UNIVERSITY OF CALIFORNIA, SAN DIEGO

From synapse to genome and back again:
A role for *Npas4* in CCK basket cell synapse plasticity

A dissertation submitted in partial satisfaction of the requirements for the degree of
Doctor of Philosophy

in

Neurosciences

by

Andrea L. Hartzell

Committee in charge:

Professor Brenda Bloodgood, Chair
Professor Jeffry Issacson
Professor Stefan Leutgeb
Professor Mark Mayford
Professor Gentry Patrick

2018

The dissertation of Andrea L. Hartzell is approved, and it is acceptable in quality and form for publication on microfilm and electronically:

_____

_____

_____

_____

_____
Chair

University of California, San Diego

2018

DEDICATION

To Luca Hartzell Brigidi, for kicking me into gear.

TABLE OF CONTENTS

LIST OF ABBREVIATIONS

ACSF	Artificial cerebro-spinal fluid
Agtx	ω Agatoxin-IVA
AMPA	α-amino-3-hydroxy-5-methyl-4-isoxazolepropionic acid
ANOVA	Analysis of Variance
AP	Action potential
AP-1	Activator protein 1 (complex)
Arc	Activity-regulated cytoskeleton-associated protein
bAP	Back-propogating action potential
BC	Basket cell
bHLH	basic helix-loop-helix
Ca	Calcium
CB1R	Cannabinoid receptor 1
CCK	Cholecystokinin
CCKBC	Cholecystokinin-expressing basket cell
ChIP-seq	Chromatin immunoprecipitation sequencing
CPP	3-((R)-2-Carboxypiperazin-4-yl)-propyl-1-phosphonic acid
Ctx	ω Conotoxin-GVIA
CV	Coefficient of variation
DAB	Diaminobenzedine
DG	Dentate gyrus
DGC	Dystrophin-glycoprotein complex
DSI	Depolarization-induced suppression of inhibition
EC	Entorhinal cortex
EE	Enriched environment or environmental enrichment

E/I	Excitation/inhibition ratio
eIPSC	Evoked inhibitory postsynaptic potential
EPSC	Excitatory postsynaptic current
EPSP	Excitatory postsynaptic potential
GABA	γ-aminobutyric acid
GABAR	γ-aminobutyric acid receptor
GAD	Glutamic acid decarboxylase
GEF	Guanine nucleotide exchange factor
GFP	Green fluorescent protein
IEG	Immediate-early gene
ITF	Inducible transcription factor
IHF	Immunohistofluorescence
IN	Inhibitory interneuron
IPSC	Inhibitory postsynaptic current
IPSP	Inhibitory postsynaptic potential
IQSec3	IQ Motif And Sec7 Domain 3 protein (SynArfGEF)
IR-DIC	Infrared differential interference contrast
ITF	Inducible transcription factor
KO	Knock out (genetic)
LEC	Lateral entorhinal cortex
MEC	Medial entorhinal cortex
mIPSC	Miniature inhibitory postsynaptic current
mRNA	Messenger RNA
N	Synapse number
NBQX	2,3-Dioxo-6-nitro-1,2,3,4-tetrahydrobenzo[f]quinoxaline-7-sulfonamide

NGS	Normal donkey serum
NMDA	N-Methyl-D-aspartic acid
nNOS	Neuronal nitric oxide synthase protein
NOS1AP	Nitric oxide synthase 1 adaptor protein
NPAS4	Neuronal PAS domain protein 4
p	postnatal day
P	Probability of release
PB	Phosphate buffer
PBS	Phosphate-buffered saline
PCL	Pyramidal cell layer
PFA	Paraformaldehyde
PN	Pyramidal neuron
PPR	Paired-pulse ratio
PV	Parvalbumin
PVBC	Parvalbumin-expressing basket cell
Q	Quantal content
RFP	Red fluorescent protein
RNAi	RNA interference
RNA-seq	RNA sequencing
ROI	Region of interest
SCA	Schaffer collateral-associated interneuron
SE	Standard environment
SEM	Standard error of the mean
SLM	Stratum lacunosum-moleculare
SO	Stratum oriens

SR	Stratum radiatum
TB	Tris buffer
uIPSC	unitary inhibitory postsynaptic currrent
VGAT	Vesicular GABA transporter
VGCC	Voltage-gated calcium channel
VGlut3	Vesicular glutamate transporter 3
WT	Wild type

LIST OF FIGURES

ACKNOWLEDGEMENTS

All of my gratitude to:

Brenda Bloodgood, for her instruction, guidance, and adventurous scientific spirit. All data and ideas presented in this dissertation result from many hours of conversation and rigorous collaboration with Brenda.

The members of the Bloodgood laboratory, for their insights, companionship, humor, and comradery. Especially to Laura Sancho, who has been on this journey with me since day one.

My committee members Jeff Isaacson, Stefan Leutgeb, Mark Mayford, and Gentry Patrick, for their mentorship and feedback. Especially to Jeff Isaacson, who helped me take the mental leap from a disorganized pile of figures to a coherent, publishable story.

My husband Stefano Brigidi, for his love and support in every aspect of life and science.

Chapter 2 is a reprint of the material as it appears in Hartzell AL, Martyniuk KM, Brigidi GS, Djaja NA, Payne, AE and Bloodgood BL (2018). *Npas4* recruits CCK basket cell synapses and enhances cannabinoid-sensitive inhibition in the mouse hippocampus. In revision. The dissertation author was the primary investigator and author of this paper.

VITA

2007-2009	Research Assistant, University of Arizona
2009-2012	Research Technician, University of Arizona
2011	Bachelor of Science, University of Arizona
2014	Teaching Assistant, University of California, San Diego
2018	Doctor of Philosophy, University of California, San Diego

PUBLICATIONS

Hartzell AL, Martyniuk KM, Brigidi GS, Payne AE, Djaja NA, Bloodgood BL. Npas4 recruits CCK basket cell synapses and enhances cannabinoid-sensitive inhibition in the mouse hippocampus. *Manuscript under revision.*

Hartzell AL, Burke SN, Rodriguez C, Lister JP, Hoang L, Friel JM, Ferng JJ, Barnes CA (2013). Transcription of the Immediate-early Gene *Arc* in the Hippocampus Reveals Activity Differences across the Transverse Axis of the CA1 Subregion. *Journal of Neuroscience* 33(8):3424-33.

Burke SN, **Hartzell AL**, Lister JP, Hoang LT, Barnes CA (2012). Layer V perirhinal cortical ensemble activity during object exploration: a comparison between young and aged rats. *Hippocampus* 22(10):2080-93.

Burke SN, Maurer AP, **Hartzell AL**, Nematollahi S, Uprety A, Wallace JL, Barnes CA (2012). Representation of three-dimensional objects by the rat perirhinal cortex. *Hippocampus* 22(10):2032-44.

Burke SN, Wallace JL, **Hartzell AL**, Nematollahi S, Plange K, Barnes CA (2011). Perirhinal Cortex-dependent Pattern Separation Deficits in Advanced Age: A Cross-species Consensus. *Behavioral Neuroscience*, Vol 125(6), Dec 2011, 836-847.

Orvis GD, **Hartzell AL**, Smith JB, Humberto Barraza L, Wilson S, Sculz KU, Turnbull DH, Joyner AL (2011). The engrailed homeobox genes are required in multiple cell lineages to coordinate sequential formation of fissures and growth of the cerebellum. *Developmental Biology.* July 2012;367(1):25-39.

FIELDS OF STUDY

Major Field: Neurosciences

Studies in Memory and Aging
Professor Carol Barnes, University of Arizona

Studies in Neural Circuitry and Plasticity
Professor Brenda Bloodgood, University of California, San Diego

ABSTRACT OF THE DISSERTATION

From synapse to genome and back again:
A role for *Npas4* in CCK basket cell synapse plasticity

by

Andrea L. Hartzell

Doctor of Philosophy in Neurosciences

University of California, San Diego, 2018

Professor Brenda Bloodgood, Chair

Experience-dependent expression of immediate-early gene transcription factors can transiently change the transcriptome of active neurons and initiate persistent changes in cellular function. However, the impact of inducible transcription factors (ITFs) on circuit connectivity and function is poorly understood. We investigate the specificity with which the ITF NPAS4 governs experience-dependent changes in inhibitory synaptic input onto CA1 pyramidal neurons (PNs). We show that novel sensory experience selectively enhances somatic inhibition mediated by cholecystokinin-expressing basket cells (CCKBCs) in an NPAS4-dependent manner. NPAS4 specifically increases the number of

synapses made onto PNs by individual CCKBCs without altering synaptic properties. Additionally, we find that sensory experience-driven NPAS4 expression enhances the amount of PN inhibition that can be suppressed by depolarization-induced suppression of inhibition (DSI), a short-term form of cannabinoid-mediated plasticity expressed at CCKBC synapses. Our results indicate that CCKBC inputs are a major target of the NPAS4-dependent transcriptional program in PNs, and consequently that NPAS4 is an important regulator of cannabinoid-sensitive inhibition in the hippocampus.

Chapter 1. Introduction

Anatomy and function of the rodent hippocampus

The hippocampus is one of the most extensively studied brain regions, attracting neuroscientists from many sub disciplines with its beautiful, laminar organization, essential role in many cognitive and behavioral processes, compelling physiological characteristics, and malfunction in widespread pathologies, especially those associated with memory and aging. While many scientists study the hippocampus in its own right, still others use it as a model system of choice in which to study general principles of neural circuit function and plasticity.

Many neuroscientists are drawn to the hippocampus because it represents a clear example of how the brain can integrate sensory input into higher-order cognitive representations, in this case by creating a cellular map of a spatial environment (**Figure 1.1**; O'Keefe and Dostrovsky, 1971). Though this property is the focus of many contemporary studies of hippocampal function, its proposed role has undergone continuous evolution since the 18th century, with the predominant hypothesis until the 1930s being that it was a part of the olfactory system (Brodal, 1947). Since then, it has been proposed to underlie emotion (Papez circuit; Papez 1937), control attention (Green and Arduini, 1954; Green and Adey, 1956; Holmes and Adey, 1960), and finally, serve as a substrate for memory (Scoville and Milner, 1957). Most contemporary research on hippocampal function focuses one of two theories: the first, based primarily on studies in human and nonhuman primates, is that it is involved in the formation of memories for facts and events that can be consciously recalled (declarative memory; Squire, 1992), or

the second, based predominantly on single unit recording studies in rodents and most relevant to the experiments described in chapter 3, that it is involved in spatial memory and navigation (O'Keefe and Dostrovsky, 1971).

The discovery of hippocampal place cells by John O'Keefe and Jonathon Dostrovsky in the early 1970s launched the contemporary wave of hippocampal research focused on spatial memory. Through single unit recordings, O'Keefe and Dostrovsky observed that a portion of hippocampal principle cells experience an increase in firing rate when an animal is in a specific location within its environment, or the cell's "place field" (**Figure 1.1**). Together, the place fields of many cells tile the animal's environment, providing the brain with a spatial map (O'Keefe and Dostrovsky, 1971; O'Keefe and Nadel, 1978; Wilson and McNaughton, 1993). While most subsequent studies focused on pyramidal cells in the hippocampus proper, granule cells in the dentate gyrus (DG) have also shown place cell activity (Jung and McNaughton, 1993; O'Keefe 1976).

The unique neuroanatomy of the hippocampus supports the cellular dynamics described above and is essential to the experiments described in chapters 2 and 3. The hippocampus shares some similarities with other brain regions, including the presence of principle neurons (PNs) with pyramidal shaped cell bodies and local inhibitory interneurons (INs). However, in other ways, the hippocampus is relatively unique, such as in the stereotyped laminar organization of fiber pathways and largely unidirectional flow of information through a tri-synaptic loop. This is in contrast to areas such as the neocortex, in which connections between subregions are generally reciprocal (Felleman and Van Essen, 1991). The hippocampal formation is composed of six regions with

distinct cytoarchitecture, including the hippocampus proper (composed of CA3, CA2, and CA1), the DG, subiculum, presubiculum, parasubiculum, and entorhinal cortex (EC) (Amaral and Lavenex, 2006). The EC is the recipient of a large portion of the neocortical inputs to the hippocampal formation, and in turn it provides the major input to the hippocampus. The axons of its principle cells form the perforant path, which provides the predominant input to the DG and sends additional direct projections to CA3 and CA1. The principle cells of the DG, the granule cells, then send their mossy fiber axons to the PNs of CA3, which in turn provide the second major input to the PNs of CA1 via the Schaffer Collateral pathway. This circuit from the EC to DG to CA3 to CA1 composes the tri-synaptic loop for which the hippocampus is well known (**Figure 1.2**). CA2 is a narrow, anomalous region situated between CA3 and CA1. While the cell bodies of its PNs are similar to those of CA3, it is not innervated by the mossy fiber axons from the DG. The PNs of region CA1, which are the focus of the experiments described in Chapters 2 and 3, form the major output of the hippocampus.

A basic knowledge of the laminar organization of CA1 is crucial to understanding the experiments presented in the following chapters (**Figure 1.3**). The principal cell layer in CA1, the pyramidal cell layer (PCL), is tightly packed with somata of PNs. The layer located deep to the PCL, called stratum oriens (SO), is home to several types of local INs, the basal dendrites of the CA1 PNs, and one portion of the Schaffer Collateral projection from CA3. Located deep to SO is the alveus, containing the axons from the CA1 PNs making their way out of the hippocampus. Superficial to the PCL, where the proximal apical dendrites of PNs are located, is stratum radiatum (SR). SR contains the other portion of the CA3 to CA1 Schaffer Collateral connection, which synapses in SR on the

proximal apical dendrites of CA1 PNs, as well as on local INs. Next to SR and forming the most superficial layer of the CA1 region is stratum lacunosum-moleculare (SLM), home to the perforant path projections from the EC directly to CA1, which synapse on the distal apical dendrites of CA1 PNs, as well as local INs.

CA1 PNs are often treated as a homogenous population, both conceptually and in biophysical and modeling studies. However, several molecular, anatomical, and functional differences have been described for PNs along the dorsal-ventral (Fanselow and Dong, 2010; Jung et al., 1994; Kjelstrup et al., 2002; Maurer et al., 2005; Moser et al., 1993; Thompson et al., 2008), proximal-distal (Graves et al., 2012; Hartzell et al., 2013; Henriksen et al., 2010; Jarsky et al., 2008), and superficial-deep axes (Danielson et al., 2016; Lee et al., 2014; Maroso et al., 2016; Mizuseki et al., 2011; Valero et al., 2015). The experiments described in chapter 2 highlight the differences between superficial (closest to SR) and deep (closest to SO) PNs. Studies from the early 1990s first demonstrated that superficial and deep PNs can be differentiated by their immunoreactivity to calbindin (Baimbridge et al., 1991) and by their zinc content (Slomianka 1992). More recently, two distinct subcircuits have been described for superficial and deep PNs, with PNs localized to the deep sublayer having higher firing rates, more frequent bursting, and stronger modulation slow wave oscillations associated with sleep, relative to superficial PNs (Muzeseki et al., 2011). Superficial and deep PNs also show opposite membrane polarization during sharp-wave ripples (Valero et al., 2015).

Superficial and deep CA1 PNs appear to participate differentially in place encoding and cognitive tasks. Interestingly, deep PNs form place fields more frequently

during exploration of a linear track or open field (Muzeseki et al., 2011), while place fields of superficial PNs are more stable than deep during head-fixed exploration of a virtual reality (Danielson et al., 2016). However, when animals undergo goal-oriented learning; deep PN place maps are preferentially stabilized, and representations of the reward zone by deep cells are predictive of task performance (Danielson et al., 2016). Together, these results suggest the existence of cognitively-relevant encoding differences between superficial and deep CA1 PNs, with superficial PNs providing a more stable map of space, while deep PNs provide a more flexible representation of an environment that is shaped by task and salient environmental features (Danielson et al., 2016). Additionally, it was recently discovered that EC projections also differentiate between superficial and deep PNs, with the medial entorhinal cortex (MEC) preferentially targeting deep PNs in proximal CA1 and the lateral entorhinal cortex (LEC) preferentially exciting superficial PNs in distal CA1 (Li et al., 2017; Masurkar et al., 2017). This connectivity difference might help explain the differential roles of proximal and distal CA1 PNs in encoding spatial versus non-spatial information (Hartzell et al., 2013; Henriksen et al., 2010).

Aside from differences in connectivity with excitatory projections, connectivity with local interneurons differs between superficial and deep PNs in CA1. Parvalbumin-expressing basket cells (PVBCs) preferentially innervate deep PNs, while superficial PNs provide more excitatory input to PVBCs (Lee et al., 2014). Cholecystokinin-expressing basket cells (CCKBCs), on the other hand, form more perisomatic boutons on superficial PNs than deep PNs (Valero et al., 2015, but see Lee et al., 2014). The distinct and complimentary roles that PVBCs and CCKBCs play in the local microcircuit, discussed

in detail in the following section, suggest compelling hypotheses regarding how this asymmetry might distinguish the ways in which superficial and deep PNs participate in hippocampal circuit operations.

Somatic inhibitory interneurons of CA1 and their role in circuit operations

On the most basic level, inhibition in the hippocampus is necessary to maintain network activity levels within an appropriate range (Dichter and Spencer, 1969; Johnston and Brown, 1981; Traub and Wong, 1982), but also to perform the more nuanced job of precisely structuring in space and time the transmission of information between neurons. Interneurons form an extremely diverse group of cells; there are over 20 unique interneuron subtypes in the hippocampus alone. This subtype classification is based on morphological, immunohistochemical, physiological, and pharmacological features, all of which contribute to the specialized role each subtype plays within the local circuit (**Figure 1.4;** Freund and Buzaki, 1996; Klausberger and Somogyi, 2008; Somogyi and Klausberger, 2005). Functional distinctions between interneuron subtypes begin with which of the four major postsynaptic PN compartments they synapse onto (soma, axon initial segment, proximal dendrites, or distal dendrites), and is further refined by cell type expression of neuropeptides, calcium binding proteins, and cellular anatomy. Neurons that utilize γ-aminobutyric acid (GABA) as their neurotransmitter provide the sole synaptic input to the somata and axon initial segments of PNs, while PN dendrites are innervated both by local GABAergic input and excitatory input from the entorhinal cortex, upstream hippocampal subregions, and thalamus (Klausberger and Somogyi, 2008).

Somatic inhibition has attracted significant attention from the research community because somatic synapses are optimally localized to control the action potential output of target cells (Cobb et al., 1995; Miles et al., 1996; Pouille and Scanziani, 2001). Somatic interneurons initiate the majority of simultaneous inhibitory postsynaptic potentials (IPSPs) recorded in nearby PNs, and indeed, single somatic IPSPs are capable of suppressing the discharge of PN action potentials (Miles et al., 1996). Thus, the potential influence of a single soma-targeting interneuron is far-reaching. On average, somatic interneurons in CA1 synapse on 22-28% of PNs within their axonal arbor, with the probability dropping from 54% for immediate neighbors to 5% for more distal neighbors (Ali et al., 1999; Halasy et al., 1996). They form 2-12 synapses onto an individual PN (Buhl et al., 1994a, b; Miles et al., 1996). In the hippocampus, rhythmic oscillations in the theta (4-7 Hz) and gamma (40-50 Hz) frequencies are observed during exploratory behavior (Bragin et al., 1995; Buzsaki and Draguhn, 2004). Perhaps unsurprisingly, somatic interneurons can entrain spontaneous firing and subthreshold oscillations in PNs at both theta (Cobb et al., 1995) and gamma (Lytton and Sejnowski, 1991; Whittington et al., 1995) frequencies. Together, these findings establish a role for somatic inhibition in gating PN output and orchestrating the coordinated activity of cohorts of nearby PNs in the hippocampus.

Somatic inhibition in CA1 can be further subdivided into that provided by each of two populations of basket cells, PVBCs and CCKBCs. The experiments described in this dissertation highlight the important physiological and pharmacological differences between these distinct classes of somatic interneurons. PVBCs and CCKBCs can be differentiated at first pass by their intrinsic properties (**Figure 1.5**). PVBCs fire narrow,

high-frequency, non-accommodating trains of action potentials (APs) in response to depolarizing current injections. CCKBCs, on the other hand, fire broader, moderately-paced, strongly accommodating APs. Furthermore, PVBCs have exceptionally large diameter dendrites (Emri et al., 2001; Nörenberg et al., 2010; Bartos et al., 2011), very fast membrane time constants (~10 ms) and low input resistances (Glickfeld and Scanziani, 2006), supporting fast propagation of excitatory postsynaptic potentials (EPSPs), while CCKBCs have slower time constants (~25 ms) and higher input resistances (Cea-del Rio et al., 2010; Glickfeld and Scanziani, 2006), allowing excitatory postsynaptic potentials (EPSPs) to arrive at the soma with longer half-durations. While both basket cell subtypes in CA1 receive feedforward excitation from all major excitatory pathways as well as feedback excitation from local CA1 PNs, PVBCs, due in large part to their intrinsic membrane properties, are readily recruited in response to excitation and exert fast, precise inhibition onto their postsynaptic targets (Doischer et al., 2008; Jonas et al., 2004; Klausberger et al., 2005). In contrast, CCKBCs are less easily recruited by excitatory inputs and integrate slower, repetitive inputs over longer time scales or coordinated input from multiple coactive input pathways (Glickfeld and Scanziani, 2006; Klausberger et al., 2005; Tukker et al., 2007). Contributing further to this difference in the probability of recruitment is the fact that PVBCs receive three times the excitatory synapses on their dendrites as CCKBCs (Gulyas et al., 1999; Mátyás et al., 2004) and experience larger excitatory postsynaptic currents (EPSCs) in response to stimulation of all three major excitatory inputs to CA1, (Schaffer Collaterals, Perforant Path, and local recurrent axons; Glickfeld and Scanziani, 2006). However, most of the relative increase

in dendritic synapse numbers relative to CCKBCs comes from Schaffer collateral inputs, biasing PVBCs to feed-forward inhibition (Glickfeld and Scanziani, 2006).

Expression of physiologically important receptors and channels further differentiates PVBCs and CCKBCs. Most relevant to this dissertation is the expression of type 1 cannabinoid receptors (CB1R) at the presynaptic terminals of CCKBCs and their absence at PVBC presynaptic terminals (Katona et al., 1999). When a postsynaptic PN is active, it synthesizes and releases endogenous cannabinoids, which signal retrogradely to the presynaptic CCKBC bouton by binding CB1Rs. CB1R activation results in antagonism of presynaptic voltage-gated calcium channels (VGCCs), causing a temporary reduction in GABAergic transmission at the synapse, a form of short-term plasticity known as depolarization-induced suppression of inhibition (DSI, **Figure 1.6**; Glickfeld and Scanziani, 2006; Katona et al., 1999; Neu et al., 2007; Wilson and Nicoll, 2001). Disinhibition of PNs due to the expression of DSI at CCKBC terminals might be permissive of long-term potentiation of excitatory inputs or other forms of plasticity (Carlson et al., 2002). Furthermore, DSI might be a potential mechanism by which a place cell achieves a high signal-to-noise ratio when an animal is inside the cell's preferred place field versus outside of it (Klausberger et al., 2005). This hypothesis is discussed in more detail in Chapter 3.

Another physiologically important difference between PVBCs and CCKBCs is the VGCC subtype that permits GABA release. GABA release from PVBC synapses is governed by P/Q-type VGCCs, whereas CCKBCs utilize N-type calcium channels (Hefft and Jonas, 2005; Poncer et al., 1997). Calcium chelator experiments have suggested a longer-lasting presynaptic calcium transient and a larger distance between the calcium

source and the sensor mediating exocytosis at N-type VGCC-containing CCKBC presynaptic boutons relative to P/Q-type VGCC-containing PVBC boutons (Hefft and Jonas, 2005). These N-type VGCC properties are thought to contribute to the characteristic asynchronous neurotransmitter release from CCKBC synapses, which extends the window of inhibition exerted on postsynaptic PNs and can result in a form of low-grade tonic inhibition (Ali and Todorova, 2010; Daw et al., 2009; Hefft and Jonas, 2005). In contrast, the tight coupling of P/Q-type VGCCs to calcium sensors at PVBC synapses contributes to the precision, speed, and efficacy of neurotransmitter release from these boutons (Bucurenciu et al., 2008).

Unsurprisingly, PVBCs and CCKBCs also play distinct roles within the neural network. Hippocampal circuit activity is characterized by the occurrence of network oscillations in gamma and theta frequencies during exploration or behavioral engagement. AP firing by PVBCs is tightly coupled to the descending phases of gamma oscillations (Bragin et al., 1995; Csicsvari et al., 2003; Gulyás et al., 2010; Klausberger et al., 2005; Mann et al., 2005; Oren et al., 2010) and underlies the emergence of gamma oscillations within the hippocampus (Bartos et al., 2007; Buzsaki and Draguhn, 2004; Cobb et al., 1995). The extensive interconnectivity of PVBCs by gap junctions allows the phasic recruitment of a small subset of cells to rapidly synchronize activity throughout the network (Vida et al., 2006; Whittington et al., 1995), orchestrating PN activity through coordinated phasic inhibition. Consistent with this, optogenetic activation or silencing of PVBCs boosts or reduces gamma oscillations, respectively (Cardin et al., 2009; Sohal et al., 2009). The activity of CCKBCs, in contrast, is less tightly coupled to gamma oscillations (Gulyás et al., 2010; Klausberger and Somogyi, 2008; Tukker et al.,

2007), but occurs regularly during the ascending phase of theta oscillations (Klausberger et al., 2005). PVBCs fire reliably during the descending phase of theta oscillations (Klausberger et al., 2005).

Sharp wave ripple episodes (120-200 Hz firing for around 100 ms in duration) occur in the hippocampus during slow-wave sleep and periods of awake rest (Buzsaki et al., 1983). PVBC firing is strongly correlated with ripple activity (Klausberger et al., 2005). CCKBC firing, on the other hand does not show any correlation to ripple episodes, with some individual CCKBCs alternating between activation or silencing during ripple events (Klausberger et al., 2005). Whether or not a CCKBC participates in a ripple episode might be determined by the recent network activity and might in turn determine which downstream PNs are activated by the ripple episode (Klausberger et al., 2005). In summary, while PVBCs serve an important role as pace makers in the hippocampal circuit, regulating oscillations and tying PN activity to the oscillatory frequency, CCKBCs might serve a more nuanced role in regulating which cohorts of PNs are active or silent during oscillations or ripple events in a manner dependent on the recent activity history of the circuit.

Somatic inhibitory interneurons in disease

In addition to their significant roles during normal circuit activity, aberrant activity of both basket cell subtypes has been associated with several neurological diseases. Disruption of PVBC function is implicated in schizophrenia through a couple of distinct mechanisms. Schizophrenia involves disruption of gamma oscillations, which are mediated by PVBCs (Lewis et al., 2012; Lisman and Buzsaki, 2008). Furthermore,

schizophrenia patients show reduced levels of $GABA_A$ receptors containing the α1 subunit, the main receptor targeted by GABA release from PVBC synapses (Glausier and Lewis, 2011).

Both PVBCs and CCKBCs have been suggested to play a role in the pathogenesis of epilepsy. In temporal lobe epilepsy induced in rodents by the muscarinic agonist pilocarpine, CCKBC boutons contacting PNs in CA1 are selectively and chronically reduced, while PVBC boutons are preserved (Wyeth et al., 2010). However, excitatory synaptic drive to PVBCs in the DG is reduced after pilocarpine-induced epilepsy, resulting in higher failure rates and smaller unitary inhibitory postsynaptic currents (uIPSCs) at basket cell-granule cell synapses (Zhang and Buckmaster, 2009). In human temporal lobe epileptic patients, a higher density of CCKBC terminals was found in the hippocampus of patients showing sclerosis and both types of somatic interneurons showed sprouting in the DG (Wittner and Maglóczky, 2017). Therefore, while the study of somatic inhibition in the healthy hippocampus will contribute to an understanding of hippocampal circuit function and information processing during essential cognitive functions, the essential role of somatic inhibition in the pathogenesis neurological disease further underscores the importance of studying this type of neurotransmission.

Structure of inhibitory synapses

Inhibitory synapses consist of GABA-releasing axonal terminals apposed to postsynaptic sites containing GABA receptors (GABARs) and several other proteins required for GABAergic transmission. GABAergic synapses can form onto dendritic shafts, spines, somata, or axon initial segments. A single rat CA1 pyramidal neuron

receives approximately 1700 inhibitory synapses, of which 40% are made onto the perisomatic region.

Though the protein content of inhibitory synapses has not been as thoroughly characterized as for excitatory synapses, recent proteomics studies have provided insight into their biochemical nature and revealed 42 characteristic proteins that are found at pre- and postsynaptic inhibitory synaptic sites (Heller et al., 2012; Loh et al., 2016). Presynaptically, the biosynthesis of GABA is achieved by the enzyme glutamic acid decarboxylase (GAD) through the decarboxylation of glutamate. Two isoforms of GAD exist in mammals, GAD67 and GAD65 (Bu et al., 1992), with largely overlapping expression in neurons (Dupuy et al., 1996; Zhao et al., 2013). Synthesized GABA is then packaged into vesicles by vesicular GABA transporter (VGAT; McIntire et al., 1997), which is used as an inhibitory synapse marker in experiments described in Chapter 2.

On the postsynaptic side, two classes of GABARs mediate the cellular response to GABA: $GABA_A$ and $GABA_B$ receptors. $GABA_A$ receptors are ionotropic and mediate a rapid response to GABA by opening a chloride-selective pore. They are pentameric receptors assembled from a pool of 19 distinct subunits, conferring specificity to distinct inhibitory synapses (Heller et al., 2012). Each subunit has sites that mediate protein-protein interactions, as well as sites for phosphorylation (Luscher et al., 2011), ubiquitination (Arancibia-Cárcamo et al., 2009), and palmitoylation (Fang et al., 2006; Keller et al., 2004). $GABA_B$ receptors, in contrast, are metabotropic G-protein coupled receptors that, when activated, lead to the opening of potassium channels (Chen et al., 2005), resulting in a slower hyperpolarization of the neuron relative to $GABA_A$ receptor activation. The scaffold protein specifically associated with GABAergic postsynaptic

sites is the cytoplasmic protein gephyrin, which directly binds to GABA receptors and is used as a postsynaptic inhibitory synapse marker in experiments described in Chapter 2.

Activity-dependent structural plasticity of inhibitory synapses

A central feature of neural circuits is the ability to adjust activity patterns in response to new experiences. Plasticity allows neural circuits to modify the computations they perform in order to encode experiences, refine behaviors, and compensate for injury. Many of these modifications have been proposed to occur through structural changes, including the formation and elimination of synapses (Feldman 2009; Leuner and Gould 2010). The relatively stable nature of structural plasticity makes it a compelling potential substrate for the long-term changes in circuit dynamics underlying learning and memory. Over the last several decades, much progress has been made toward understanding activity-dependent structural plasticity of glutamatergic synapses, but structural plasticity of inhibitory GABAergic neurotransmission is still a comparatively young field. Inhibitory synapses can shape the activity of postsynaptic targets in myriad ways depending on the interneuron subtype and how it is excited, the location of the inhibitory synapses on the postsynaptic cell, and the types of plasticity capable of being expressed at the synapses. An interesting question to consider, therefore, is how the activity history of a principle neuron might be capable of altering its future activity by driving the formation or elimination of inhibitory synapses. Recently, several examples of this phenomenon have been described, after large-scale, dramatic manipulations of neural activity as well as in response to fine-scale, ethologically relevant activity paradigms. The resultant forms of inhibitory structural plasticity range from global changes in inhibitory

synapse numbers that are important for homeostasis, to more sparse or localized changes that shape the information received from upstream inputs.

Over the last several years, beautiful imaging work has allowed the dynamics of inhibitory synapse structural plasticity to be observed at baseline and after the manipulation of experience. Imaging of mature IN axons and PN dendrites *in vitro* has revealed that new GABAergic synapses form at pre-existing axonal-dendritic crossings (Wierenga et al., 2008). *In vivo* imaging of mature inhibitory axons led to the observation that a portion of presynaptic boutons turn over with time, and that this rate can be manipulated by behavioral intervention (Chen et al., 2011, Chen et al., 2012; Keck et al., 2011). Most recently, two-photon *in vivo* daily imaging of synapses in the mouse visual cortex demonstrated that inhibitory synapses often disappear and reappear at the same location (Villa et al., 2016). As tools for probing neural circuits become more sophisticated, studies are beginning to identify examples of activity-dependent structural plasticity of synapses made by individual subtypes of interneurons, in some instances driven by learning-related stimuli. This makes it possible to begin to untangle the functional consequences of different flavors of activity-dependent inhibitory synapse structural plasticity.

Experiments in acute and cultured brain slices from mouse cortex have provided evidence for a role of activity-dependent inhibitory structural plasticity in homeostasis and maintaining the balance of excitation and inhibition (E/I balance). PNs in the adult visual cortex maintain stable E/I ratios despite changing levels of excitation, because increased excitation results in a proportional increase in the engagement of inhibitory neurons (Anderson et al., 2000; Atallah and Scanziani, 2009; Okun and Lampl, 2008;

Shu et al., 2003). In layer 2/3 of the murine visual cortex, E/I ratios are not only maintained, but are stable across PNs, with individual neurons receiving inhibition proportional to excitation (Xue et al., 2014). This maintenance of E/I ratio is mediated by synaptic input from PV- expressing interneurons. Manipulating the excitability of PNs results in an activity-driven change in PV interneuron-mediated inhibition in order to restore E/I balance (Xue et al., 2014). PV interneurons are ideally suited for the maintenance of E/I balance due to their rapid, reliable recruitment as circuit activity levels increase (Doischer et al., 2008; Jonas et al., 2004; Klausberger et al., 2005).

Another body of work describing a role for activity-dependent structural plasticity of inhibitory synapses in homeostasis or E/I balance takes place in the barrel fields of mouse somatosensory cortex and involves the quantification of inhibitory synapses after robust manipulation of input or cellular excitability. When rats are sensory deprived from birth by the continuous removal of rows of whiskers, the number and proportion of GABA-immunoreactive synaptic puncta is significantly reduced in layer IV of the corresponding somatosensory cortex (Micheva and Beaulie, 1995). In a later study, ultrastructural analysis after whisker stimulation for 24 hours revealed an increase in both excitatory and inhibitory synaptic puncta in the corresponding cortical barrel (Knott et al., 2002). Four days after stimulation, the increase in inhibitory synaptic puncta persists, despite the total synaptic density returning to baseline levels. These anatomical changes correspond with altered response properties of cortical neurons to whisker deflection (Knott et al., 2002).

While the above studies establish a role for activity-dependent structural plasticity of inhibitory synapses in maintenance of homeostasis or E/I balance, other studies have

described inhibitory structural plasticity mechanisms that have the potential to alter the temporal or spatial structure of excitation received by the postsynaptic cell. Inhibitory synapses that share a spine with an excitatory synapse, found to comprise around a third of all dendritic inhibitory synapses, have a turnover rate three times higher than those made onto the dendritic shaft or occupying a spine in the absence of an excitatory synapse (Chen et al., 2012). Interestingly, on dendritic spines dually innervated by excitatory and inhibitory synapses, the excitatory synapse is stable while the inhibitory synapse frequently is pruned and reforms, allowing for dynamic control of the efficacy of the excitatory input on a synapse-by-synapse basis (Chen et al., 2012; Villa et al., 2016). These observations imply that the efficacy of individual excitatory synapses has the potential to be modulated by local structural plasticity of inhibitory synapses, resulting in changes in dendritic integration and information processing by postsynaptic principle cells. The next major challenge for the field will be to 1) mechanistically link increases in cellular activity to structural plasticity of inhibitory synapses, and 2) to fully understand the functional consequences of these long-lasting, persistent changes in circuit connectivity on information processing within neural circuits.

Immediate-early genes in hippocampal circuits

One way in which transient increases in neural activity can initiate widespread, persistent changes in cellular and circuit function is through the induction of activity-dependent gene expression. The immediate-early genes (IEGs) are the first group of genes to be transcribed after a neuron is active. This group of genes includes transcription factors, cytoskeletal proteins, growth factors, metabolic enzymes, and signal transduction pathway components (**Figure 1.7;** Lanahan and Worley, 1998; Sun and Lin, 2016). Many

of these genes, such as *c-fos*, activity-regulated cytoskeleton associated protein (*Arc)*, early growth response 1 (*Egr-1/* zif268*)*, and neuronal PAS domain protein 4 (*Npas4)* are associated with plasticity and are rapidly and selectively upregulated in brain regions associated with learning and memory, such as the hippocampus (Minatohara et al., 2015). IEG expression has therefore become a popular tool for marking neuronal populations active during various learning and memory tasks. Recent optogenetic studies have demonstrated that the population of neurons that expresses IEGs such as *c-fos* or *Arc* in response to a memory task encode information that is necessary and sufficient for memory recall, suggesting that IEG-expressing cells might be involved in the memory trace (for examples see Garner et al., 2012; Liu et al., 2012; Ramirez et al., 2013). However, despite their widespread use as tools, the molecular and cellular mechanisms linking IEG expression to mnemonically-relevant changes for cells and circuits remain relatively unknown.

One exception is the IEG *Arc*, which encodes an effector protein with a direct connection to memory (Peebles et al., 2010; Plath et al., 2006; Yamada et al., 2011) and a known role in reshaping synaptic properties (Chowdhury et al., 2006; Shepard et al., 2006). *Arc* messenger RNA (mRNA) can be observed in nuclei within minutes of neural activity and quickly translocates into the cytoplasm and subsequently the dendrites of active cells (Guzowski et al., 1999; Steward et al., 1998), where Arc protein can be observed in spines near active synapses (**Figure 1.8;** Chowdhury et al., 2006; Moga et al., 2004; Rodriguez et al., 2005; Steward et al., 2014). There, Arc protein interacts with other postsynaptic proteins such as endophilin, dynamin (Chowdhury et al., 2006; Rial Verde et al., 2006), and TARPγ2 (Zhang et al., 2015) to regulate endocytosis of α-amino-

3-hydroxy-5-methyl-4-isoxazolepropionic acid (AMPA) receptors. *Arc* overexpression or knockout decreases or increases AMPA receptor at the synapse, respectively (Chowdhury et al., 2006). Consistent with this function, perturbing *Arc* expression affects homeostatic synaptic scaling (McCurry et al., 2010; Sheperd et al., 2006) and the induction of long-term depression (Park et al., 2008; Plath et al., 2006). These roles also implicate *Arc* expression in behavior and cognition; indeed, *Arc* knockout (KO) mice show impaired consolidation of spatial and fear memories (Peebles et al., 2010; Plath et al., 2006; Yamada et al., 2011).

In addition to its role in AMPA receptor endocytosis, it was recently discovered that Arc protein also has a role in mediating intercellular signaling between neurons. Arc protein exhibits structural similarities to retroviral Gag proteins, including self-assembly into oligomers that resemble virus-like capsids (Ashley et al., 2018; Pastuzyn et al., 2018). Arc capsids containing *Arc* mRNA are released from neurons in extracellular vesicles and are endocytosed by other cells, allowing *Arc* mRNA to be delivered into target cells, where it can undergo activity-dependent translation (Ashley et al., 2018; Pastuzyn et al., 2018).

The subset of IEGs that encodes inducible transcription factors (ITFs) is optimally suited to dramatically alter cellular function by regulating the expression of large families of target genes. However, even less is known about the functional consequences of ITF expression than those of IEGs encoding effector proteins. The most well-known ITFs, *c-fos*, encodes a transcription factor that participates in the Activator protein 1 (AP-1) complex by interacting with a member of the *jun* family (Jun, JunB, and JunD). The consensus sequence recognized by the AP-1 complex is known, however the target genes

have not been fully characterized (for review see Alberini, 2009; Sheng and Greenberg, 1990) and the effect of activity-induced *c-fos* expression or AP-1 activation on neuronal function, especially within the adult brain, has not been fully described. Gene knockout experiments have suggested that Fos and Jun family proteins have largely overlapping functions, but other functions appear to be biased to individual isoforms. For example, knock-down of *c-jun*, but not *junB*, inhibits sequence learning (Tischmeyer et al., 1994). However, for many studies implying isoform specificity in learning and memory tasks, conflicting studies also exist.

Npas4 is an immediate-early gene regulator of inhibitory synapses

One ITF for which a function relevant to neural circuits has been recently described is encoded by the gene *Npas4*. *Npas4* is a member of the basic helix-loop-helix (bHLH)/ PAS family of transcription factors that has been implicated in acute responses to environmental and physiological stimuli. Even amongst IEGs, *Npas4* has several unique features that make it an ideal candidate for mechanistically linking neuronal activity to long-lasting changes in neuronal information processing. In the brain, *Npas4* is exclusively expressed in neurons, and solely in response to increased intracellular calcium associated with neural activity (Lin et al., 2008; Ramamoorthi et al., 2011). This is in contrast to other IEGs, including *Fos*, *Arc*, and *Zif268*, that can be induced by cytokines, growth factors, and neurotrophins (**Figure 1.9)**. Finally, *Npas4* is unique amongst IEGs in that its expression has been shown to regulate structural synapse plasticity, including both inhibitory synapses made onto principle cells and excitatory synapses made onto INs (Bloodgood et al., 2013; Lin et al., 2008; Spiegel et al., 2014), and is required for the formation of long-term memories (Ploski et al., 2011;

Ramamoorthi et al., 2011). Consistent with a role in regulating inhibition, constitutive *Npas4* KO mice are hyperactive, aggressive, and seizure prone compared to wildtype (WT) littermates (Coutellier et al., 2012; Lin et al., 2008).

Npas4 first emerged as a candidate for regulating inhibitory synapse development in 2008 by a DNA microarray screen that aimed to identify genes that were induced by activity in neurons, predicted to encode transcription factors, and upregulated during the developmental window for inhibitory synapse formation. The known transcription factor *Npas4* was the sole gene out of over 300 candidates to meet all three criteria, and was the most highly induced transcription factor in this screen (Lin et al., 2008). In culture, its induction depends on calcium influx through L-type VGCCs and is partly dependent on N-methyl-D-aspartate (NMDA) and AMPA receptors (Lin et al., 2008). *In vivo*, *Npas4* is expressed in brain regions in response to salient stimuli, such as the visual cortex of dark-reared mice in response to visual stimulation (**Figure 1.10;** Lin et al., 2008), the hippocampus in response to exposure to environmental enrichment (Bloodgood et al., 2013) or contextual fear conditioning (Ramamoorthi et al., 2011; Weng et al., 2018), the olfactory bulb after olfactory sensory input (Yoshihara et al., 2014) and in the barrel cortex in response to whisker stimulation conditioning (Kaliszewska and Kossut, 2015).

The effect of *Npas4* on inhibitory synapse development was first discovered by RNA interference (RNAi)-mediated knockdown in cultured hippocampal neurons and immunostaining for pre- and postsynaptic proteins. Expression of an RNAi targeting *Npas4*, but not a scrambled RNAi control, significantly reduced the number of putative inhibitory synaptic puncta. This result was confirmed by comparing spontaneous miniature inhibitory postsynaptic currents (mIPSCs) between WT PNs and PNs

transfected with an RNAi against *Npas4* in organotypic hippocampal cultures. In *Npas4* knockdown neurons, the mIPSC inter-event interval was increased while the amplitude was decreased, indicating a decrease in inhibitory synapse number (Lin et al., 2008). These results led to the conceptualization of activity-induced *Npas4* as a homeostatic regulator of inhibition, increasing the number of inhibitory synapses in response to increased activity.

The role of *Npas4* in inhibitory synapse regulation *in vivo* was established by experiments in acute hippocampal slices taken from *Npas4* conditional knockout animals ($Npas4^{f/f}$) in which a small population of PNs was virally infected with Cre recombinase (Bloodgood et al., 2013). Inducing *Npas4* expression in these animals through exposing them to an enriched environment or through kainic acid-induced seizure resulted in less frequent and smaller amplitude mIPSCs in *Npas4* KO PNs relative to neighboring WT cells (Bloodgood et al., 2013).

This result was further refined by stimulating axons within discrete layers of CA1 (SO, PCL, SR, and SLM) and comparing evoked inhibitory postsynaptic current (eIPSC) amplitudes between neighboring WT and *Npas4* KO PNs (**Figure 1.11**). In mice housed in an enriched environment, stimulation in the PCL generated smaller eIPSCs in *Npas4* KO PNs than WT PNs. By contrast, stimulation in SR generated larger eIPSCs in *Npas4* KO PNs relative to WT PNs. No difference was detected when slices were stimulated in SO or SLM (Bloodgood et al., 2013). This finding necessitated a reinterpretation of the functional role of *Npas4*; instead of a homeostatic regulator of inhibitory synapses, *Npas4* plays a more computationally complex role in reorganizing inhibitory synaptic input onto PNs in a domain-specific manner. However, this domain-specific phenotype combined

with the complexity of IN subtypes in the hippocampus suggests the possibility that *Npas4* might be a regulator of inhibitory synapses made by specific IN subtypes, rather than homogeneously regulating all inhibitory synapses within a particular somato-dendritic domain. In order to understand the functional consequences of *Npas4*-mediated inhibitory synapse structural plasticity, the next step is to identify the interneuron subtypes that are regulated downstream of *Npas4* expression.

As a transcription factor, *Npas4* has the potential to regulate numerous downstream target genes and affect many aspects of cell biology. 270 unique genes were identified via DNA microarray that were upregulated or downregulated in control neurons relative to neurons in which *Npas4* was knocked down. These potential *Npas4* target genes include IEGs, other transcription factors, ion channels, kinases, phosphatases, and synaptic proteins involved in ubiquitination, trafficking, and receptor endocytosis, and over 90 genes that are as of yet uncharacterized (**Figure 1.12;** Lin et al., 2008). In order to make progress toward understanding the mechanistic link between *Npas4* expression and inhibitory synapse reorganization, target genes were identified via chromatin immunoprecipitation sequencing (ChIP-seq) and RNA sequencing (RNA-seq) that had NPAS4 bound close to the gene and where mRNA transcribed near the NPAS4 peak was strongly induced. This list of target genes is enriched for secreted molecules and proteins involved in the processing and trafficking of secreted molecules, opening the possibility that NPAS4 initiates communication with presynaptic neurons via a secreted factor. For these candidates, short hairpin-mediated knockdown was performed in hippocampal organotypic cultures in order to identify putative target genes that affect mIPSC frequency or amplitude, resulting in 16 genes that might mediate the effects of

Npas4 expression on inhibitory synapse reorganization (Bloodgood et al., 2013). Therefore, despite the identification of putative *Npas4* target genes involved in inhibitory synapse regulation *in vitro*, it remains unknown how the expression of *Npas4* mediates domain-specific inhibitory synapse structural plasticity in behaving animals, and, importantly, whether the relevant inhibitory synapses arise from functionally distinct subtypes of dendrite-targeting interneurons.

Conclusions and perspectives

The discovery that *Npas4* does not simply provide homeostatic regulation of excitability, but instead regulates inhibitory synapses domain-specifically in hippocampal PNs, suggests that *Npas4* expression might profoundly affect information processing in the postsynaptic neuron. Furthermore, this opens the door to the possibility that *Npas4*-mediated regulation of inhibitory synapses might have even more layers of specificity, down to the level of individual interneuron subtypes. For example, *Npas4* expression increases the number of inhibitory synapses onto the somata of PNs in CA1 (Bloodgood et al., 2013). Somatic inhibition in the hippocampus is provided by two interneuron subtypes with distinct and well-studied roles in the hippocampal circuit, CCKBCs and PVBCs. Does *Npas4* recruit both subtypes of inhibitory synapses to PN somata, or is it possible that activity-dependent *Npas4* expression recruits synapses from only one basket cell subtype? The answer to this question is fundamental to understanding how activity-dependent *Npas4* expression changes information processing by individual postsynaptic PNs and ultimately how NPAS4 alters a PNs role in the hippocampal circuit. Luckily, in the case of somatic inhibition, many molecular and pharmacological tools exist that can

reliably distinguish between CCKBCs and PVBCs, making this question experimentally tractable.

Similar to somatic inhibition, inhibitory synapses formed onto the proximal apical dendrites in SR, the other PN domain in which *Npas4* regulates inhibitory synapses, are made predominantly by two interneuron subtypes, the cholecystokinin-expressing Schaffer Collateral-Associated IN (SCA) and the parvalbumin-expressing bistratified IN. Unfortunately, while much is known about the functional role of dendritic inhibition in general, the specific roles of individual dendrite-targeting interneuron subtypes are not as well-understood as their soma-targeting counterparts. Furthermore, less is known about the receptor and channel expression profiles of dendritic interneurons in the hippocampus, resulting in fewer pharmacological and molecular tools with which to target these cell types. Currently, therefore, answering this question requires a candidate-based approach in which strength of inhibition between individual INs and PNs is recorded and subtypes identified post hoc based on morphology, physiology, and molecular expression profiles.

The experiments described in Chapter 2 take advantage of electrophysiological, pharmacological, and molecular tools to address the question of how activity-dependent *Npas4* expression regulates somatic inhibition by CCKBCs and PVBCs onto CA1 PNs. The results show that *Npas4* exclusively regulates somatic inhibition by CCKBCs, while PVBC synapses are unaffected. This finding suggests many interesting hypotheses regarding how activity-dependent *Npas4* expression might shape activity patterns and plasticity. Indeed, we demonstrate that this *Npas4*-mediated recruitment of somatic CCKBC synapses results in an increase in the proportion of somatic inhibition received

by a PN that is susceptible to DSI. The next steps are to 1) work out the mechanistic link between *Npas4* expression and recruitment of CCKBC synapses, 2) to understand the complete consequences of CCKBC synapse recruitment on hippocampal circuit function, including how place cell activity might be shaped by this phenotype, and 3) to investigate the interneuron subtypes that make the synapses regulated by *Npas4* expression in the proximal dendrites. Hypotheses and preliminary data toward these goals are discussed in Chapter 3.

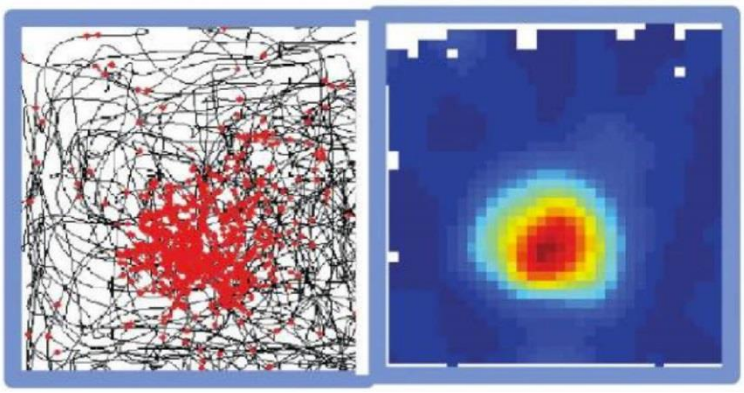

Figure 1.1 Place cell in the rodent hippocampus

An example of a hippocampal pyramidal cell showing place cell activity. (Left) The black trace shows a rat's trajectory throughout a square arena, with spike locations shown as red dots. (Right) Rate map of the cell's firing with red showing high activity and blue showing low activity. Reprinted with permission from Moser, M. B., Rowland, D. C., & Moser, E. I. (2015). Place cells, grid cells, and memory. Cold Spring Harb Perspect Biol, 7(2), a021808. doi:10.1101/cshperspect.a021808.

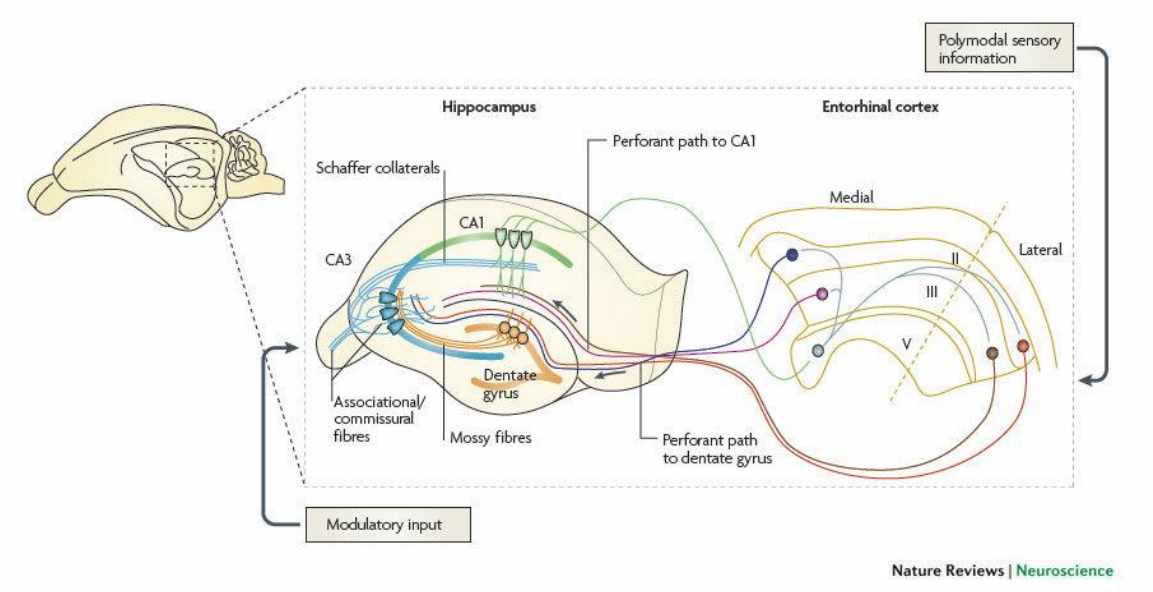

Figure 1.2 The "tri-synaptic loop" of the rodent hippocampus.

The entorhinal cortex (EC) is the recipient of a large portion of the neocortical inputs to the hippocampal formation, and in turn it provides the major input to the hippocampus. The axons of its layer II principle cells form the perforant path, which provides the predominant input to the DG and also projects to CA3, while the layer III principle cells send a direct projection to CA1. The principle cells of the dentate gyrus (DG), the granule cells, then send their mossy fiber axons to the PNs of CA3, which in turn provide the second major input to the PNs of CA1 via the Schaffer Collateral pathway. This circuit from the EC to DG to CA3 to CA1 composes the hippocampal "tri-synaptic loop". The PNs of region CA1 form the major output of the hippocampus. Reprinted with permission from Neves, G., Cooke, S. F., & Bliss, T. V. (2008). Synaptic plasticity, memory and the hippocampus: a neural network approach to causality. Nat Rev Neurosci, 9(1), 65-75. doi:10.1038/nrn2303.

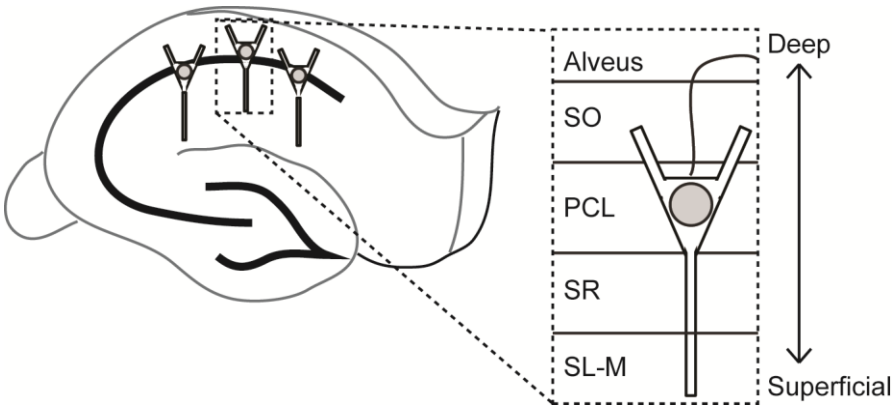

Figure 1.3 Layers of hippocampal area CA1

The principal cell layer in CA1, the pyramidal cell layer (PCL), is tightly packed with somata of PNs. The layer located deep to the PCL, called stratum oriens (SO), is home to several types of local INs, the basal dendrites of the CA1 PNs, and one portion of the Schaffer Collateral projection from CA3. Located deep to SO is the alveus, containing the axons from the CA1 PNs making their way out of the hippocampus. Superficial to the PCL, where the proximal apical dendrites of PNs are located, is stratum radiatum (SR). SR contains the other portion of the CA3 to CA1 Schaffer Collateral connection, which synapses in SR on the proximal apical dendrites of CA1 PNs, as well as on local INs. Next to SR and forming the most superficial layer of the CA1 region is stratum lacunosum-moleculare (SLM), home to the perforant path projections from the EC directly to CA1, which synapse on the distal apical dendrites of CA1 PNs, as well as local INs.

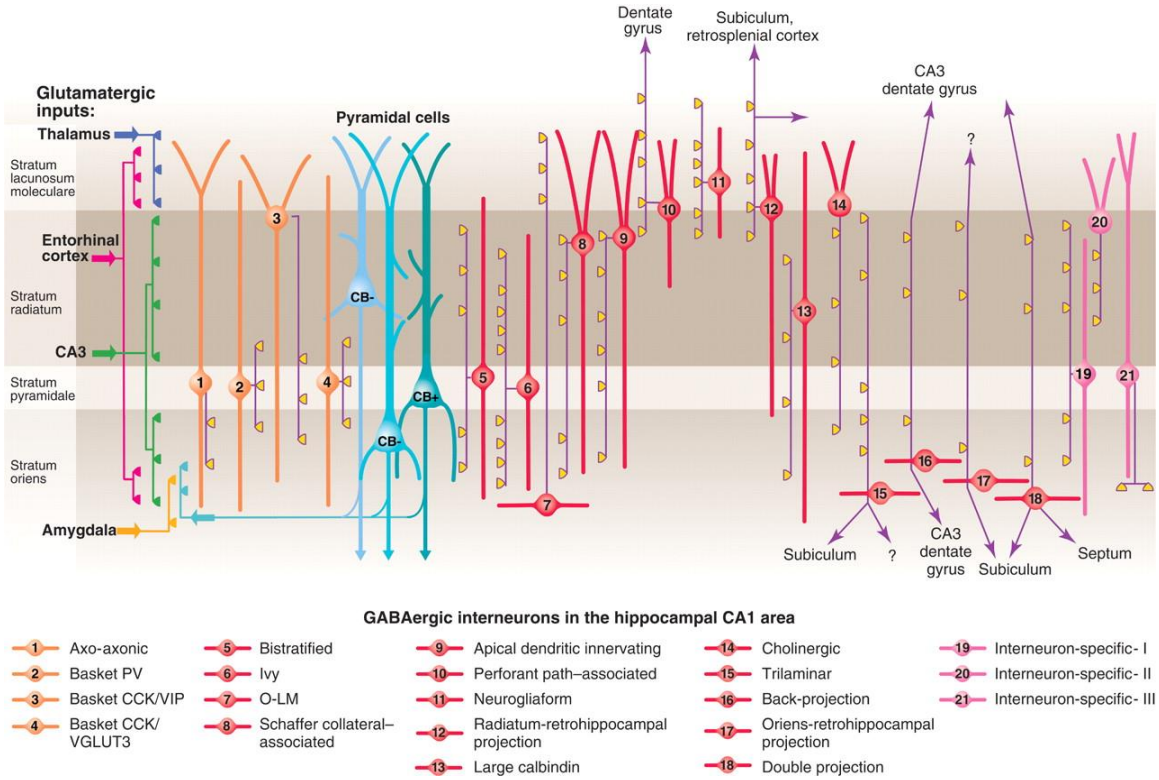

Figure 1.4 Interneuron diversity in the hippocampus

Interneurons form an extremely diverse group; there are over 20 unique interneuron subtypes in the hippocampus alone. This subtype classification is based on morphological, immunohistochemical, physiological, and pharmacological features, all of which contribute to the specialized role each subtype plays within the local circuit Functional distinctions between interneuron subtypes begin with which of four postsynaptic PN compartment they contact (soma, axon initial segment, proximal dendrites, or distal dendrites). GABAergic synapses provide the sole input to the somata and axon initial segments of PNs, while PN dendrites are innervated both by local GABAergic input and excitatory input from the entorhinal cortex, upstream hippocampal subregions, and thalamus. From Klausberger, T. and Somogyi, P. (2008). Neuronal diversity and temporal dynamics: the unity of hippocampal circuit operations. Science 321(5885):53-57. Reprinted with permission from AAAS.

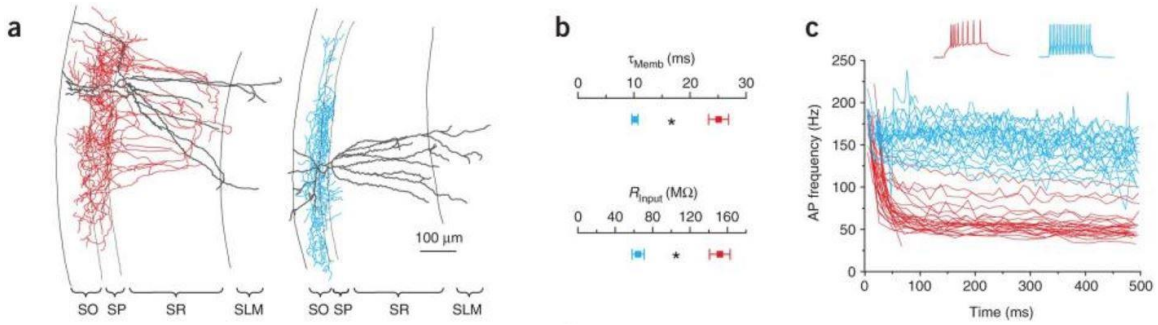

Figure 1.5 Morphology and intrinsic physiological signatures of CCK and PV basket cells

Somatic inhibition in CA1 is provided by cholecystokinin-expressing and parvalbumin-expressing basket cells (CCKBCs and PVBCs, respectively) that can be differentiated by their intrinsic physiological properties. (A) Both CCKBCs (red) and PVBCs (blue) have dense axon ramifying along the pyramidal cell layer and dendrites that extend into stratum radiatum and stratum Lacunosum-moleculare. (B) PVBCs have very fast membrane time constants (~10 ms) and low input resistance (Glickfeld and Scanziani, 200), while CCKBCs have slower time constants (~25 ms) and higher input resistance (Glickfeld and Scanziani, 2006; Cea-del Rio et al., 2010). (C) PVBCs fire fast, non-accommodating trains of action potentials (APs) in response to depolarizing current injections. CCKBCs, on the other hand, fire moderately-paced, strongly accommodating APs. Reprinted with permission from Glickfeld, L. L., & Scanziani, M. (2006). Distinct timing in the activity of cannabinoid-sensitive and cannabinoid-insensitive basket cells. Nat Neurosci, 9(6), 807-815. doi:10.1038/nn1688.

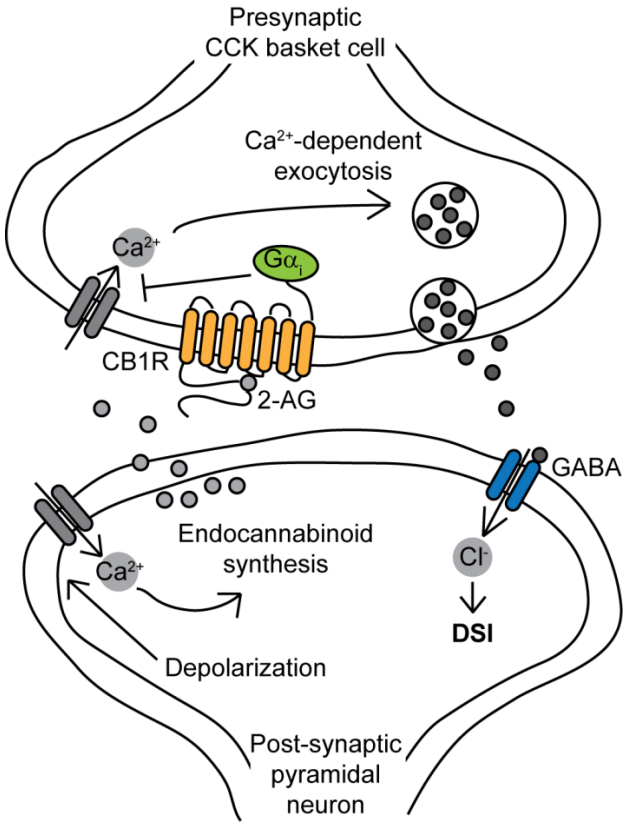

Figure 1.6 Depolarization-induced suppression of inhibition (DSI) at CCKBC-PN synapse

When a postsynaptic PN is active, it synthesizes and releases endogenous cannabinoids, which signal retrogradely to the presynaptic CCKBC bouton by binding CB1Rs. CB1R activation results in antagonism of synaptic voltage-gated calcium channels, causing a temporary reduction in GABAergic release from the synapse, a form of short-term plasticity known as depolarization-induced suppression of inhibition (DSI). This form of short term inhibitory plasticity is expressed at CCKBC-PN synapses in the hippocampus (Katona et al., 1999; Wilson and Nicoll, 2001; Glickfeld and Scanziani, 2006; Neu et al., 2007).

Gene	Full Name	Neuron-Specific	mRNA Peak Time[a]	Cellular Function	Roles in Synaptic Plasticity	Learning and Memory Paradigm Tested
Fos	FBJ osteosarcoma oncogene	No	Early	Transcription factor	LTP	Morris water maze; fear conditioning
Zif268 (*Egr1*)	Early growth response 1	No	Early	Transcription factor	LTP	Morris water maze; conditioned taste aversion; objection recognition
Cebp	CCAAT/enhancer binding protein	No	Late	Transcription factor	LTF[b], LTP	Inhibitory avoidance; Morris water maze
Npas4	Neuronal PAS domain protein 4	Yes	Early	Transcription factor	Not characterized	Fear conditioning
Nr4a1 (*Nur77*)	Nuclear receptor subfamily 4 group A member 1	No	Early	Transcription factor	LTP	Fear conditioning
Arc (*Arg3.1*)	Activity-regulated cytoskeleton-associated protein	No	Early	Cytoskeletal associated protein	LTP, LTD, Homeostatic scaling	Morris water maze; fear conditioning; objection recognition
Bdnf	Brain-derived neurotrophic factor	No	Late	Neurotrophic factors	LTP	Morris water maze; fear conditioning
Narp (*Nptx2*)	Neuronal pentraxin 2	No	Late	Secreted proteins	Homeostatic scaling	Food devaluation; extinction of conditioned place preference
Homer1a	Homer scaffolding protein 1	No	Late	Synaptic scaffolding proteins	Homeostatic scaling	Morris water maze
Cpg15	Neuritin 1	No	Late	Extracellular membrane-anchored proteins	Not characterized	Morris water maze; fear conditioning

Figure 1.7 Charateristics of some well-known IEGs

The immediate-early gene (IEG) family is the first group of genes to be transcribed after a neuron is active. This group of genes includes transcription factors, cytoskeletal proteins, growth factors, metabolic enzymes, and signal transduction pathway components. Many of these genes are associated with plasticity and are rapidly and selectively upregulated in brain regions associated with learning and memory, such as the hippocampus. Reprinted with permission from Sun, X., & Lin, Y. (2016). Npas4: Linking Neuronal Activity to Memory. Trends Neurosci, 39(4), 264-275. doi:10.1016/j.tins.2016.02.003.

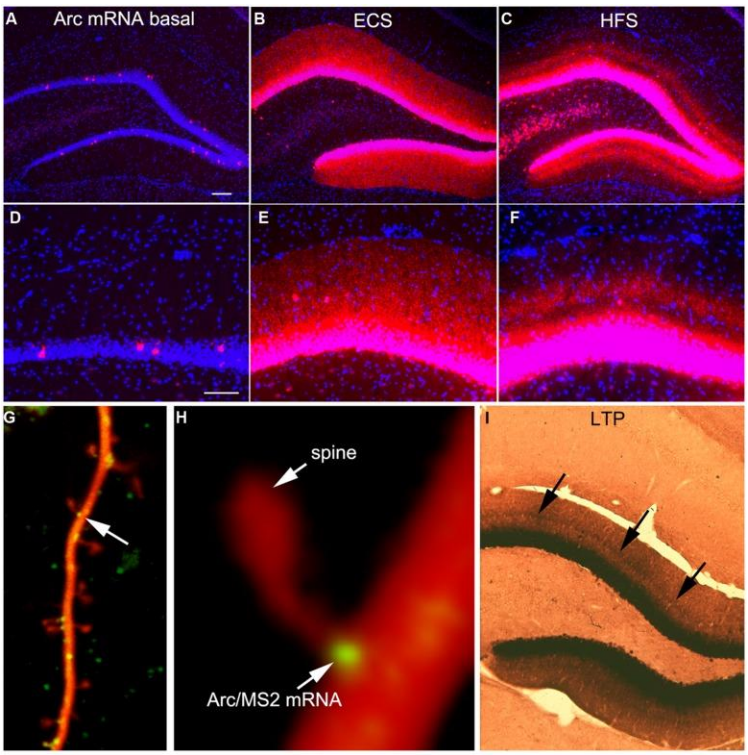

Figure 1.8 Activity-dependent expression of *Arc* mRNA and trafficking to dendrites and spines

The IEG *Arc* is expressed in neurons following neural activity. Its mRNA can be observed in nuclei within minutes of neural activity and quickly translocates into the cytoplasm and subsequently the dendrites of active cells, where it can be observed in spines near active synapses. (A) *Arc* mRNA (red) in the rat dentate gyrus under basal conditions. (B) *Arc* mRNA two hours after electroconvulsive seizure. (C) Localization of *Arc* mRNA to the middle molecular layer of the dentate gyrus after high-frequency stimulation of the medial perforant path. (D-F) High magnification images of A-C. (G) *Arc* mRNA particles in a dendrite from a cultured neuron. (H) Higher magnification view of an *Arc* particle at the base of a dendritic spine. (I) *In situ* hybridization for *Arc* mRNA two hours after LTP induction by 20 high frequency trains. Reprinted with permission from Steward, O., Farris, S., Pirbhoy, P. S., Darnell, J., & Driesche, S. J. (2014). Localization and local translation of Arc/Arg3.1 mRNA at synapses: some observations and paradoxes. Front Mol Neurosci, 7, 101. doi:10.3389/fnmol.2014.00101

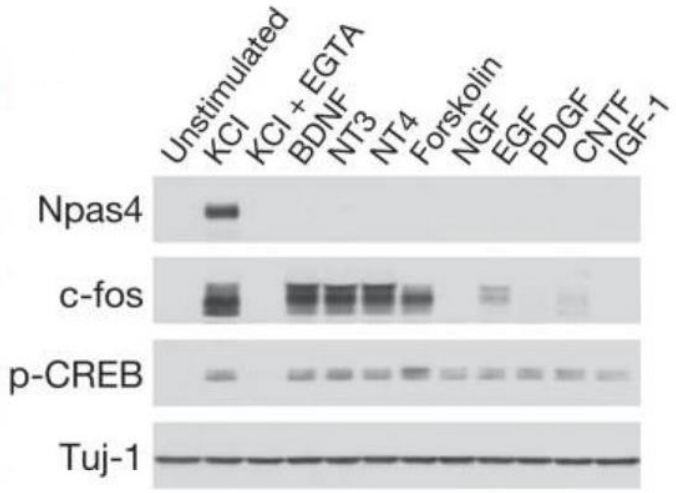

Figure 1.9 Npas4 is selectively expressed in response to calcium influx

In the brain, *Npas4* is expressed solely in response to increased intracellular calcium associated with neural activity. This is in contrast to other IEGs, including *c-fos*, that can be induced by cytokines, growth factors, neurotrophins, and elevated protein kinase A activity. Reprinted with permission from Lin, Y., Bloodgood, B. L., Hauser, J. L., Lapan, A. D., Koon, A. C., Kim, T. K., . . . Greenberg, M. E. (2008). Activity-dependent regulation of inhibitory synapse development by npas4. Nature, 455(7217), 1198-1204. doi:10.1038/nature07319.

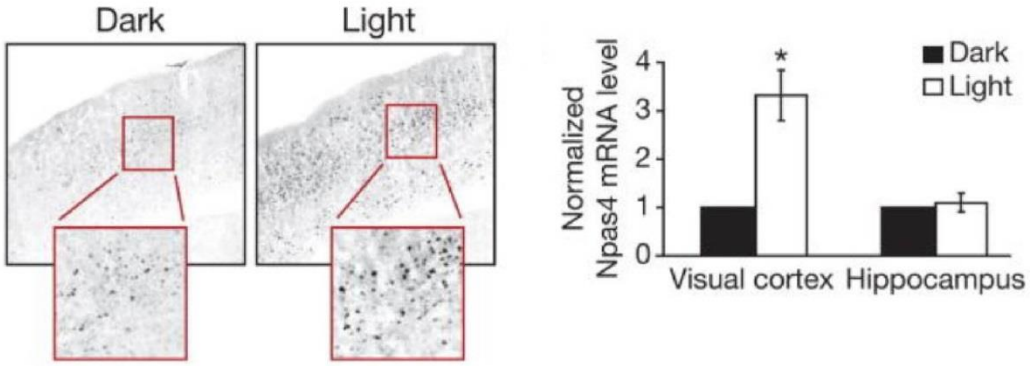

Figure 1.10 *Npas4* is induced in the mouse visual cortex in response to visual stimuli

In vivo, *Npas4* is expressed in brain regions in response to salient stimuli. (Right) In the visual cortex of dark-reared mice, *Npas4* mRNA is expressed in neurons after exposure to visual stimuli. (Left) Quantification of *Npas4* mRNA levels in visual cortex and hippocampus after exposure to light. Reprinted with permission from Lin, Y., Bloodgood, B. L., Hauser, J. L., Lapan, A. D., Koon, A. C., Kim, T. K., . . . Greenberg, M. E. (2008). Activity-dependent regulation of inhibitory synapse development by npas4. Nature, 455(7217), 1198-1204. doi:10.1038/nature07319.

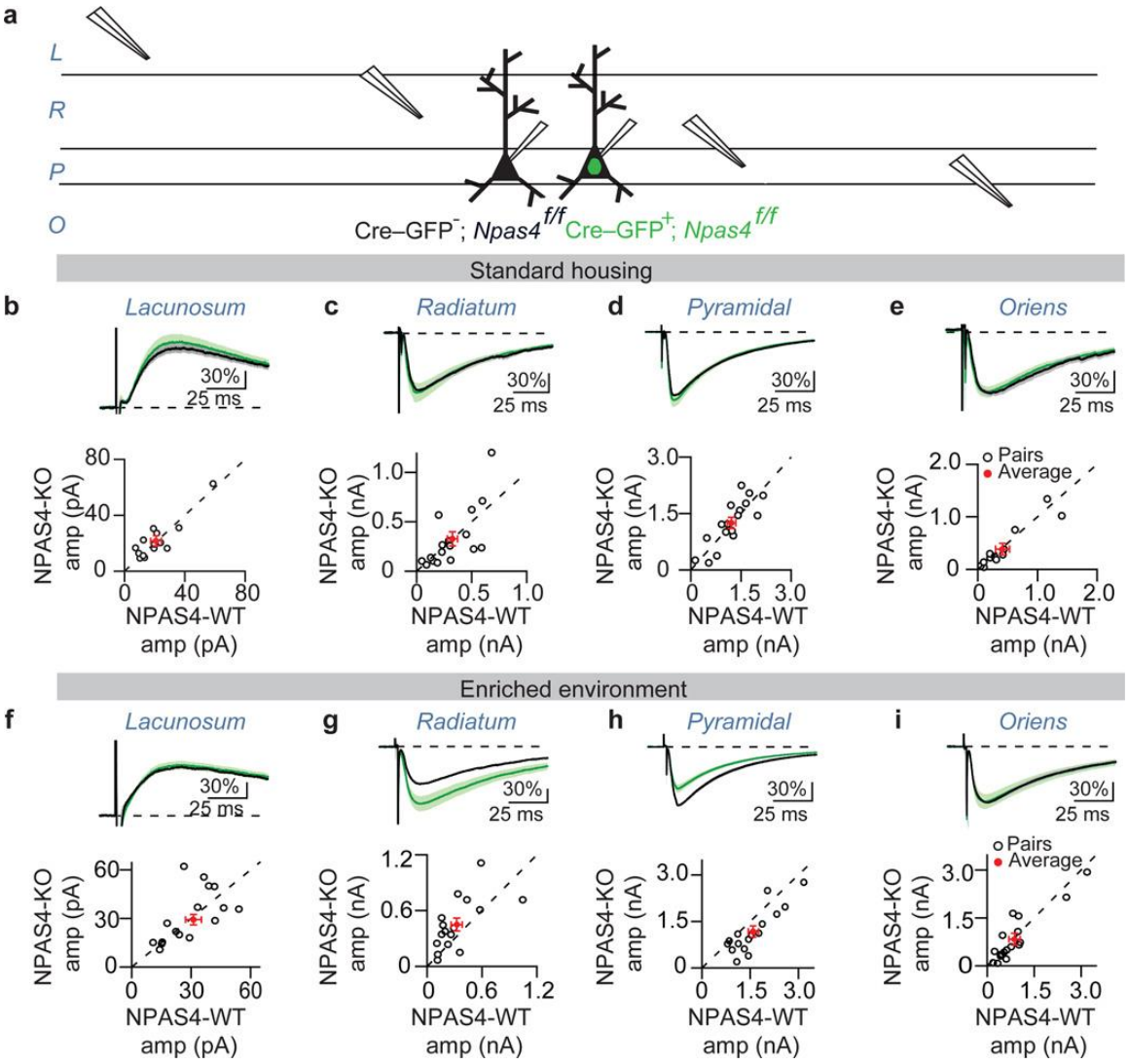

Figure 1.11 *Npas4* regulates inhibition in a domain-specific manner in CA1

(A) Acute hippocampal slices were made from *Npas4* conditional knock out mice in which a sparse population of knockout (KO) neurons was generated with expression of a Cre virus. Inhibitory postsynaptic currents (IPSCs) were evoked in all layers across the somato-dendritic axis in CA1. (B-E) In mice from standard housing, in which *Npas4* expression is almost absent, wild type (WT) and *Npas4* KO pyramidal neurons have similar amplitude IPSCs evoked by stimulating in all layers across the somato-dendritic axis in CA1. (F-I) In mice housed in an enriched environment, stimulation in the PCL generates smaller IPSCs in *Npas4* KO neurons than in WT PNs. By contrast, stimulation in SR generates larger IPSCs in *Npas4* KO neurons relative to WT neurons. No difference was detected when slices were stimulated in SO or SLM. Reprinted with permission from Bloodgood, B. L., Sharma, N., Browne, H. A., Trepman, A. Z., & Greenberg, M. E. (2013). The activity-dependent transcription factor npas4 regulates domain-specific inhibition. Nature, 503(7474), 121-125. doi:10.1038/nature12743

Figure 1.12 Putative *Npas4* target genes

As a transcription factor, *Npas4* has the potential to regulate numerous downstream target genes and affect many aspects of cell biology. (A) 270 unique genes were identified via DNA microarray that were upregulated or downregulated in control neurons relative to neurons in which *Npas4* was knocked down. (B) These potential *Npas4* target genes include other IEGs, other transcription factors, channel proteins, kinases, phosphatases, and synaptic proteins involved in ubiquitination, trafficking, and receptor endocytosis, and over 90 genes that are as of yet uncharacterized. (C) BDNF expression is reduced by *Npas4* knockdown. (D) BDNF levels are constitutively reduced in *Npas4* knockout mice relative to wildtype littermates. (E) NPAS4 interacts with two BDNF promoters in stimulated cells. Reprinted with permission from Lin, Y., Bloodgood, B. L., Hauser, J. L., Lapan, A. D., Koon, A. C., Kim, T. K., . . . Greenberg, M. E. (2008). Activity-dependent regulation of inhibitory synapse development by npas4. Nature, 455(7217), 1198-1204. doi:10.1038/nature07319.

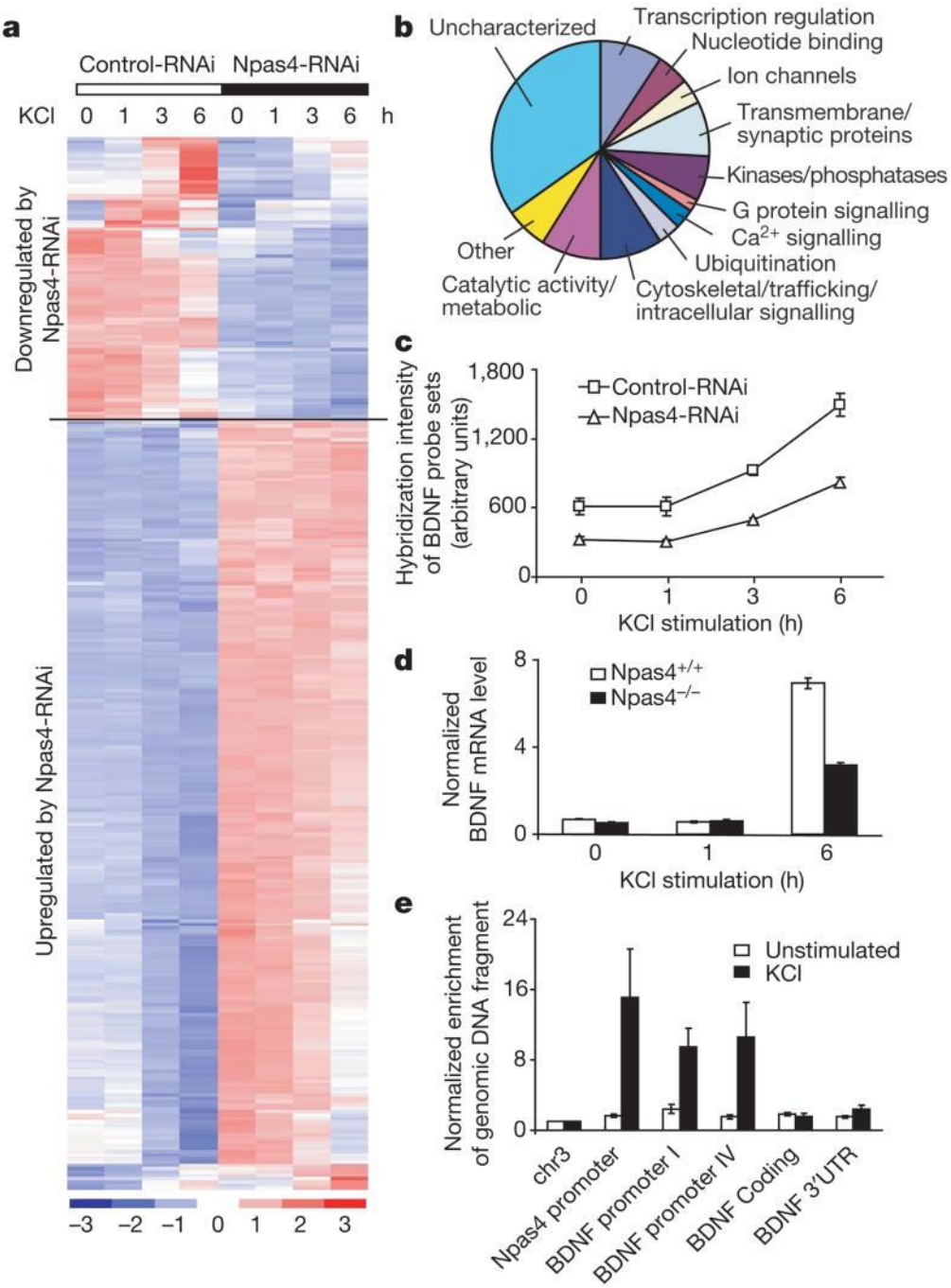
a
Control-RNAi
Npas4-RNAi
KCl 0 1 3 6 0 1 3 6 h
Downregulated by Npas4-RNAi
Upregulated by Npas4-RNAi
−3 −2 −1 0 1 2 3
b
Uncharacterized
Transcription regulation
Nucleotide binding
Ion channels
Transmembrane/ synaptic proteins
Kinases/phosphatases
G protein signalling
Ca2+ signalling
Ubiquitination
Cytoskeletal/trafficking/ intracellular signalling
Other
Catalytic activity/ metabolic
c
Hybridization intensity of BDNF probe sets (arbitrary units)
1,800
1,200
600
0
Control-RNAi
Npas4-RNAi
0 1 3 6
KCl stimulation (h)
d
Normalized BDNF mRNA level
8
4
0
Npas4+/+
Npas4−/−
0 1 6
KCl stimulation (h)
e
Normalized enrichment of genomic DNA fragment
24
16
8
0
Unstimulated
KCl
chr3
Npas4 promoter
BDNF promoter I
BDNF promoter IV
BDNF Coding
BDNF 3′UTR

References

Alberini, C. M. (2009). Transcription factors in long-term memory and synaptic plasticity. Physiol Rev, 89(1), 121-145. doi:10.1152/physrev.00017.2008

Ali, A.B., Bannister, A.P., & Thompson, A.M. (1999). IPSPs elicited in CA1 pyramidal cells by putative basket cells in slices of adult rat hippocampus. Eur. J. Neurosci. 11: 1741-1753.

Ali, A. B., & Todorova, M. (2010). Asynchronous release of GABA via tonic cannabinoid receptor activation at identified interneuron synapses in rat CA1. Eur J Neurosci, 31(7), 1196-1207. doi:10.1111/j.1460-9568.2010.07165.x

Amaral, D. and Lavenex, P. (2006) Hippocampal Neuroanatomy. In: Andersen, P., Morris, R., Amaral, D., Bliss, T. and O'Keefe, J., Eds., The Hippocampus Book, Oxford University Press, Oxford, 37-115.

Anderson, J. S., Carandini, M., & Ferster, D. (2000). Orientation tuning of input conductance, excitation, and inhibition in cat primary visual cortex. J Neurophysiol, 84(2), 909-926. doi:10.1152/jn.2000.84.2.909

Arancibia-Carcamo, I. L., Yuen, E. Y., Muir, J., Lumb, M. J., Michels, G., Saliba, R. S., . . . Moss, S. J. (2009). Ubiquitin-dependent lysosomal targeting of GABA(A) receptors regulates neuronal inhibition. Proc Natl Acad Sci U S A, 106(41), 17552-17557. doi:10.1073/pnas.0905502106

Ashley, J., Cordy, B., Lucia, D., Fradkin, L. G., Budnik, V., & Thomson, T. (2018). Retrovirus-like Gag Protein Arc1 Binds RNA and Traffics across Synaptic Boutons. Cell, 172(1-2), 262-274.e211. doi:10.1016/j.cell.2017.12.022

Atallah, B. V., & Scanziani, M. (2009). Instantaneous modulation of gamma oscillation frequency by balancing excitation with inhibition. Neuron, 62(4), 566-577. doi:10.1016/j.neuron.2009.04.027

Baimbridge, K.G., Peet, M.J., McLennan, H., & Church, J. (1991) Bursting response to current-evoked depolarization in rat CA1 pyramidal neurons is correlated with Lucifer yellow dye coupling but not with the presence of calbindin-D28K. Synapse 7(4): 269-277.

Bartos, M., Vida, I., & Jonas, P. (2007). Synaptic mechanisms of synchronized gamma oscillations in inhibitory interneuron networks. Nat Rev Neurosci, 8(1), 45-56. doi:10.1038/nrn2044

Bartos, M., Alle, H., & Vida, I. (2011). Role of microcircuit structure and input integration in hippocampal interneuron recruitment and plasticity. Neuropharmacology 60(5): 730-739.

Bloodgood, B. L., Sharma, N., Browne, H. A., Trepman, A. Z., & Greenberg, M. E. (2013). The activity-dependent transcription factor npas4 regulates domain-specific inhibition. Nature, 503(7474), 121-125. doi:10.1038/nature12743

Bragin, A., Jandó, G., Nádasdy, Z., Hetke, J., Wise, K, & Buzsáki, G. (1995). Gamma (40-100 Hz) oscillation in the hippocampus of the behaving rat. J. Neurosci. 15(1 Pt 1): 47-60.

Brodal, A. (1947). The hippocampus and the sense of smell: A review. Brain 7(2), 179-222.

Bu, D. F., Erlander, M. G., Hitz, B. C., Tillakaratne, N. J., Kaufman, D. L., Wagner-McPherson, C. B., . . . Tobin, A. J. (1992). Two human glutamate decarboxylases, 65-kDa GAD and 67-kDa GAD, are each encoded by a single gene. Proc Natl Acad Sci U S A, 89(6), 2115-2119.

Bucurenciu, I., Kulik, A., Schwaller, B., Frotscher, M., & Jonas, P. (2008). Nanodomain coupling between Ca2+ channels and Ca2+ sensors promotes fast and efficient transmitter release at a cortical GABAergic synapse. Neuron, 57(4), 536-545. doi:10.1016/j.neuron.2007.12.026

Buhl, E.H., Halasy, K., Somogyi, P. (1994). Diverse sources of hippocampal unitary inhibitory postsynaptic potentials and the number of synaptic release sites. Nature 368(6474): 823-828.

Buzsaki, G., Leung, L. W., & Vanderwolf, C. H. (1983). Cellular bases of hippocampal EEG in the behaving rat. Brain Res, 287(2), 139-171.

Buzsáki, G. and Draguhn, A. (2004). Neuronal oscillations in cortical networks. Science 304(5679): 1926-1929.

Cardin, J. A., Carlen, M., Meletis, K., Knoblich, U., Zhang, F., Deisseroth, K., . . . Moore, C. I. (2009). Driving fast-spiking cells induces gamma rhythm and controls sensory responses. Nature, 459(7247), 663-667. doi:10.1038/nature08002

Carlson, G., Wang, Y., & Alger, B. E. (2002). Endocannabinoids facilitate the induction of ltp in the hippocampus. Nat Neurosci, 5(8), 723-724. doi:10.1038/nn879

Cea-del Rio, C. A., Lawrence, J.J., Tricoire, L., Erdelyi, F., Szabo, G., McBain, C.J. (2010). M3 muscarinic acetylcholine receptor expression confers differential cholinergic modulation to neurochemically distinct hippocampal basket cell subtypes. J Neurosci 30(17): 6011-6024.

Chen, X., & Johnston, D. (2005). Constitutively active G-protein-gated inwardly rectifying K+ channels in dendrites of hippocampal CA1 pyramidal neurons. J Neurosci, 25(15), 3787-3792. doi:10.1523/jneurosci.5312-04.2005

Chen, J. L., Lin, W. C., Cha, J. W., So, P. T., Kubota, Y., & Nedivi, E. (2011). Structural basis for the role of inhibition in facilitating adult brain plasticity. Nat Neurosci, 14(5), 587-594. doi:10.1038/nn.2799

Chen, J. L., Villa, K. L., Cha, J. W., So, P. T., Kubota, Y., & Nedivi, E. (2012). Clustered dynamics of inhibitory synapses and dendritic spines in the adult neocortex. Neuron, 74(2), 361-373. doi:10.1016/j.neuron.2012.02.030

Chowdhury, S., Shepherd, J. D., Okuno, H., Lyford, G., Petralia, R. S., Plath, N., . . . Worley, P. F. (2006). Arc/Arg3.1 interacts with the endocytic machinery to regulate AMPA receptor trafficking. Neuron, 52(3), 445-459. doi:10.1016/j.neuron.2006.08.033

Cobb, S.R., Buhl, E.H., Halasy, K., Paulsen, O., Somogyi, P. (1995). Synchronization of neuronal activity in hippocampus by individual GABAergic interneurons. Nature 378(6552): 75-78.

Coutellier, L., Beraki, S., Ardestani, P. M., Saw, N. L., & Shamloo, M. (2012). Npas4: a neuronal transcription factor with a key role in social and cognitive functions relevant to developmental disorders. PLoS One, 7(9), e46604. doi:10.1371/journal.pone.0046604

Csicsvari, J., Jamieson, B., Wise, K. D., & Buzsaki, G. (2003). Mechanisms of gamma oscillations in the hippocampus of the behaving rat. Neuron, 37(2), 311-322.

Danielson, N. B., Zaremba, J. D., Kaifosh, P., Bowler, J., Ladow, M., & Losonczy, A. (2016). Sublayer-specific coding dynamics during spatial navigation and learning in hippocampal area CA1. Neuron, 91(3), 652–665. http://doi.org/10.1016/j.neuron.2016.06.020

Daw, M. I., Tricoire, L., Erdelyi, F., Szabo, G., & McBain, C. J. (2009). Asynchronous transmitter release from cholecystokinin-containing inhibitory interneurons is widespread and target-cell independent. J Neurosci, 29(36), 11112-11122. doi:10.1523/jneurosci.5760-08.2009

Dicther, M. and Spencer, W.A. (1969). Penicillin-induced interictal discharges from the cat hippocampus. II. Mechanisms underlying origin and restriction. J Neurophysiol. 32(5): 663-687.

Doischer, D., Hosp, J. A., Yanagawa, Y., Obata, K., Jonas, P., Vida, I., & Bartos, M. (2008). Postnatal differentiation of basket cells from slow to fast signaling devices. J Neurosci, 28(48), 12956-12968. doi:10.1523/jneurosci.2890-08.2008

Dupuy, S. T., & Houser, C. R. (1996). Prominent expression of two forms of glutamate decarboxylase in the embryonic and early postnatal rat hippocampal formation. J Neurosci, 16(21), 6919-6932.

Emri, Z., Antal, K., Gulyás, A.I., Megías, M., Freund, T.F. (2001). Electrotonic profile and passive propagation of synaptic potentials in three subpopulations of hippocampal CA1 interneurons. Neuroscience 104(4): 1013-1026.

Fang, C., Deng, L., Keller, C. A., Fukata, M., Fukata, Y., Chen, G., & Luscher, B. (2006). GODZ-mediated palmitoylation of GABA(A) receptors is required for normal assembly and function of GABAergic inhibitory synapses. J Neurosci, 26(49), 12758-12768. doi:10.1523/jneurosci.4214-06.2006

Fanselow, M. and Dong, H. (2010). Are the dorsal and ventral hippocampus functionally distinct structures? Neuron 65(1): 7-19.

Feldman, D. E. (2009). Synaptic Mechanisms for Plasticity in Neocortex. Annual review of neuroscience, 32, 33-55. doi:10.1146/annurev.neuro.051508.135516

Fellman, D. and Van Essen, D. (1991). Distributed hierarchical processing in the primate cerebral cortex. Cereb. Cortex 1(1): 1-47.

Freund, T.F. and Buzsáki, G. (1996). Interneurons of the hippocampus. Hippocampus 6(4): 347-470.

Garner, A. R., Rowland, D. C., Hwang, S. Y., Baumgaertel, K., Roth, B. L., Kentros, C., & Mayford, M. (2012). Generation of a synthetic memory trace. Science, 335(6075), 1513-1516. doi:10.1126/science.1214985

Glausier, J. R., & Lewis, D. A. (2011). Selective pyramidal cell reduction of GABA(A) receptor alpha1 subunit messenger RNA expression in schizophrenia. Neuropsychopharmacology, 36(10), 2103-2110. doi:10.1038/npp.2011.102

Glickfeld, L. L., & Scanziani, M. (2006). Distinct timing in the activity of cannabinoid-sensitive and cannabinoid-insensitive basket cells. Nat Neurosci, 9(6), 807-815. doi:10.1038/nn1688

Graves, A. R., Moore, S. J., Bloss, E. B., Mensh, B. D., Kath, W. L., & Spruston, N. (2012). Hippocampal pyramidal neurons comprise two distinct cell types that are countermodulated by metabotropic receptors. Neuron, 76(4), 776–789. http://doi.org/10.1016/j.neuron.2012.09.036

Green J. and Arduini A. (1954) Hippocampal electrical activity in arousal. J. Neurophysiol. 17(6): 533-557.

Green, J. and Adey, W. (1956) Electrophysiological studies of hippocampal connections and excitability. Electroenceph. Clin. Neurophysiol. 8: 245 262.

Gulyas, A. I., Megias, M., Emri, Z., & Freund, T. F. (1999). Total number and ratio of excitatory and inhibitory synapses converging onto single interneurons of different types in the CA1 area of the rat hippocampus. J Neurosci, 19(22), 10082-10097.

Gulyas, A. I., Szabo, G. G., Ulbert, I., Holderith, N., Monyer, H., Erdelyi, F., . . . Hajos, N. (2010). Parvalbumin-containing fast-spiking basket cells generate the field potential oscillations induced by cholinergic receptor activation in the hippocampus. J Neurosci, 30(45), 15134-15145. doi:10.1523/jneurosci.4104-10.2010

Guzowski, J. F., McNaughton, B. L., Barnes, C. A., & Worley, P. F. (1999). Environment-specific expression of the immediate-early gene Arc in hippocampal neuronal ensembles. Nat Neurosci, 2(12), 1120-1124. doi:10.1038/16046

Haider, B., Duque, A., Hasenstaub, A. R., & McCormick, D. A. (2006). Neocortical network activity in vivo is generated through a dynamic balance of excitation and inhibition. J Neurosci, 26(17), 4535-4545. doi:10.1523/jneurosci.5297-05.2006

Halasy, K., Buhl, E.H., Lörinczi, Z., Tamás, G., Somogyi, P. (1996). Synaptic target selectivity and input of GABAergic basket and bistratified interneurons in the CA1 area of the rat hippocampus. Hippocampus 6(3): 306-329.

Hartzell, A. L., Burke, S. N., Hoang, L. T., Lister, J. P., Rodriguez, C. N., & Barnes, C. A. (2013). Transcription of the Immediate-early Gene Arc in CA1 of the Hippocampus Reveals Activity Differences along the Proximodistal Axis that are Attenuated by Advanced Age. The Journal of Neuroscience 33(8), 3424–3433. http://doi.org/10.1523/JNEUROSCI.4727-12.2013

Hefft, S., & Jonas, P. (2005). Asynchronous GABA release generates long-lasting inhibition at a hippocampal interneuron-principal neuron synapse. Nat Neurosci, 8(10), 1319-1328. doi:10.1038/nn1542

Heller, E. A., Zhang, W., Selimi, F., Earnheart, J. C., Slimak, M. A., Santos-Torres, J., . . . Heintz, N. (2012). The biochemical anatomy of cortical inhibitory synapses. PLoS One, 7(6), e39572. doi:10.1371/journal.pone.0039572

Henriksen, E. J., Colgin, L. L., Barnes, C. A., Witter, M. P., Moser, M.-B., & Moser, E. I. (2010). Spatial representation along the proximodistal axis of CA1. Neuron, 68(1), 127–137. http://doi.org/10.1016/j.neuron.2010.08.042

Holmes, J. and Adey, W. (1960). Electrical activity of the entorhinal cortex during conditioned behavior. Amer. J. Physiol. 199: 741-744.

Jarsky, T., Mady, R., Kennedy, B., Spruston, N. (2008). Distribution of bursting neurons in the CA1 region and subiculum of the rat hippocampus. J. Comp. Neurol. 506(1): 535-547.

Johnston, D., and Brown, T.H. (1981). Giant synaptic potential hypothesis for epileptiform activity. Science 211: 294-297.

Jonas, P., Bischofberger, J., Fricker, D., & Miles, R. (2004). Interneuron Diversity series: Fast in, fast out--temporal and spatial signal processing in hippocampal interneurons. Trends Neurosci 27(1): 30-40.

Jung, M. and McNaughton, B. (1993). Spatial selectivity of unit activity in the hippocampal granular layer. Hippocampus 3(2): 165-182.

Jung, M., Wiener, S., and McNaughton, B. (1994). Comparison of spatial firing characteristics of units in dorsal and ventral hippocampus of the rat. J. Neurosci. 14(12): 7347-7356.

Kaliszewska, A., & Kossut, M. (2015). Npas4 expression in two experimental models of the barrel cortex plasticity. Neural Plast, 2015, 175701. doi:10.1155/2015/175701

Katona, I., Sperlagh, B., Sik, A., Kafalvi, A., Vizi, E. S., Mackie, K., & Freund, T. F. (1999). Presynaptically located CB1 cannabinoid receptors regulate GABA release from axon terminals of specific hippocampal interneurons. J Neurosci, 19(11), 4544-4558.

Keck, T., Scheuss, V., Jacobsen, R. I., Wierenga, C. J., Eysel, U. T., Bonhoeffer, T., & Hubener, M. (2011). Loss of sensory input causes rapid structural changes of inhibitory neurons in adult mouse visual cortex. Neuron, 71(5), 869-882. doi:10.1016/j.neuron.2011.06.034

Keller, C. A., Yuan, X., Panzanelli, P., Martin, M. L., Alldred, M., Sassoe-Pognetto, M., & Luscher, B. (2004). The gamma2 subunit of GABA(A) receptors is a substrate for palmitoylation by GODZ. J Neurosci, 24(26), 5881-5891. doi:10.1523/jneurosci.1037-04.2004

Kjelstrup, K., Tuvnes, F., Steffenach, H., Murison, R., Moser, E., Moser, M. (2002). Reduced fear expression after lesions of the ventral hippocampus. Proceedings of the National Academy of Science 99(16): 10825-10830.

Klausberger, T., Marton, L. F., O'Neill, J., Huck, J. H., Dalezios, Y., Fuentealba, P., . . . Somogyi, P. (2005). Complementary roles of cholecystokinin- and parvalbumin-expressing GABAergic neurons in hippocampal network oscillations. J Neurosci, 25(42), 9782-9793. doi:10.1523/jneurosci.3269-05.2005

Klausberger, T. and Somogyi, P. (2008). Neuronal diversity and temporal dynamics: the unity of hippocampal circuit operations. Science 321(5885):53-57.

Knott, G. W., Quairiaux, C., Genoud, C., & Welker, E. (2002). Formation of dendritic spines with GABAergic synapses induced by whisker stimulation in adult mice. Neuron, 34(2), 265-273.

Lanahan, A., & Worley, P. (1998). Immediate-early genes and synaptic function. Neurobiol Learn Mem, 70(1-2), 37-43. doi:10.1006/nlme.1998.3836

Lee, S.-H., Marchionni, I., Bezaire, M., Varga, C., Danielson, N., Lovett-Barron, M., … Soltesz, I. (2014). Parvalbumin-Positive Basket Cells Differentiate Among Hippocampal Pyramidal Cells. Neuron, 82(5), 1129–1144. http://doi.org/10.1016/j.neuron.2014.03.034

Leuner, B., & Gould, E. (2010). Structural Plasticity and Hippocampal Function. Annual review of psychology, 61, 111-C113. doi:10.1146/annurev.psych.093008.100359

Lewis, D. A., Curley, A. A., Glausier, J. R., & Volk, D. W. (2012). Cortical parvalbumin interneurons and cognitive dysfunction in schizophrenia. Trends Neurosci, 35(1), 57-67. doi:10.1016/j.tins.2011.10.004

Li, Y., Xu, J., Liu, Y., Zhu, J., Liu, N., Zeng, W., Huang, N., Rasch, M.J., Jiang, H., Gu, X., Li, X., Luo, M., Li, C., Teng, J., Chen, J., Zeng, S., Lin, L., & Zhang, X. (2017). A distinct entorhinal cortex to hippocampal CA1 direct circuit for olfactory associative learning. Nat. Neurosci. 20(4): 559-570.

Lin, Y., Bloodgood, B. L., Hauser, J. L., Lapan, A. D., Koon, A. C., Kim, T. K., . . . Greenberg, M. E. (2008). Activity-dependent regulation of inhibitory synapse development by npas4. Nature, 455(7217), 1198-1204. doi:10.1038/nature07319

Lisman, J., & Buzsaki, G. (2008). A neural coding scheme formed by the combined function of gamma and theta oscillations. Schizophr Bull, 34(5), 974-980. doi:10.1093/schbul/sbn060

Liu, X., Ramirez, S., Pang, P. T., Puryear, C. B., Govindarajan, A., Deisseroth, K., & Tonegawa, S. (2012). Optogenetic stimulation of a hippocampal engram activates fear memory recall. Nature, 484(7394), 381-385. doi:10.1038/nature11028

Loh, K. H., Stawski, P. S., Draycott, A. S., Udeshi, N. D., Lehrman, E. K., Wilton, D. K., . . . Ting, A. Y. (2016). Proteomic Analysis of Unbounded Cellular Compartments: Synaptic Clefts. Cell, 166(5), 1295-1307.e1221. doi:10.1016/j.cell.2016.07.041

Luscher, B., Fuchs, T., & Kilpatrick, C. L. (2011). GABAA receptor trafficking-mediated plasticity of inhibitory synapses. Neuron, 70(3), 385-409. doi:10.1016/j.neuron.2011.03.024

Lytton, W.W. and Sejnowski, T.J. (1991). Simulations of cortical pyramidal neurons synchronized by inhibitory interneurons. J. Neurophysiol. 66(3): 1059-1079.

Mann, E. O., Suckling, J. M., Hajos, N., Greenfield, S. A., & Paulsen, O. (2005). Perisomatic feedback inhibition underlies cholinergically induced fast network oscillations in the rat hippocampus in vitro. Neuron, 45(1), 105-117. doi:10.1016/j.neuron.2004.12.016

Maroso, M., Szabo, G. G., Kim, H. K., Alexander, A., Bui, A. D., Lee, S.-H., … Soltesz, I. (2016). Cannabinoid control of learning and memory through HCN channels. Neuron, 89(5), 1059–1073. http://doi.org/10.1016/j.neuron.2016.01.023

Masurkar, A.V., Srinivas, K.V., Brann, D.H., Warren, R., Lowes, D.C., Siegelbaum, S.A. (2017). Medial and lateral entorhinal cortex differentially excite deep versus superficial CA1 pyramidal neurons. Cell Reports 18(1): 148-160.

Matyas, F., Freund, T. F., & Gulyas, A. I. (2004). Convergence of excitatory and inhibitory inputs onto CCK-containing basket cells in the CA1 area of the rat hippocampus. Eur J Neurosci, 19(5), 1243-1256. doi:10.1111/j.1460-9568.2004.03225.x

Maurer, A., Vanrhoads, S., Sutherland, G., Lipa, P., and McNaughton, B. (2005). Self-motion and the origin of differential spatial scaling along the septo-temporal axis of the hippocampus. Hippocampus 15: 841-852.

McCurry, C. L., Shepherd, J. D., Tropea, D., Wang, K. H., Bear, M. F., & Sur, M. (2010). Loss of Arc renders the visual cortex impervious to the effects of sensory experience or deprivation. Nat Neurosci, 13(4), 450-457. doi:10.1038/nn.2508

McIntire, S. L., Reimer, R. J., Schuske, K., Edwards, R. H., & Jorgensen, E. M. (1997). Identification and characterization of the vesicular GABA transporter. Nature, 389(6653), 870-876. doi:10.1038/39908

Micheva, K. D., & Beaulieu, C. (1995). Neonatal sensory deprivation induces selective changes in the quantitative distribution of GABA-immunoreactive neurons in the rat barrel field cortex. J Comp Neurol, 361(4), 574-584. doi:10.1002/cne.903610403

Miles, R., Tóth, K., Gulyás, A.I., Hájos, N., & Freund, T.F. (1996). Differences between somatic and dendritic inhibition in the hippocampus. Neuron 16(4): 815-823.

Minatohara, K., Akiyoshi, M., & Okuno, H. (2015). Role of Immediate-Early Genes in Synaptic Plasticity and Neuronal Ensembles Underlying the Memory Trace. Front Mol Neurosci, 8, 78. doi:10.3389/fnmol.2015.00078

Mizuseki, K., Diba, K., Pastalkova, E., & Buzsáki, G. (2011). Hippocampal CA1 pyramidal cells form functionally distinct sublayers. Nature Neuroscience, 14(9), 1174–1181. http://doi.org/10.1038/nn.2894

Moga, D. E., Calhoun, M. E., Chowdhury, A., Worley, P., Morrison, J. H., & Shapiro, M. L. (2004). Activity-regulated cytoskeletal-associated protein is localized to recently activated excitatory synapses. Neuroscience, 125(1), 7-11. doi:10.1016/j.neuroscience.2004.02.004

Moser, E., Moser, M. B., & Andersen, P. (1993). Spatial learning impairment parallels the magnitude of dorsal hippocampal lesions, but is hardly present following ventral lesions. J Neurosci, 13(9), 3916-3925

Moser, M. B., Rowland, D. C., & Moser, E. I. (2015). Place cells, grid cells, and memory. Cold Spring Harb Perspect Biol, 7(2), a021808. doi:10.1101/cshperspect.a021808

Neu, A., Foldy, C., & Soltesz, I. (2007). Postsynaptic origin of CB1-dependent tonic inhibition of GABA release at cholecystokinin-positive basket cell to pyramidal cell synapses in the CA1 region of the rat hippocampus. J Physiol, 578(Pt 1), 233-247. doi:10.1113/jphysiol.2006.115691

Neves, G., Cooke, S. F., & Bliss, T. V. (2008). Synaptic plasticity, memory and the hippocampus: a neural network approach to causality. Nat Rev Neurosci, 9(1), 65-75. doi:10.1038/nrn2303

Nörenberg, A., Hu, H., Vida, I., Bartos, M., Jonas, P. (2010). Distinct nonuniform cable properties optimize rapid and efficient activation of fast-spiking GABAergic interneurons. Proc. Natl. Acad. Sci. 107(2): 894-899.

O'Keefe, J. (1976). Place units in the hippocampus of the freely moving rat. Experimental Neurology 51(1): 78-109.

O'Keefe, J., & Dostrovsky, J. (1971). The hippocampus as a spatial map. Preliminary evidence from unit activity in the freely-moving rat. Brain Res, 34(1), 171-175.

O'Keefe, J. and Nadel, L. (1978). The hippocampus as a cognitive map. Oxford University Press, Oxford.

Okun, M., & Lampl, I. (2008). Instantaneous correlation of excitation and inhibition during ongoing and sensory-evoked activities. Nat Neurosci, 11(5), 535-537. doi:10.1038/nn.2105

Oren, I., Hajos, N., & Paulsen, O. (2010). Identification of the current generator underlying cholinergically induced gamma frequency field potential oscillations in the hippocampal CA3 region. J Physiol, 588(Pt 5), 785-797. doi:10.1113/jphysiol.2009.180851

Papez, J. (1937) A proposed mechanism of emotion. Arch. Neurol. Psychiat. (Chic.) 38: 725-743.

Park, S., Park, J. M., Kim, S., Kim, J. A., Shepherd, J. D., Smith-Hicks, C. L., . . . Worley, P. F. (2008). Elongation factor 2 and fragile X mental retardation protein control the dynamic translation of Arc/Arg3.1 essential for mGluR-LTD. Neuron, 59(1), 70-83. doi:10.1016/j.neuron.2008.05.023

Pastuzyn, E. D., Day, C. E., Kearns, R. B., Kyrke-Smith, M., Taibi, A. V., McCormick, J., . . . Shepherd, J. D. (2018). The Neuronal Gene Arc Encodes a Repurposed Retrotransposon Gag Protein that Mediates Intercellular RNA Transfer. Cell, 172(1-2), 275-288.e218. doi:10.1016/j.cell.2017.12.024

Peebles, C. L., Yoo, J., Thwin, M. T., Palop, J. J., Noebels, J. L., & Finkbeiner, S. (2010). Arc regulates spine morphology and maintains network stability in vivo. Proc Natl Acad Sci U S A, 107(42), 18173-18178. doi:10.1073/pnas.1006546107

Plath, N., Ohana, O., Dammermann, B., Errington, M. L., Schmitz, D., Gross, C., . . . Kuhl, D. (2006). Arc/Arg3.1 is essential for the consolidation of synaptic plasticity and memories. Neuron, 52(3), 437-444. doi:10.1016/j.neuron.2006.08.024

Ploski, J. E., Monsey, M. S., Nguyen, T., DiLeone, R. J., & Schafe, G. E. (2011). The neuronal PAS domain protein 4 (Npas4) is required for new and reactivated fear memories. PLoS One, 6(8), e23760. doi:10.1371/journal.pone.0023760

Poncer, J. C., McKinney, R. A., Gahwiler, B. H., & Thompson, S. M. (1997). Either N- or P-type calcium channels mediate GABA release at distinct hippocampal inhibitory synapses. Neuron, 18(3), 463-472.

Pouille, F., & Scanziani, M. (2001). Enforcement of temporal fidelity in pyramidal cells by somatic feed-forward inhibition. Science, 293(5532), 1159-1163. doi:10.1126/science.1060342

Ramamoorthi, K., Fropf, R., Belfort, G. M., Fitzmaurice, H. L., McKinney, R. M., Neve, R. L., . . . Lin, Y. (2011). Npas4 regulates a transcriptional program in CA3 required for contextual memory formation. Science, 334(6063), 1669-1675. doi:10.1126/science.1208049

Ramirez, S., Liu, X., Lin, P. A., Suh, J., Pignatelli, M., Redondo, R. L., . . . Tonegawa, S. (2013). Creating a false memory in the hippocampus. Science, 341(6144), 387-391. doi:10.1126/science.1239073

Rial Verde, E. M., Lee-Osbourne, J., Worley, P. F., Malinow, R., & Cline, H. T. (2006). Increased expression of the immediate-early gene arc/arg3.1 reduces AMPA receptor-mediated synaptic transmission. Neuron, 52(3), 461-474. doi:10.1016/j.neuron.2006.09.031

Rodriguez, J. J., Davies, H. A., Silva, A. T., De Souza, I. E., Peddie, C. J., Colyer, F. M., . . . Stewart, M. G. (2005). Long-term potentiation in the rat dentate gyrus is associated with enhanced Arc/Arg3.1 protein expression in spines, dendrites and glia. Eur J Neurosci, 21(9), 2384-2396. doi:10.1111/j.1460-9568.2005.04068.x

Scotter, E., Graham, S., & Glass M. (2009) Cannabinoid Receptor Signal Transduction Pathways. In: Reggio P.H. (eds) The Cannabinoid Receptors. The Receptors. Humana Press.

Scoville, W. and Milner, B. (1957). Loss of recent memory after bilateral hippocampal lesions. J. Neurol. Neurosurg. Psychiatry 20(1): 11-21.

Sheng, M., & Greenberg, M. E. (1990). The regulation and function of c-fos and other immediate early genes in the nervous system. Neuron, 4(4), 477-485.

Shu, Y., Hasenstaub, A., & McCormick, D. A. (2003). Turning on and off recurrent balanced cortical activity. Nature, 423(6937), 288-293. doi:10.1038/nature01616

Shepherd, J. D., Rumbaugh, G., Wu, J., Chowdhury, S., Plath, N., Kuhl, D., . . . Worley, P. F. (2006). Arc/Arg3.1 mediates homeostatic synaptic scaling of AMPA receptors. Neuron, 52(3), 475-484. doi:10.1016/j.neuron.2006.08.034

Sohal, V. S., Zhang, F., Yizhar, O., & Deisseroth, K. (2009). Parvalbumin neurons and gamma rhythms enhance cortical circuit performance. Nature, 459(7247), 698-702. doi:10.1038/nature07991

Somogyi P., Klausberger, T. (2005). Defined types of cortical interneurone structure space and spike timing in the hippocampus. J. Physiol. 562(Pt 1): 9-26.

Spiegel, I., Mardinly, A. R., Gabel, H. W., Bazinet, J. E., Couch, C. H., Tzeng, C. P., . . . Greenberg, M. E. (2014). Npas4 regulates excitatory-inhibitory balance within neural circuits through cell-type-specific gene programs. Cell, 157(5), 1216-1229. doi:10.1016/j.cell.2014.03.058

Squire, L. R. (1992). Declarative and Nondeclarative Memory: Multiple Brain Systems Supporting Learning and Memory. Journal of Cognitive Neuroscience 4(3): 232-243.

Steward, O., Wallace, C. S., Lyford, G. L., & Worley, P. F. (1998). Synaptic activation causes the mRNA for the IEG Arc to localize selectively near activated postsynaptic sites on dendrites. Neuron, 21(4), 741-751.

Steward, O., Farris, S., Pirbhoy, P. S., Darnell, J., & Driesche, S. J. (2014). Localization and local translation of Arc/Arg3.1 mRNA at synapses: some observations and paradoxes. Front Mol Neurosci, 7, 101. doi:10.3389/fnmol.2014.00101

Sun, X., & Lin, Y. (2016). Npas4: Linking Neuronal Activity to Memory. Trends Neurosci, 39(4), 264-275. doi:10.1016/j.tins.2016.02.003

Thompson, C.L., Pathak, S.D., Jeromin, A., Ng, L.L., MacPherson, C.R., Mortrud, M.T., Cusick, A., Riley, Z.L., Sunkin, S.M., Bernard, A., Puchalski, R.B., Gage, F.H., Jones, A.R., Bajic, V.B., Hawrylycz, M.J., Lein, E.S. (2008). Genomic anatomy of the hippocampus. Neuron 60(6): 1010-1021.

Tischmeyer, W., Grimm, R., Schicknick, H., Brysch, W., & Schlingensiepen, K. H. (1994). Sequence-specific impairment of learning by c-jun antisense oligonucleotides. Neuroreport, 5(12), 1501-1504.

Traub, R.D. and Wong, R.K. (1982). Cellular mechanisms of neuronal synchronization in epilepsy. Science 216: 745-747.

Tukker, J. J., Fuentealba, P., Hartwich, K., Somogyi, P., & Klausberger, T. (2007). Cell type-specific tuning of hippocampal interneuron firing during gamma oscillations in vivo. J Neurosci, 27(31), 8184-8189. doi:10.1523/jneurosci.1685-07.2007

Valero, M., Cid, E., Averkin, R. G., Aguilar, J., Sanchez-Aguilera, A., Viney, T. J., … de la Prida, L. M. (2015). Determinants of different deep and superficial CA1 pyramidal cell dynamics during sharp-wave ripples. Nature Neuroscience, 18(9), 1281–1290. http://doi.org/10.1038/nn.4074

Vida, I., Bartos, M., & Jonas, P. (2006). Shunting inhibition improves robustness of gamma oscillations in hippocampal interneuron networks by homogenizing firing rates. Neuron, 49(1), 107-117. doi:10.1016/j.neuron.2005.11.036

Villa, K. L., Berry, K. P., Subramanian, J., Cha, J. W., Oh, W. C., Kwon, H. B., . . . Nedivi, E. (2016). Inhibitory Synapses Are Repeatedly Assembled and Removed at Persistent Sites In Vivo. Neuron, 89(4), 756-769. doi:10.1016/j.neuron.2016.01.010

Weng, F. J., Garcia, R. I., Lutzu, S., Alvina, K., Zhang, Y., Dushko, M., . . . Lin, Y. (2018). Npas4 Is a Critical Regulator of Learning-Induced Plasticity at Mossy Fiber-CA3 Synapses during Contextual Memory Formation. Neuron, 97(5), 1137-1152.e1135. doi:10.1016/j.neuron.2018.01.026

Whittington, M.A., Traub, R.D., & Jefferys, J.G. (1995). Synchronized oscillations in interneuron networks driven by metabotropic glutamate receptor activation. Nature 373(6515): 612-615.

Wierenga, C. J., Becker, N., & Bonhoeffer, T. (2008). GABAergic synapses are formed without the involvement of dendritic protrusions. Nat Neurosci, 11(9), 1044-1052. doi:10.1038/nn.2180

Wilson, M. and McNaughton, B. (1993). Dynamics of the hippocampal ensemble code for space. Science 261(5124): 1055-1058.

Wilson, R. I., & Nicoll, R. A. (2001). Endogenous cannabinoids mediate retrograde signalling at hippocampal synapses. Nature, 410(6828), 588-592. doi:10.1038/35069076

Wittner, L., & Magloczky, Z. (2017). Synaptic Reorganization of the Perisomatic Inhibitory Network in Hippocampi of Temporal Lobe Epileptic Patients. Biomed Res Int, 2017, 7154295. doi:10.1155/2017/7154295

Wyeth, M. S., Zhang, N., Mody, I., & Houser, C. R. (2010). Selective reduction of cholecystokinin-positive basket cell innervation in a model of temporal lobe epilepsy. J Neurosci, 30(26), 8993-9006. doi:10.1523/jneurosci.1183-10.2010

Xue, M., Atallah, B. V., & Scanziani, M. (2014). Equalizing excitation-inhibition ratios across visual cortical neurons. Nature, 511(7511), 596-600. doi:10.1038/nature13321

Yamamada, K., Homma, C., Tanemura, K., Ikeda, T., Itohara, S., Nagoaka, Y. (2011). Analyses of fear memory in Arc/ Arg3.1-deficient mice: intact short-term emmory and impaired long-term and remote member. Scientific Research 1(1): 1-8. doi: 10.4236/wjns.2011.11001

Yoshihara, S., Takahashi, H., Nishimura, N., Kinoshita, M., Asahina, R., Kitsuki, M., . . . Tsuboi, A. (2014). Npas4 regulates Mdm2 and thus Dcx in experience-dependent dendritic spine development of newborn olfactory bulb interneurons. Cell Rep, 8(3), 843-857. doi:10.1016/j.celrep.2014.06.056

Zhang, W., & Buckmaster, P. S. (2009). Dysfunction of the dentate basket cell circuit in a rat model of temporal lobe epilepsy. J Neurosci, 29(24), 7846-7856. doi:10.1523/jneurosci.6199-08.2009

Zhang, W., Wu, J., Ward, M. D., Yang, S., Chuang, Y. A., Xiao, M., . . . Worley, P. F. (2015). Structural basis of arc binding to synaptic proteins: implications for cognitive disease. Neuron, 86(2), 490-500. doi:10.1016/j.neuron.2015.03.030

Zhao, C., Eisinger, B., & Gammie, S. C. (2013). Characterization of GABAergic neurons in the mouse lateral septum: a double fluorescence in situ hybridization and immunohistochemical study using tyramide signal amplification. PLoS One, 8(8), e73750. doi:10.1371/journal.pone.0073750

Chapter 2. The IEG *Npas4* recruits CCK basket cell synapses and enhances-mediated plasticity in the mouse hippocampus

Summary

Experience-dependent expression of immediate-early gene transcription factors can transiently change the transcriptome of active neurons and initiate persistent changes in cellular function. However, the impact of inducible transcription factors (ITFs) on circuit connectivity and function is poorly understood. We investigate the specificity with which the ITF NPAS4 governs experience-dependent changes in inhibitory synaptic input onto CA1 pyramidal neurons (PNs). We show that novel sensory experience selectively enhances somatic inhibition mediated by cholecystokinin-expressing basket cells (CCKBCs) in an NPAS4-dependent manner. NPAS4 specifically increases the number of synapses made onto PNs by individual CCKBCs without altering synaptic properties. Additionally, we find that sensory experience-driven NPAS4 expression enhances depolarization-induced suppression of inhibition (DSI), a short-term form of cannabinoid-mediated plasticity expressed at CCKBC synapses. Our results indicate that CCKBC inputs are a major target of the NPAS4-dependent transcriptional program in PNs and that NPAS4 is an important regulator of plasticity mediated by endogenous cannabinoids.

Introduction

Immediate-early gene (IEG) transcription factors are expressed in response to sensory experiences and are routinely used to identify task-relevant neurons (Bullitt, 1990; Guenthner, Miyamichi, Yang, Heller, & Luo, 2013; Renier et al., 2016; Ye et al.,

2016), including those associated with memory formation and behavioral plasticity (Alen, Ramirez-Lopez, Gomez de Heras, Rodriguez de Fonseca, & Orio, 2013; Cai et al., 2016; Cowansage et al., 2014; Garner et al., 2012; Mayford & Reijmers, 2015). In spite of their wide-spread use as tools, surprisingly little is known about how inducible transcription factors (ITFs) alter connectivity between specific neuron subtypes, influence plasticity, or impact circuit function (Minatohara, Akiyoshi, & Okuno, 2015).

The ITF neuronal PAS domain protein 4 (NPAS4) is expressed exclusively in response to membrane depolarization (Lin et al., 2008), explicitly linking it to the activity history of the neuron. Behaviorally-induced NPAS4 directs the reorganization of inhibition along the somato-dendritic axis of hippocampal PNs, enhancing somatic inhibition and reducing inhibition in the proximal dendrites (Bloodgood, Sharma, Browne, Trepman, & Greenberg, 2013). NPAS4 is therefore poised to convert transient increases in neuronal activity into long-lasting changes in how PNs are functionally embedded in the local inhibitory circuit. However, whether expression of NPAS4 in PNs leads to the regulation of synapses made by specific inhibitory neuron subtypes is unknown.

Inhibitory neuron subtypes are highly heterogeneous, each with distinct functions within the local circuit. In CA1 of the hippocampus, somatic inhibition is provided by cholecystokinin- (CCK) and parvalbumin (PV)-expressing basket cells (BCs), which have distinct and complementary roles in gating PN output. This provides a straight-forward system in which to ask if NPAS4 regulates distinct subtypes of inhibitory inputs. Fast-spiking PVBCs provide reliable, precisely timed neurotransmission in response to predominantly feedforward synaptic input (Glickfeld & Scanziani, 2006), positioning

them to finely regulate the timing of PN action potential (AP) firing (Pouille & Scanziani, 2001). In contrast, CCKBCs elicit slower and less reliable, asynchronous inhibition (Daw, Tricoire, Erdelyi, Szabo, & McBain, 2009; Hefft & Jonas, 2005) in response to the summation of both feedforward and feedback synaptic input (Glickfeld & Scanziani, 2006). Importantly, CCKBCs express a variety of neuromodulatory receptors, including cannabinoid receptors (CB1Rs) localized to their axon terminals (Dudok et al., 2015; Glickfeld, Atallah, & Scanziani, 2008; Katona et al., 1999). Indeed, activation of CCKBC CB1Rs by endocannabinoids, released from postsynaptic PNs, underlies depolarization-induced suppression of inhibition (DSI) (Wilson & Nicoll, 2001), a form of retrograde signaling that confers onto active PNs a transient window of increased excitability and plasticity (Carlson, Wang, & Alger, 2002; Chevaleyre & Castillo, 2004; Zhu & Lovinger, 2007). Activity-driven NPAS4 expression increases somatic inhibition onto PNs, but it is unknown whether this synaptic regulation is interneuron subtype-specific. Given the marked differences between PV- and CCKBCs, the functional significance of experience-driven modulation of somatic inhibition will be determined by the subtype(s) of basket cells regulated by NPAS4-expression.

Using behavioral manipulations in combination with electrophysiological, pharmacological, and anatomical approaches, we show that novel sensory experiences selectively increase the number of inhibitory synapses made by individual CCKBCs onto CA1 PNs through an NPAS4-dependent mechanism. Moreover, we find that this interneuron subtype-specific circuit change strongly enhances DSI expression by active PNs.

Results

Npas4 is expressed in response to environmental enrichment

We manipulated the sensory experiences of juvenile wild-type (WT) mice by housing littermates in an enriched environment (EE), consisting of a running wheel and several novel objects that were regularly refreshed (**Figure 2.1A**, see Methods for details). After four days in EE, hippocampi were removed, sectioned, and immunostained with antibodies recognizing NPAS4 and the neuronal marker NeuN. Comparable immunostaining was performed on sections from age-matched mice housed in unenriched, standard environments (SE). We observed a significant increase in NPAS4-positive neurons in CA1 from mice allowed to explore an EE relative to those maintained in an SE (**Figure 2.1B-C**; SE: 3.4 ± 0.6 %, EE: 11.2 ± 0.5%; $p<0.001$, Mann-Whitney U Test), similar in magnitude to what has been previously reported (Bloodgood et al., 2013) and indicating that many CA1 cells were recently active. As NPAS4 protein is rapidly produced and degraded (Lin et al., 2008), this is likely a significant underestimate of the percentage of neurons that expressed NPAS4 over the duration of the four days in EE.

Recent studies indicate functional distinctions between PNs in the superficial (closest to stratum radiatum, SR) and deep (closest to stratum oriens, SO) subregions of CA1 (Geiller, Royer, & Choi, 2017), including gene expression profiles (Cembrowski, Wang, Sugino, Shields, & Spruston, 2016), firing patterns (Baimbridge, Peet, McLennan, & Church, 1991), and connectivity with excitatory (Masurkar et al., 2017) and inhibitory neurons (Lee et al., 2014; Valero et al., 2015). We therefore asked whether superficial and deep CA1 PNs express NPAS4 equivalently in response to exploration of an EE. We observed no significant difference in the percentage of NPAS4-positive cells

between these subregions (**Figure 2.2**; superficial: 11.3% ± 0.8 of neurons, deep: 10.3% ± 1.0 of neurons, p=0.662, Mann-Whitney U Test), suggesting that experience-driven NPAS4 expression is similar among superficial and deep CA1 PNs.

NPAS4 underlies an experience-dependent enhancement of somatic inhibition in superficial CA1

We visualized somatic inhibitory synapses in CA1 using immunohistochemistry and made the unexpected observation that NPAS4 expression most prominently affects inhibitory synapses onto superficial CA1 pyramidal cells. The CA1 region of the hippocampus from *Npas4*$^{f/f}$ mice was densely infected with adeno-associated viruses (AAV) encoding mRFP (AAV-mRFP) in one hemisphere and Cre-GFP (AAV-Cre-GFP) in the other, enabling within animal comparisons of wild type (WT) and *Npas4* knockout (KO) hemispheres (**Figure 2.1D**), respectively. Four days after surgery, allowing time for virus expression, *Npas4* excision, and degradation of preexisting NPAS4 protein, mice were housed for an additional four days in SE or EE, then hippocampi were removed, fixed, and sectioned. To detect inhibitory synapses, sections in which >95% of PNs were infected were stained with antibodies recognizing presynaptic vesicular GABA transporter (VGAT) protein and the inhibitory postsynaptic scaffolding protein gephyrin. The overlap of immunofluorescence within the pyramidal cell layer was quantified as a proxy for somatic inhibitory synapses.

In mice housed in SE, WT and KO hemispheres had equivalent immunofluorescence (**Figure 2.1E-F**; WT: 208.0 ± 4.4 A.U., KO: 203.8 ± 5.6 A.U.;

p>0.05, ANOVA with Bonferroni post hoc test), indicating somatic inhibition of WT and KO neurons is similar in mice maintained in SE. In contrast, and consistent with what has been described previously (Bloodgood et al., 2013), we detected a highly significant NPAS4-dependent increase in somatic inhibitory synapses in tissue from mice housed in EE (**Figure 2.1E-F**; WT: 277.3 ± 14.2 A.U., KO: 209.4 ± 6.8 A.U., p<0.001, ANOVA with Bonferroni post hoc test). Surprisingly, analyzing superficial and deep subregions separately revealed that the increase in inhibitory synapses was significant only within superficial, and not deep, CA1, despite comparable experience-driven NPAS4 expression in both subregions (**Figure 2.1G**; superficial – WT: 60.5 ± 4.5 A.U., 107.8 ± 14.0 A.U., KO: 57.8 ± 15.7 A.U., 60.0 ± 7.7; deep – WT: 147.5 ± 7.3 A.U., 163.4 ± 8.7 A.U., KO: 143.5 ± 5.4 A.U., 157.2 ± 4.7 A.U. for SE and EE, respectively, superficial WT vs KO for EE p<0.001, p>0.05 for all other comparisons).

Does this sublayer-specific change in immunofluorescence translate into a sublayer-specific change in synaptic response? We next asked if novel sensory experiences lead to the enhancement of somatic inhibitory postsynaptic currents (IPSCs) preferentially within superficial CA1. To answer this question, the CA1 region of the hippocampus was infected with AAV-Cre-GFP to generate a sparse population of *Npas4* KO neurons within a larger population of WT neurons (**Figure 2.1H**). Four days after virus injection, animals were housed in an SE or EE for four to seven days and then acute hippocampal slices were prepared. Simultaneous whole-cell voltage clamp recordings were obtained from neighboring WT and *Npas4* KO PNs within superficial or deep subregions of CA1. Inhibitory postsynaptic currents were evoked (eIPSCs) by focal stimulation of axons in the pyramidal cell layer and monosynaptic inhibitory currents

were isolated by bath application of NMDA and AMPA receptor antagonists (**Figure 2.1I**, 10 μM CPP and NBQX, respectively). Consistent with our immunohistochemistry data, we measured no systematic difference in eIPSC amplitudes between WT and KO neurons in mice from SE (**Figure 2.1J and M**; WT: 1059.9 ± 198.9 pA, KO: 1119.8 ± 192.5 pA, p=0.93, Wilcoxon Signed-rank Test). However, housing mice in an EE resulted in considerably larger eIPSCs in WT neurons relative to neighboring *Npas4* KO neurons when the pair of PNs was localized to superficial CA1 (**Figure 2.1K and M**; WT: 1035.3 ± 196.9 pA, KO: 715.2 ± 116.1 pA, p=0.04, Wilcoxon Signed-rank Test). No significant difference in eIPSC amplitude was measured when recording from neighboring WT and KO neurons in deep CA1 (**Figure 2.1L and M**; WT: 1146.4 ± 150.6 pA, KO: 1011.1 ± 194.5 pA, p=0.37, Wilcoxon Signed-rank Test). Thus, experience-driven NPAS4 expression increases somatic inhibitory currents preferentially in superficial CA1 PNs.

NPAS4 exclusively regulates CCKBC, not PVBC, synapses in CA1

Recent work has revealed new aspects of the precision with which basket cells innervate postsynaptic targets, including basket cell subtype-specific preferences for PNs in superficial or deep CA1. Inhibition from CCKBCs is stronger onto superficial CA1 PNs ((Lee et al., 2014; Valero et al., 2015), while PVBCs provide stronger inhibition to PNs in deep CA1 (Lee et al., 2014) However, it is unclear if these synaptic preferences are influenced by expression of NPAS4 in postsynaptic PNs.

To determine whether the NPAS4-dependent increase in somatic inhibition observed in superficial CA1 is attributed to CCK or PVBC synapses exclusively or inhibitory synapses in general, we took advantage of key molecular differences between these populations of neurons to visualize inhibitory synapses. Synapses made by CCK and PVBCs can be distinguished immunohistochemically via the mutually exclusive expression of the presynaptic cannabinoid receptor (CB1R) and calcium binding protein parvalbumin (PV), respectively (**Figure 2.3A**). Thus, we visualized inhibitory synapses made by CCK or PVBCs by staining sections with antibodies recognizing VGAT, gephyrin, and CB1R or PV and quantified the triple overlap to measure synapses made by the respective cell type. Importantly, neither *Cnr1* nor *Pvalb* genes, encoding CB1R or PV, respectively, appear to be direct targets of NPAS4 (Lin 2008). Furthermore, only a fraction CCK- and PV-expressing neurons induce NPAS4 in response to depolarization (Spiegel et al., 2014). Finally, within-animal comparisons of *Npas4* WT and KO hemispheres control for potential experience-dependent differences in CB1R or PV expression levels (Donato et al., 2013).

Immunofluorescence corresponding to CCKBC synapses was equivalent between *Npas4* WT and KO hemispheres, in both superficial and deep CA1, when mice were housed in SE (**Figure 2.3B-C**; SE: superficial – WT: 68.93 ± 3.09 A.U., KO: 66.85 ± 7.65 A.U.; deep – WT: 37.91 ± 3.00 A.U., KO: 36.47 ± 2.23 A.U., $p>0.05$ for all comparisons, ANOVA with Bonferroni post hoc test). Increased sensory experience associated with EE, however, lead to a significant increase in immunofluorescence in superficial CA1 from WT hemispheres that were not present in the KO hemispheres (**Figure 2.3B-C**; EE: superficial – WT: 159.51 ± 28.30 A.U., KO: 67.87 ± 9.45 A.U.,

p<0.001, ANOVA with Bonferroni post hoc test). No significant change was detected in deep CA1 (EE: deep – WT: 40.43 ± 3.38 A.U., KO: 36.24 ± 3.05 A.U., p>0.05, ANOVA with Bonferroni post hoc test). These data suggest that activity-driven NPAS4 expression impacts CCKBC synapses and recapitulates our results from evaluating all somatic inhibitory synapses.

In order to determine whether this change in the immunofluorescent detection of CCKBC synapses translates into changes in functional connectivity, we sought to directly measure inhibition from CCKBCs onto CA1 PNs. Stimulation of axons in the cell body layer produces an eIPSC that is a mixture of CCK and PVBC inputs. These cell types utilize distinct subtypes of voltage-gated calcium (Ca) channels (VGCCs) to trigger neurotransmitter release (N- and P/Q-type, respectively; **Figure 2.3A**; (Hefft & Jonas, 2005; Poncer, McKinney, Gahwiler, & Thompson, 1997), enabling the pharmacological isolation of CCKBC neurotransmission by blocking P/Q-type VGCCs (300 nM ω-agatoxin IVA, Mintz et al., 1992). Juvenile mice were stereotaxically infected with AAV-Cre-GFP in order to generate a sparse population of *Npas4* knockout neurons in CA1 (as in **Figure 2.1H**). After four days, mice were housed in an EE for an additional four days and acute slices were prepared as above. In superficial CA1, when P/Q-type VGCCs were antagonized and eIPSCs were evoked by electrical stimulation of axons in the pyramidal cell layer, eIPSCs originating from CCKBCs were ~30% smaller in *Npas4* KO neurons than neighboring WT neurons (**Figure 2.3D and F**; WT: 552.47 ± 104.75 pA, KO: 389. 80 ± 121.90 pA, p=0.03, Wilcoxon Signed-rank Test). Similar recordings made from PNs in deep CA1 revealed a trend towards WT neurons having larger eIPSC, although the difference was not significant (**Figure 2.3E and F**; WT: 1402.8 ± 341.2, KO

1081.1 ± 231.9, p=0.12, Wilcoxon Signed-rank Test). Thus, novel sensory experiences drive an *Npas4*-dependent increase in CCKBC input onto CA1 PNs that is most pronounced in superficial CA1 PNs.

NPAS4-dependent regulation of CCKBC inputs does not preclude the possibility that NPAS4 expression may also regulate PVBC inputs. To test possibility, we performed analogous experiments to those described above, but with immunostaining for PV and pharmacological isolation of PVBC neurotransmission by antagonizing N-type VGCCs (1 μM ω-conotoxin GVIA, **Figure 2.3A**) to prevent neurotransmission from CCKBCs. We did not detect any experience- or NPAS4-dependent change in PVBC synapses visualized immunohistochemically (**Figure 2.4A-B**; SE: superficial – WT: 53.68 ± 4.88 A.U., KO: 56.34 ± 13.13 A.U.; deep – WT: 116.15 ± 9.31 A.U., KO: 119.94 ± 5.85 A.U.; EE: superficial – WT: 55.76 ± 5.30 A.U., KO: 54.86 ± 1.94 A.U.; deep – WT: 136.32 ± 8.25 A.U., KO: 127.93 ± 14.02 A.U.; $p>0.05$ for all comparisons, ANOVA with Bonferroni post hoc test). Moreover, we observed no difference in eIPSC amplitudes recorded from *Npas4* WT and KO neuron neighbors when transmission from PVCBs was pharmacologically isolated (**Figure 2.4C**; WT: 679.55 ± 150.68 pA, KO: 738.63 ± 179.41 pA, p=0.65, Wilcoxon Signed-rank Test). These results indicate that expression of NPAS4 in active CA1 PNs leads to the selective increase of CCKBC inputs without significantly impacting PVBC synapses.

NPAS4 strengthens CCKBC input by increasing the number of synapses made by individual CCKBCs onto a PN

We next sought to determine if the mechanism underlying the regulation of CCKBC synapses by NPAS4 involves changes in synapse number, synaptic strength, release probability, or a combination of synaptic changes. First, to determine how expression of NPAS4 in PNs drives an increase in the strength of inhibition, we recorded from pairs of synaptically connected CCKBCs and PNs. Though genetic strategies exist to visually identify CCK-expressing inhibitory neurons, including Cre- and Flp-dependent intersectional strategies (Basu et al., 2013), these methods are incompatible with our use of Cre to manipulate *Npas4* in *Npas4*$^{f/f}$ animals as they would result in the excision of *Npas4* from CCK inhibitory neurons. To circumvent this limitation, we identified CCKBCs by a combination of their location, electrophysiological signatures, and morphology. We sparsely manipulated *Npas4,* as described above, and housed the animals in an EE to reveal NPAS4-dependent changes in CCKBC inhibition. Acute slices were prepared and whole-cell current clamp recordings made from putative CCK inhibitory neurons. Recordings were made in the presence of AM251 (5□M) to antagonized CB1Rs and remove the confound of tonic activation of the receptor on uIPSC properties. We took advantage of the distinct intrinsic electrophysiological properties of CCK and PV inhibitory neurons to distinguish between the two classes of neurons. Non-infected (WT) cells were targeted that had large somata in superficial CA1 or stratum radiatum (Bartos & Elgueta, 2012; Wisden et al., 2002) and electrical properties consistent with a CCK, and not PV, inhibitory neuron identity (**Figure 2.5A-C**; (Glickfeld & Scanziani, 2006; Wisden et al., 2002). Inhibitory neurons were filled

with biocytin through the patch pipette for post hoc morphological analysis (**Figure 2.6D-F**, **Figure 2.7B**).

After identifying an inhibitory neuron with CCK-like electrical properties, we established a whole-cell recording from a synaptically connected WT or KO PN and measured the unitary inhibitory postsynaptic current (uIPSC) evoked in response to a single AP (**Figure 2.5D and E**, **Figure 2.6A**). CCK inhibitory neurons are themselves a heterogeneous population of neurons in CA1, comprised of basket cells and dendrite-targeting Schaffer collateral-associated (SCA) inhibitory neurons. To eliminate the latter from our analysis, which have largely indistinguishable physiological properties to CCKBCs (Cope et al., 2002), we excluded pairs for which the uIPSC success rate was less than 60% (**Figure 2.6B-C**; (Younts & Castillo, 2014). These putative SCA neurons tended to evoke smaller amplitude uIPSCs with slower rise times (**Figure 2.6A-C**), consistent with currents that are filtered by extensive stretches of dendrite (Maccaferri, Roberts, Szucs, Cottingham, & Somogyi, 2000). Lastly, when possible, the presynaptic neurons' morphology was reconstructed (**Figure 2.6D-F**) and pairs omitted if the presynaptic neuron did not have a basket cell-like morphology (for example **Figure 2.6F**). Based on these criteria, we analyzed properties of synaptic connectivity between CCKBCs and WT or *Npas4* KO PNs.

We measured significantly different uIPSC amplitudes in postsynaptic WT and KO PNs in response to single APs evoked in a CCKBC. On average, uIPSC amplitudes in WT PNs were more than twice as large as those measured in KO PNs (**Figure 2.5E-G**; WT = 450.64 ± 127.29 pA, KO = 183.97 ± 62.70 pA, p=0.044, Mann-Whitney U Test), demonstrating that NPAS4 increases the strength of individual CCKBC-PN connections.

Despite different uIPSC amplitudes, the rise times (10-90% of peak) and decay time constants (τ) of the currents were indistinguishable between the two genotypes (**Figure 2.5G-I**; rise time – WT: 1.13 ± 0.10 ms, KO: 1.06 ± 0.09 ms, p=0.92; τ - WT: 14.35 ± 0.83 ms, KO: 13.45 ± 1.01 ms, p=0.49, Mann-Whitney U Test), suggesting that the synapses made onto WT and KO PNs have similar postsynaptic receptor compositions (Gingrich, Roberts, & Kass, 1995; Lavoie & Twyman, 1996; Mody & Pearce, 2004; Thomson, Bannister, Hughes, & Pawelzik, 2000).

We next sought to determine if NPAS4 regulates the numbers of synapses (N), the presynaptic probability of release (P), or the magnitude of the postsynaptic response (quantal amplitude, Q). We first determined the rate of successes and failures of transmission from individual CCKBCs onto WT and KO PNs. While there were few failures recorded in both genotypes, uIPSCs recorded in *Npas4* KO PNs had a significantly lower success rate than WT neurons (**Figure 2.8A**; WT: 0.94 ± 0.02, KO 0.82 ± 0.04; p=0.01, Mann-Whitney U Test; 60-100 trials per connected pair, APs evoked at 0.1 Hz). One potential explanation for this difference in success rate is that NPAS4 might regulate release probability at individual CCKBC synaptic contacts. To test this possibility, we measured postsynaptic responses to pairs of APs and calculated paired pulse ratios (PPRs). Changes in this short-term plasticity are generally attributed to shifts in P (Regehr, 2012). However, PPRs were indistinguishable between WT and KO pairs for all inter-spike-intervals tested (**Figure 2.8B**; 20ms – WT: 0.81 ± 0.11, KO: 1.04 ± 0.18; p=0.65, 50ms – WT: 0.85 ± 0.13, KO: 0.99 ± 0.12; p=0.55, 200ms – WT: 0.83 ± 0.04, KO: 0.78 ± 0.10, p=0.46, and 1000ms – WT: 0.94 ± 0.07, KO: 0.83 ± 0.17, p=0.34) suggesting that the probability of release onto WT and KO neurons is unchanged.

Similarly, the latency to uIPSC onset was unchanged between the two PN genotypes (**Figure 2.9**; WT: 1.65 ± 0.12, KO: 1.66 ± 0.17, p=0.80, Mann-Whitney U Test), providing further evidence for similar presynaptic organization between synapses converging on *Npas4* WT and KO neurons (Boudkkazi et al., 2007; Boudkkazi, Fronzaroli-Molinieres, & Debanne, 2011; Sabatini & Regehr, 1999).

If release probability at CCKBC synapses onto WT and KO neurons is indistinguishable, an NPAS4-mediated increase in the number of CCKBC synapses formed onto PNs is the most parsimonious mechanism to account for the lower success rate of uIPSCs in *Npas4* KO neurons (Del Castillo & Katz, 1954). To confirm this and investigate possible changes in Q, we calculated the coefficient of variation (CV) and variance of the uIPSC amplitude recorded from each PN and compared this to the mean uIPSC amplitude. Comparing the CV for each PN's uIPSC amplitude to the mean response revealed a strong negative correlation across all cells, with smaller amplitude uIPSCs having larger CVs (**Figure 2.8C**). The average CV for WT PNs was half that measured from KO neurons (**Figure 2.8D**; WT: 44.17 ± 5.90, KO: 79.40 ± 9.80, p=0.008, Mann-Whitney U Test), indicating that the difference in uIPSC amplitudes between WT and *Npas4* KO neurons is due to a change in N and not Q (Berninger, Schinder, & Poo, 1999; Kerchner & Nicoll, 2008; Le Bé, Silberberg, Wang, & Markram, 2007). Moreover, variance-mean analysis of uIPSC amplitudes shows a linear relationship for both CCKBC- WT PN and CCKBC- KO PN pairs (**Figure 2.8E**; WT: R2 = 0.89, KO: R2 = 0.84; (Foster & Regehr, 2004). Strikingly, the linear fits of the WT and KO data sets are essentially superimposable (slope – WT: 55.55 ± 4.73, KO: 54.91 ±

5.46), confirming that the probability of release is unchanged and indicating the quantal amplitude is ~55pA in both genotypes (Reid & Clements, 1999).

Variance-mean analysis provides an indirect measurement of Q. To measure this directly we took advantage of the fact that CCKBCs generate significant asynchronous release, which is quantal in nature (Daw et al., 2009; Hefft & Jonas, 2005). A series of 20 APs were evoked at 40 Hz in the CCKBC and the amplitude of asynchronous events quantified during the first 100 ms after the last spike (**Figure 2.8F**). These amplitudes were comparable between WT and KO neurons (**Figure 2.8G**; WT: 57.37 pA ± 3.62, KO: 61.67 pA ± 6.50, p=0.48, Mann-Whitney U Test) and in close agreement with our estimate of Q from the variance-mean analysis. Thus, we conclude NPAS4 regulates the number of synapses made by an individual CCKBC onto a PN and does not significantly change the probability of release at individual synapses or the quantal size. Based on our measurements, CCKBCs make, on average, eight synapses onto WT (1-29 synapses) and three onto *Npas4* KOs neurons (1-13 synapses) in animals exposed to sensory experience.

Sensory experience enhances DSI expression in CA1 PNs through an *Npas4*-dependent mechanism

Membrane depolarization triggers the production of endocannabinoids by PNs, which act retrogradely by binding presynaptic CB1Rs, resulting in the transient suppression of inhibitory transmission (DSI) (Wilson & Nicoll, 2001). CCKBCs are notable for their expression of CB1Rs and cannabinoid-mediated plasticity (Glickfeld & Scanziani, 2006). We thus considered the possibility that animals housed in an EE, which

leads to more CCKBC synapses, might have more prominent DSI than those maintained in SE. CA1 of *Npas4*$^{f/f}$ mice was sparsely infected with AAV-Cre-GFP and mice were housed in an SE or EE as described above. Spontaneous IPSCs were recorded from WT and KO PNs and DSI was induced by switching into current clamp and triggering 30 APs at 25 Hz (Dubruc, Dupret, & Caillard, 2013) (Figure 6A-B). In WT PNs from mice housed in SE, spontaneous IPSCs were suppressed by approximately 25% (DSI magnitude, **Figure 2.10C**) after the spike train. Notably, the magnitude of DSI in animals exposed to EE was nearly two-fold larger relative to animals in SE (**Figure 2.10B-C**, DSI magnitude, WT – SE: 26% ± 7, EE: 48% ± 4, p=0.038, Mann-Whitney U Test). As NPAS4 expression in PNs is required for the experience-driven increase in CCKBC synapse number, we hypothesized that experience-induced enhancement of DSI would also require NPAS4. Indeed, the magnitude of DSI measured in *Npas4* KO PNs from SE and EE conditions was comparable to that measured in WT neurons in standard conditions and significantly less than WT cells in animals exposed to EE (Figure **2.10B-C**, DSI magnitude, KO – SE: 0.31 ± 0.06, EE: 0.29 ± 0.05, EE WT vs EE KO p=0.016, Mann-Whitney U Test). Finally, DSI was completely prevented by bath application of the CB1R receptor antagonist AM251 (**Figure 2.10B-C**, DSI magnitude, WT: 0.03 ± 0.07, KO: -0.03 ± 0.01, p=0.46, Mann-Whitney U Test), confirming that this effect is due to endocannabinoid-mediated DSI. Together, our results support a model of experience-dependent regulation of CCKBC synapses by postsynaptic NPAS4 expression, and demonstrate that NPAS4 enhances endocannabinoid-mediated plasticity in CA1 of the hippocampus.

Discussion

The expression of IEG transcription factors is routinely used to label task-relevant neurons, but we have little insight into how these molecules shape neuronal information processing and contribute to future representations of an animal's environment. *Npas4* is the first known example of an IEG that regulates inhibitory synapses, presenting an opportunity for detailed mechanistic investigation of IEG's role in flexibly adjusting circuit operations. Determining the identity of inhibitory synapses regulated by NPAS4 is critical for understanding how this IEG could alter circuit function. Additionally, uncovering the precise way in which inhibition is enhanced provides a basis for future studies aimed at uncovering the molecular mechanism by which NPAS4 achieves this strengthening of inhibition.

Here, we have taken advantage of mutually exclusive receptor and channel expression and electrophysiological signatures of PV- and CCKBCs to reveal the identity of somatic inhibitory synapses regulated by NPAS4. We demonstrate that experience-driven NPAS4 expression recruits synapses made by CCKBCs, but neither environmental enrichment nor NPAS4 significantly affects synapses made by PVBCs in CA1 (**Figures 2.3-2.5, Figure 2.7**). This phenotype is most prominent in superficial CA1, where CCKBCs most extensively synapse, enhancing the gradient of CCKBC inhibition along the superficial to deep axis and reinforcing the idea that superficial and deep CA1 PNs form separate microcircuits (Danielson et al., 2016; Geiller et al., 2017). Moreover, we find this activity-dependent gene program increases the number of CCKBC synapses, whereas their synaptic properties are indistinguishable from the CCKBC synapses existing prior to NPAS4 expression (**Figure 2.5 and 2.8**). Intriguingly, these findings

indicate that CCKBCs and PNs communicate through a unique signaling pathway that is dynamically established by the expression of an IEG transcription factor in the postsynaptic PN. The next challenge will be to elucidate the molecular mechanism by which experience-driven NPAS4 in PNs specifically communicates with CCKBCs to signal the need for more synapses. Recent work has revealed that the formation of CCKBC synapses relies on postsynaptic expression of the dystroglycan complex (Fruh et al., 2016), while formation of PVBC synapses does not. Dystroglycans, and the proteins that associate with them, are compelling candidates through which NPAS4 may regulate CCKBC synapses, although others may yet be identified.

In comparison to PVBCs, CCKBCs are less well-studied. A distinguishing characteristic of CCKBCs is the sensitivity of their synapses to cannabinoids, and consequently their susceptibility to dynamic regulation by the postsynaptic PN through DSI. Here, we have uncovered an experience-driven enhancement of DSI that requires NPAS4 expression (**Figure 2.10**), generating several intriguing hypotheses about how expression of this ITF might shape PN network dynamics. For example, our data imply that PNs in which NPAS4 is expressed will be subject to enhanced CCKBC inhibition, thus reducing CA1 PN spiking during low to moderate network activity. However, when PN activity levels surpass the threshold for triggering cannabinoid production, leading to the temporary suppression of transmission from CCKBCs through DSI, a temporal window will open in which the PN can disinhibit itself, generate more APs, and lower the threshold for plasticity. More broadly, a function of NPAS4 expression may be to reduce noise and increase signal within the local microcircuit by refining PN firing (Bartos & Elgueta, 2012). As DSI of CCKBC synapses can also facilitate the induction of long-term

potentiation (LTP) in PNs (Carlson et al., 2002), this window of disinhibition may facilitate LTP at inputs active during DSI and help to coordinate plasticity of common inputs to NPAS4-expressing neurons.

There is accumulating evidence supporting a role for CCKBCs in shaping hippocampal circuit function. Indeed, abnormal wiring of CCK inhibitory neurons disrupts the spatial coherence of place fields (Del Pino et al., 2017), and the opposing gradients of inhibition from PV and CCKBCs along the superficial to deep axis of the hippocampus underlie the heterogeneity of PN spiking associated with sharp wave ripples (Valero et al., 2015). Thus, NPAS4-dependent recruitment of CCKBC inputs may play a role in the spatial coherence of place fields and increase the difference in firing patterns observed during active and resting behavior states.

Notably, exposure of animals to EE induced NPAS4 in similar numbers of PNs localized to both superficial and deep CA1, yet we did not detect a significant effect of EE or a requirement of NPAS4 in regulating somatic inhibition in the deep subregion. This sublayer specificity may indicate that NPAS4 regulates target genes that selectively recruit CCKBC boutons to both superficial and deep PNs, but a preexisting preference of CCKBC axons for superficial CA1 is the limiting organizational feature. Alternatively, different types of behavioral manipulations may reveal a more significant NPAS4-mediated inhibitory synapse phenotype in deep CA1 PNS. It is also worth noting that while we do not observe a significant change in somatic inhibition of PNs in deep CA1, NPAS4 is expression in these cells may regulate other populations of synapses, such as those in the proximal dendrites (Bloodgood et al., 2013).

Acknowledgements

This work was supported by grants from the Pew Charitable Trust (00028631), the Searle Scholars Program (14-SSP-184), the Whitehall Foundation (2013-12-88) (B.L.B.), and the National Science Foundation (2013154395) (A.L.H.). We thank A. Payne, G. Higerd, A. Kazi, K. Mendoza, and G. Moore for technical assistance. We thank J. Isaacson, M. Scanziani, T. Komiyama and members of the lab for critical reading of the manuscript and thoughtful feedback. We are particularly grateful to J. Isaacson for his ongoing and thoughtful discussions during the preparation of this manuscript.

Author contributions

A.L.H. and B.L.B. conceived of the study and designed all experiments. A.L.H., K.M.M, and B.L.B. co-wrote the manuscript. A.L.H. performed all electrophysiology experiments, surgeries, immunohistochemistry and all data analysis. K.M.M. performed surgeries and immunohistochemistry. G.S.B. performed immunohistochemistry and image quantification. N.A.D. performed immunohistochemistry.

Materials and methods

Animal Husbandry and Handling

Animals were handled according to protocols approved by the UC San Diego Institutional Animal Care and Use Committee and were in accordance with federal guidelines. The animal lines used were wildtype (WT; C57BL/6J, JAX000664) and

Npas4f/f (Lin et al., 2008). Both female and male mice were used. All experiments were performed on animals between postnatal days 21-28 (p21-28) before weaning. For experiments in which mice were injected with virus followed by housing in an enriched environment (**Figures 2.3-2.10**), four days after surgery (P17) animals (dam and pups) were moved to a larger cage containing a running wheel, hut, tunnel, and several other objects. To maximize novelty, new objects were introduced and cage was rearranged every other day. All experiments were conducted on mice housed in an enriched environment for 4-7 days or on mice from standard mouse housing as indicated.

Stereotaxic Viral Injection Surgeries

All surgeries were performed according to protocols approved by the UC San Diego Institutional Animal Care and Use Committee and were in accordance with federal guidelines. Stereotaxic viral injection surgeries were performed on P14 mice. Animals were administered Flunixin (2.5 mg/ kg) subcutaneously pre-operatively and post-operatively every 12h for 72 hr. Animals were deeply anesthetized with isoflurane for the duration of the surgery (initially 3-4% in O2, then maintained at 2%) and body temperature was maintained at 37°C. The fur covering the scalp was shaved and scalp was cleaned with three iterations of betadine and 70% ethanol before an incision was made to expose the skull. A small burr hole was drilled through the skull over the CA1 region of the hippocampus bilaterally (medial/lateral: ± 3.1 mm; anterior/posterior: −2.4 mm; dorsal/ventral: 2.8 mm and 2.9 mm below the dura) and virus was injected (350 nL at each dorsal/ventral site for a total of 700 nL; 150 nL min−1). Each virus was

diluted 2:1 in phosphate-buffered saline (PBS). Three minutes post-injection, the needle was retracted, the scalp sutured and the mouse was recovered at 37°C before being returned to its home cage.

Virus production

AAV-Cre–GFP was custom produced by the UNC Vector Core with a plasmid provided by M. During (Ohio State University). AAV-TurboRFP was a stock virus produced by the Penn Vector Core (AAV1.hWyn.TurboRFP.WPRE.rBG).

Acute Slice Preparation

Transverse hippocampal slices were prepared from Npas4f/f mice (P21-P28) seven to 15 days after stereotaxic injection of Cre-GFP AAV into CA1. Animals were anesthetized briefly by inhaled isoflurane and decapitated. The cerebral hemispheres were removed and bathed for three minutes in a cold slushy of choline-based dissection solution containing (in mM): 110 choline-Cl, 25 NaHCO3, 1.25 Na2HPO4, 2.5 KCl, 7 MgCl2, 25 glucose, 0.5 CaCl2, 11.6 ascorbic acid, 3.1 pyruvic acid and equilibrated with 95% O2/ 5% CO2. Blocking cuts were made to isolate the portion of the cerebral hemispheres containing the hippocampus and the tissue was transferred to a slicing chamber containing choline artificial cerebrospinal fluid (choline-ACSF). Slices (300 μM) were cut with a Leica VT1000s vibratome (Leica Instruments) and transferred to a recovery chamber with ACSF consisting of (in mM): 127 NaCl, 25 NaHCO3, 1.25

Na2HPO4, 2.5 KCl, 2 CaCl2, 1 MgCl2, 25 glucose, saturated with 95% O2/ 5% CO2. Slices were recovered for 30 min at 31° C and maintained at room temperature for the duration of the experiment (4-6 hours).

Electrophysiology and Pharmacology

For experiments performed in tissue from AAV-Cre-GFP injected mice, infection density varied with distance from the injection site and slices were selected in which ~5-25% of neurons were infected. Whole-cell voltage clamp recordings were obtained from CA1 pyramidal neurons and inhibitory neurons visualized with infrared differential interference contrast (IR-DIC) microscopy. Neurons were clamped at -70 mV. During recordings, slices were perfused with ACSF (2-4 mL/ min) bubbled with 95% O2/ 5% CO2 and heated to 31°C. For pyramidal neuron recordings, patch pipettes (open pipette resistance 2-4 MΩ) were filled with an internal solution containing (in mM) 147 CsCl, 5 Na2-phosphocreatine, 10 HEPES, 2 MgATP, 0.3 Na2GTP and 2 EGTA (pH=7.3, osmolarity=300 mOsm) and supplemented with QX-314 (5 mM), except in DSI experiments. For experiments in which eIPSCs in WT and *Npas4* KO pyramidal cell pairs were recorded, extracellular stimulation of local axons within specific lamina of the hippocampus was delivered by current injection through a theta glass stimulating electrode that was placed in the center of the relevant layer (along the radial axis of CA1) and within 100–300 μm laterally of the patched pair. eIPSCs were pharmacologically isolated with CPP (10 μM) and NBQX (10 μM) in all experiments as well as Agtx-IVA (0.3 μM) or Ctx-GIVA (1 μM) where indicated. For inhibitory neuron- pyramidal cell

connected pair experiments, inhibitory neurons were patched with pipettes filled with an internal solution containing (in mM): 147 K-gluconate, 20 KCl, 10 Na2-phosphocreatine, 10 HEPES, 2 Na-ATP, 0.3 Na-GTP, 5 MgCl2, 0.2 EGTA, and 3% biocytin (Sigma Aldrich B4261) (pH=7.3, osmolarity=300 mOsm). Interneurons were held in current clamp at a resting membrane potential of -70 mV. For DSI experiments, spontaneous inhibitory activity was induced in acute slices with carbachol (5 µM). DSI was induced in pyramidal cells by triggering 30 action potentials at 25 Hz.

Biocytin visualization and Reconstructions

Interneurons recorded with an internal solution containing 3% biocytin were labeled using a diaminobenzene (DAB) reaction, as previously described with modifications (Marx, Gunter, Hucko, Radnikow, & Feldmeyer, 2012). Briefly, cells were held for 15-30 min. After gently detaching from the cell, slices were placed in 4% paraformaldehyde (PFA) and fixed overnight. After fixation slices were stored in PBS until processing. All the following steps were carried out at 4°C on a rotating platform and all washes were 10 min, unless otherwise noted. Slices were washed 6x in 100mM phosphate buffer (PB; consisting of NaH2PO4- and NaPO4-, pH 7.4), incubated for 20 minutes in PB + 3% H2O2, washed 4x in PB, then incubated overnight in a permeabilization buffer (3% Triton X-100, 2% normal goat serum (NGS) in PB). The next day, slices were washed 1x in PB, incubated for 2 hours in a ‘pre-incubation’ buffer (0.5% Triton X-100, 0.5% NGS in PB), then incubated in a biotinylation buffer (pre-incubation buffer + ABC solutions (ThermoScientific 32050; 1% of “Reagent A” Avidin + 1% “Reagent B” biotinylated

horseradish peroxidase) for 2 hours. Slices were then washed 3x in PB, 2x in Tris Buffer (TB; 50mM Tris base, pH 7.4), incubated for 10 min at room temperature in DAB solution 1 (1% Imidazole, 1 tablet / 2mL DAB (Sigma Aldrich D5905), in TB), and then incubated in DAB solution 2 (1% Imidazole, 1% Ammonium nickel sulfate hydrate (NH4)2Ni(SO4)2, 1 tablet / 2mL DAB, 3% H2O2, in TB) for 2 – 10 min at room temperature, or until the slices turned visibly dark purple. Slices were immediately washed in PB for 1 min, followed by 2x washes in PB. Slices were then mounted on slides (Superfrost/Plus, Fisher Scientific) and air dried overnight. The following day, slices were dehydrated and cleared with the following steps (6 min each): 30% ethanol, 50% ethanol, 70% ethanol, 96% ethanol, 100% ethanol, 100% ethanol, xylenes, xylenes, xylenes. Slices were then cover slipped with Krystalon (EMD Millipore) and dried overnight in the chemical fume hood. Biocytin-filled inhibitory neurons were reconstructed on an Olympus DSU microscope using Neurolucida software (MBF Bioscience).

Immunohistochemistry

For labeling of PV- and CB1R-positive inhibitory synapses, p14 mice were stereotaxically injected with AAV-Cre-GFP into CA1 of the right hemisphere and AAV-TurboRFP into CA1 of the left hemisphere. After 4 days of recovery from surgery and 4-7 days in an enriched environment or standard housing, mice were anesthetized briefly with isoflurane and decapitated. Hippocampi were rapidly dissected in ice-cold dissection media consisting of (in mM): 1 CaCl2, 5 MgCl2, 10 glucose, 4 KCl, 26 NaHCO3, 218

sucrose, 1.3 NaH2PO4·H2O, 30 HEPES. Hippocampi were immediately drop fixed in 4% PFA in PBS at 4°C for 2 hours followed by overnight incubation in 30% sucrose in PBS. Cryoprotected tissue was stored in Tissue-Tec O.C.T. at -20°C, sectioned at 20 μM (Leica CM1950 cryostat) and mounted on slides (Superfrost/Plus, Fisher Scientific).

For NPAS4 and inhibitory synapse immunostaining, hippocampal sections were blocked in 5% goat serum and 0.2% Triton X-100 in PBS overnight at 4°C. Sections were incubated in primary antibody overnight at 4°C in blocking solution, washed three times in PBS, and incubated overnight in a species-matched secondary at 4°C, and washed again three times in PBS. Slices were briefly dipped in ddH_2O and cover slipped with Fluoromount (Electron Microscopy Sciences). See Table 1 for antibodies and concentrations used for all IHC experiments.

Confocal imaging

All slices and tissue sections were imaged using an Olympus Fluoview 1000 confocal microscope (× 10/.4, × 20/0.75, and × 60/1.42 (oil) plan-apochromat objectives; UC San Diego School of Medicine Microscopy Core, supported by NINDS grant NS047101). Identical acquisition parameters were used for all slices or tissue within a single experiment. The levels, contrast, and brightness of confocal images were moderately adjusted in Photoshop CS6 software (Adobe Systems, Inc.) for illustrative purposes using scientifically accepted procedures.

Image Quantification

Confocal images for a particular experiment were subjectively thresholded using ImageJ software and the threshold was kept consistent across images from all conditions obtained for a single experiment. For immunohistochemistry experiments (Fig. 1), the integrated density (the product of the area and mean grey value, termed immunohistofluorescence (IHF) of the overlap of the three fluorescent signals was quantified within regions of interest (ROIs) for superficial and deep CA1 using ImageJ software (National Institute of Health). Puncta were defined as a thresholded fluorescence cluster with an area ≥0.05 μm2. Superficial and deep CA1 ROIs were 25 μM deep bins (along superficial to deep axis) aligned to the superficial and deep edges of the CA1 stratum pyramidale, respectively (Lee et al., 2014). IHF was normalized to cell number within each ROI as determined by DAPI counterstaining.

Electrophysiology Analysis

Electrophysiology data were acquired using ScanImage software (Pologruto, Sabatini, & Svoboda, 2003) and a Multiclamp 700B amplifier, and digitized with a DigiData 1440 data acquisition board (Axon Instruments). Data were sampled at 10 kHz and filtered at 6 kHz. Off-line data analysis was performed using custom software written in Igor Pro by A.L.H. and B.L.B. (Wavemetrics).

Experiments were discarded if the holding current for pyramidal cells with CsCl-based internal solution was greater than −500 pA or if the series resistance was greater than 25 MΩ. In experiments in which direct comparisons were made between two

neurons, recordings were discarded if the series resistance differed by more than 20% between the two recordings. All recordings were performed at 31°C.

The amplitudes of eIPSCs and uIPSCs were calculated by averaging the amplitude 0.5 ms before to 2 ms after the peak of the current. Data are shown as positive values for clarity. For connected inhibitory neuron- pyramidal cell paired recordings, paired pulse ratios (PPR) were calculated by recording a template uIPSC for each cell, normalizing it to the peak of the first pulse of the PPR wave, subtracting the template wave from the PPR wave, and then measuring the corrected amplitude of the second peak. Asynchronous event amplitudes were measured for events greater than 15 pA within the 100 ms following the end of a 20 AP train delivered at 40 Hz to the CCKBC. Asynchronous event amplitudes were only counted for cells in which the spontaneous event frequency recorded for the cell was less than 40% that of the event frequency recorded during the asynchronous release analysis window. Slopes of the rise times of the uIPSCs were measured by normalizing the uIPSC, then measuring the slope between 10-90% of the uIPSC peak. For DSI experiments, the DSI magnitude was reported as the ratio of the total inhibitory current per second averaged over 4 s after DSI to the total inhibitory current per second for averaged for 10 s before DSI induction.

Statistics

All values are expressed as mean ± SEM. Box plots are displayed as the median (center line), 75-25% (upper and lower box), and 90-10% (whiskers). For all electrophysiology experiments, ‘n' refers to the number of cells or pairs recorded per

condition and are biological replicates. For immunohistochemistry and FISH experiments, 'n' refers to tissue sections used per condition, obtained from a specified number of separate mice and are biological replicates. The aforementioned values can be found in the figure legends. Our sample sizes were not pre-determined, and are similar to those reported in the literature. Data collection was not performed blind to the conditions of the experiment and we did not use any specific randomization procedure other than to assign litters of mice to one of two experimental housing conditions in an alternating manner. Analysis was done blind to condition and when possible experiments were designed to allow for within-animal comparisons between WT and Npas4 KO pyramidal cells. All statistical analysis was performed in Prism (GraphPad Software, Inc., La Jolla, CA) and nonparametric statistical tests were used. Wilcoxon signed-rank tests were performed for paired data and Mann-Whitney U Tests were used for unpaired data. However, in experiments involving ≥2 independent variables, where n was too small to determine distribution, a normal distribution was assumed and analysis of variance (ANOVA) with Bonferroni post-hoc tests were performed. Statistical significance was assumed when $P<0.05$. In all figures, *$P<0.05$, **$P<0.01$ and ***$P<0.001$ as determined in Prism software. All figures were generated using Illustrator CS6 software (Adobe Systems, Inc.).

Figure 2.1 NPAS4 enhances somatic inhibition on superficial CA1 pyramidal neurons

(A) Cartoon of standard environment (SE) and enriched environment (EE). (B) Confocal images of mouse hippocampi from SE (top) and EE (bottom) stained with antibodies recognizing NPAS4 (cyan) and NeuN (magenta). Left: Box indicates region imaged at high magnification and quantified for NPAS4-positive neurons. Scale bar = 200 μm. Right: Higher magnification boxed region on left. Scale bar = 50 μm. (C) Quantification of NPAS4-positive neurons in CA1 in mice from SE and EE (n=10 sections over 3 mice per condition). * indicates $p<0.05$. (D) Schematic of stereotaxic AAV infection of CA1 in Npas4f/f mice. Hippocampi were infected with AAV-Cre-GFP (left) and AAV-RFP (right) in the contralateral hemisphere. (E) Representative images of gephyrin (red), VGAT (green) and merged IHC from WT and Npas4 KO hemispheres from mice housed in SE and EE. Gray outlines in merged images represent cell body outlines in WT condition (mRFP expression) or cell nuclei in Npas4 KO condition (Cre-GFP expression). (F) Quantification of inhibitory synapses (overlap of VGAT and gephyrin immunofluorescence) in WT and Npas4 KO hemispheres from mice housed in SE and EE (SE: n=10-11 sections over 5 mice; EE: n=9-11 sections over 6 mice). Scale bar = 20 □m. (F) Quantification of inhibitory synapses (overlap of gephyrin and VGAT) in CA1 of WT and Npas4 KO hemispheres from mice housed in SE and EE (SE: n=3-4 sections per condition from 3 mice; EE: n=5 sections per condition from 3 mice). (G) Quantification of inhibitory synapses (overlap of gephyrin and VGAT in superficial vs deep CA1 of WT and Npas4 KO hemispheres from mice housed in SE and EE (SE: n=7 sections across 3 mice, EE: n=4-6 sections across 3 mice). *** indicates $p<0.001$. (H) Example DIC image of an acute hippocampal slice with overlay of fluorescence from AAV-Cre-GFP expression in CA1. (I) Schematic of paired recordings from neighboring WT and Npas4 KO neurons with stimulation of axons in stratum pyramidale. Example eIPSCs are shown. (J) Standard environment: example eIPSC from WT (black) and KO (green) PNs in superficial CA1 (left). Pairwise comparison of eIPSCs recorded in neighboring WT and Npas4 KO neurons (gray, right, n=11 pairs). (K) Enriched environment: example eIPSC from WT (black) and KO (green) PNs in superficial CA1 (left). Pairwise comparison of eIPSCs recorded in neighboring WT and Npas4 KO neurons from mice housed in EE (gray, right, n=14 pairs). (L) Enriched environment: example eIPSC from WT (black) and KO (green) PNs in deep CA1 (left). Pairwise comparison of eIPSCs recorded from neighboring deep WT and Npas4 KO PNs (right, n=11 pairs). For (J-L), open circles indicate individual pairs, the darker circle is the example trace, and the closed circle indicated the mean ± SEM. (M) The ratio of eIPSCs recorded from WT and KO pairs across SE, EE and CA1 subregions, normalized to the sum of the WT and KO eIPSC amplitudes.

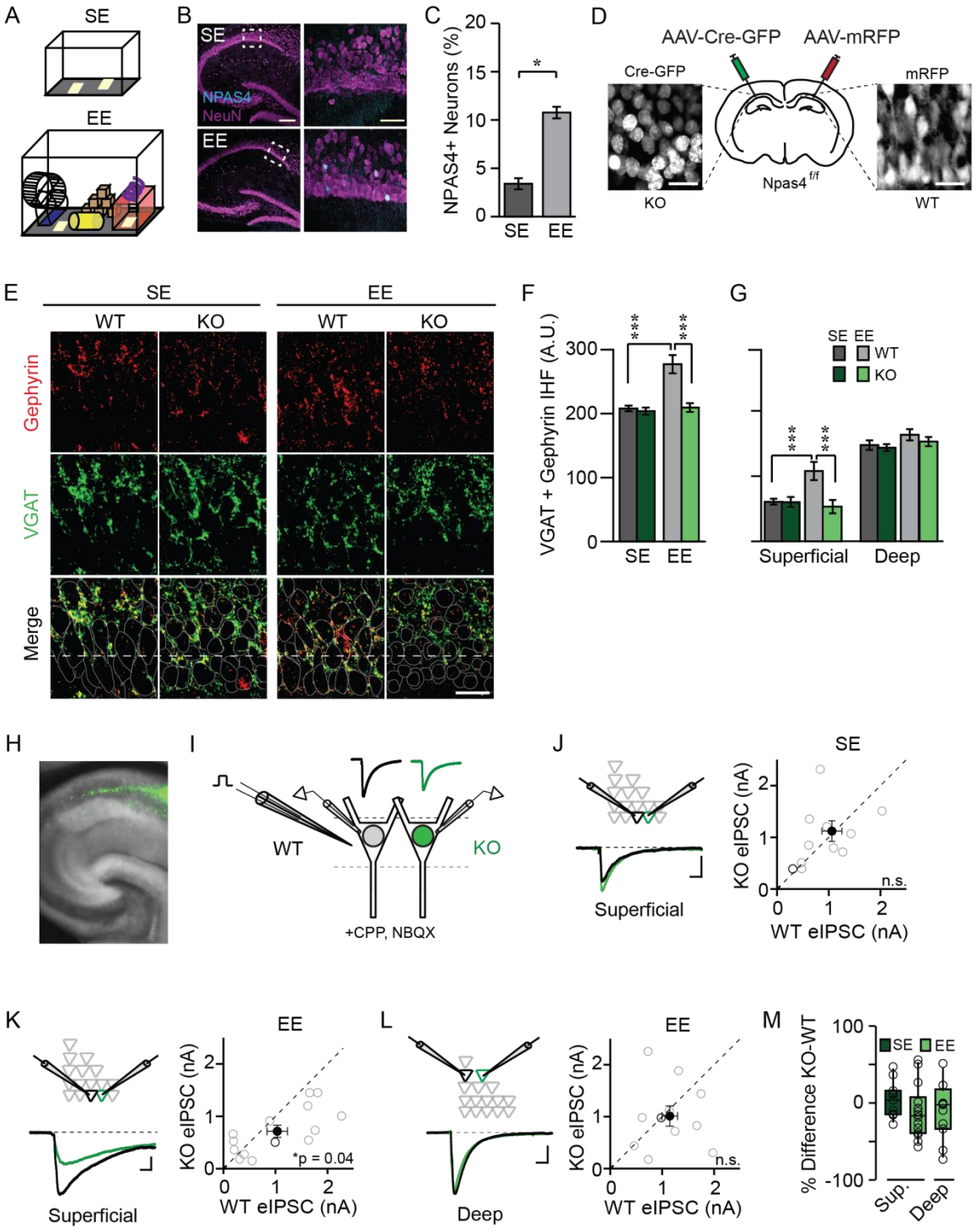
A
SE
EE
B
SE
EE
NPAS4
NeuN
C
NPAS4+ Neurons (%)
20
15
10
5
0
*
SE
EE
D
AAV-Cre-GFP
AAV-mRFP
Cre-GFP
mRFP
Npas4 f/f
KO
WT
E
SE
EE
WT
KO
WT
KO
Gephyrin
VGAT
Merge
F
VGAT + Gephyrin IHF (A.U.)
300
200
100
0
***
***
SE
EE
G
SE EE
WT
KO
***
***
Superficial
Deep
H
I
WT
KO
+CPP, NBQX
J
Superficial
SE
KO eIPSC (nA)
WT eIPSC (nA)
n.s.
K
Superficial
EE
KO eIPSC (nA)
WT eIPSC (nA)
*p = 0.04
L
Deep
EE
KO eIPSC (nA)
WT eIPSC (nA)
n.s.
M
% Difference KO-WT
100
0
-100
SE
EE
Sup.
Deep

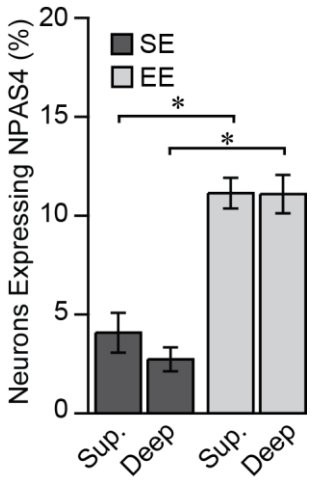

Figure 2.2 Superficial and deep CA1 PNs express NPAS4 equivalently after exploration of an EE

Quantification of NPAS4-positive neurons in superficial and deep CA1 PNs in mice from SE and EE (n=10 sections over 3 mice per condition). * indicates $p<0.05$.

Figure 2.3 NPAS4 regulates CCKBC input onto PNs in superficial CA1

(A) Schematic representation of PN with CCKBC and PVBC synaptic input. CCKBC boutons contain CB1Rs and utilize N-type VGCCs for neurotransmission; PVBCs express PV and utilize P/Q-type VGCCs for neurotransmission. (B) Representative images of gephyrin (red), VGAT (green), CB1R (blue) and merged IHC from WT and Npas4 KO hemispheres from mice housed in SE and EE. Gray outlines in merged images represent cell body outlines in WT condition (mRFP expression) or cell nuclei in Npas4 KO condition (Cre-GFP expression). (C) Quantification of CCKBC synapses (overlap of gephyrin, VGAT, and CB1R) in superficial vs deep CA1 of WT and Npas4 KO hemispheres from mice housed in SE and EE (SE: n=7 sections across 3 mice, EE: n=4-6 sections across 3 mice). *** indicates $p<0.001$. (D) ω-Agtx-IVA (0.3 μM) is used to isolate synaptic release from CCKBCs. Example eIPSCs from WT (black) and Npas4 KO PNs in superficial CA1 (left) of enriched mice. Pairwise comparison of eIPSCs recorded in neighboring WT and Npas4 KO neurons (right, n=16 pairs). (E) ω-Agtx-IVA (0.3 μM) is used to isolate synaptic release from CCKBCs. Example eIPSCs from WT (black) and Npas4 KO PNs in deep CA1 (left) of enriched mice. Pairwise comparison of eIPSCs recorded in neighboring WT and Npas4 KO neurons (right, n=13 pairs). (F) The ratio of eIPSCs recorded from WT and KO pairs across CA1 subregions, normalized by the sum of the WT and KO eIPSC amplitudes.

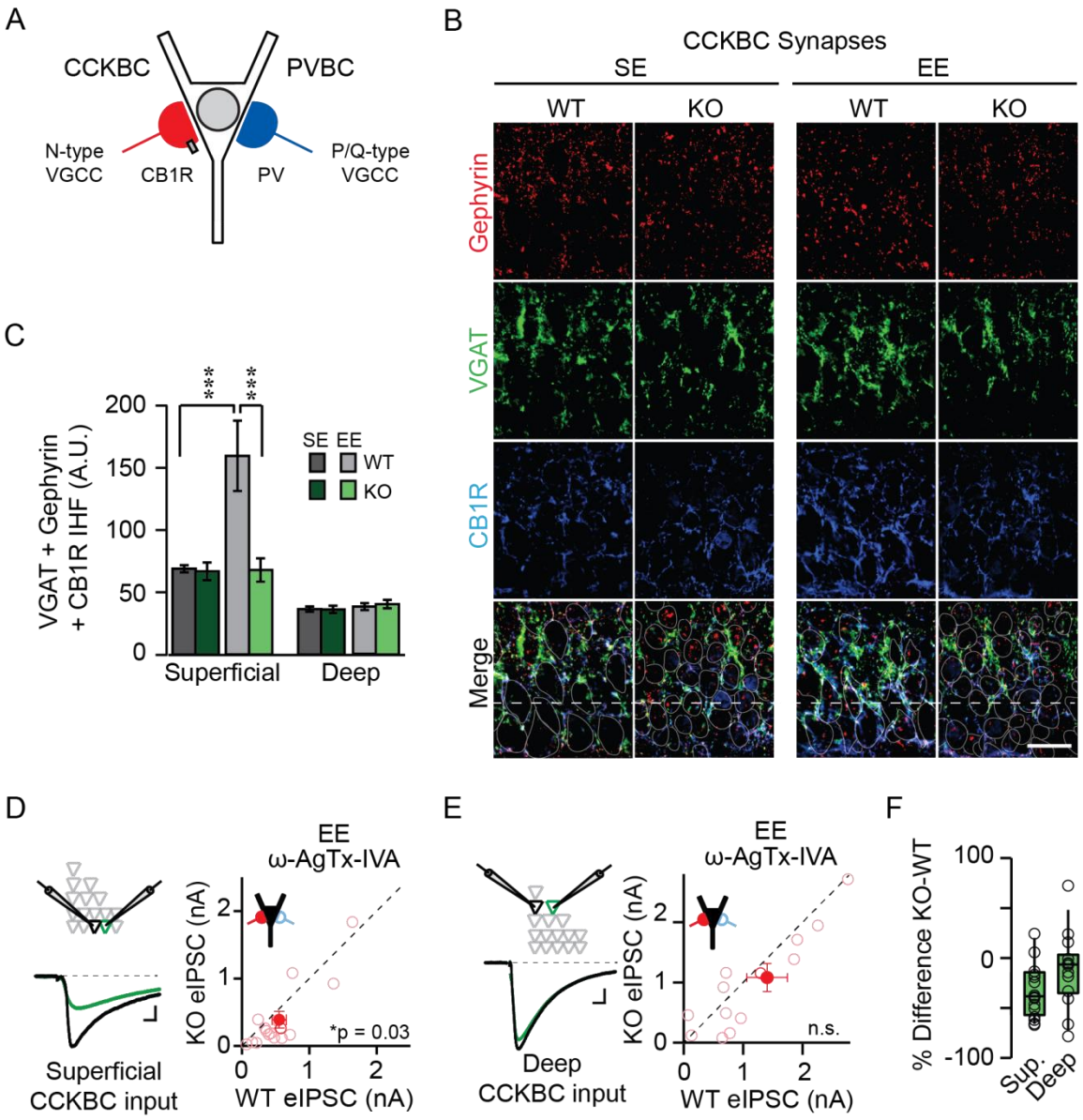
A
CCKBC
PVBC
N-type VGCC
CB1R
PV
P/Q-type VGCC
B
CCKBC Synapses
SE
EE
WT
KO
WT
KO
Gephyrin
VGAT
CB1R
Merge
C
VGAT + Gephyrin + CB1R IHF (A.U.)
200
150
100
50
0
***
***
SE EE
WT
KO
Superficial
Deep
D
EE
ω-AgTx-IVA
KO eIPSC (nA)
WT eIPSC (nA)
*p = 0.03
Superficial CCKBC input
E
EE
ω-AgTx-IVA
KO eIPSC (nA)
WT eIPSC (nA)
n.s.
Deep CCKBC input
F
% Difference KO-WT
100
0
-100
Sup.
Deep

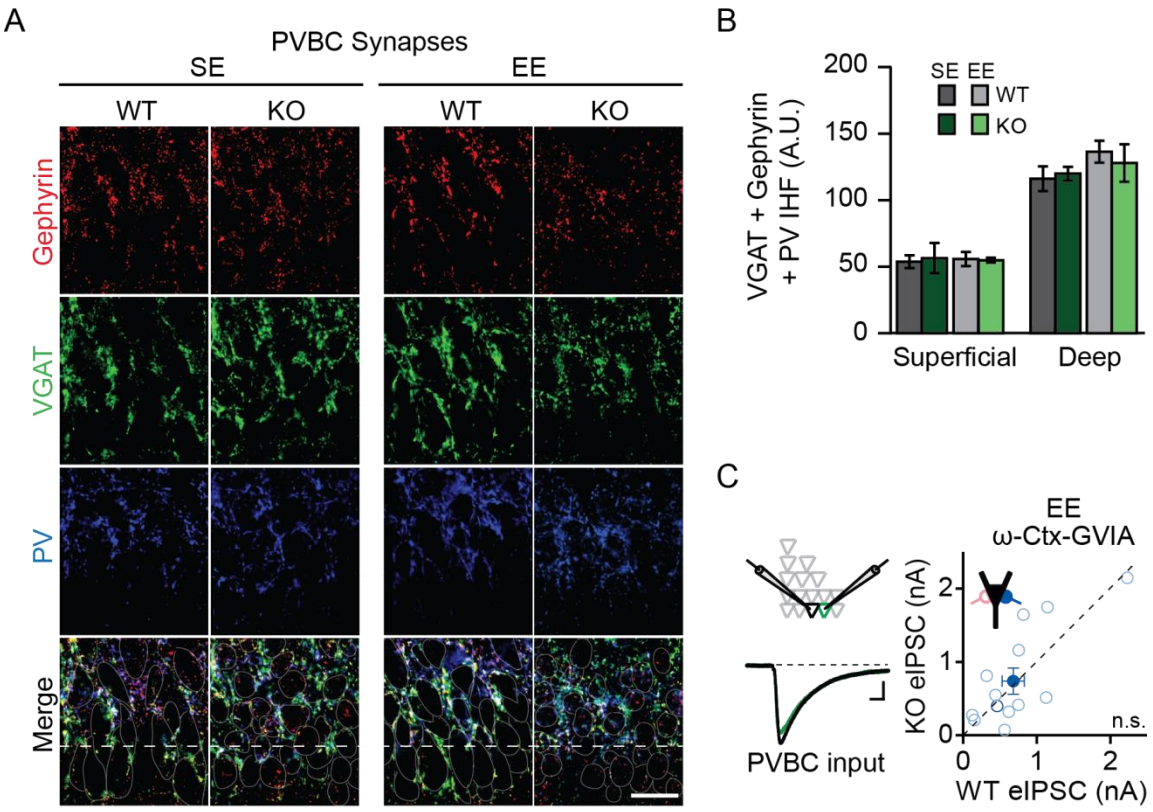

Figure 2.4 NPAS4 does not regulate PVBC input into PNs in CA1

(A) Representative images of gephyrin (red), VGAT (green), PV (blue) and merged IHC from WT and Npas4 KO hemispheres from mice housed in SE and EE. Gray outlines in merged images represent cell body outlines in WT condition (mRFP expression) or cell nuclei in Npas4 KO condition (Cre-GFP expression). Scale bar = 20 □m. (B) Quantification of PVBC synapses (overlap of gephyrin, VGAT, and PV) in superficial vs deep CA1 of WT and Npas4 KO hemispheres from mice housed in SE and EE (SE: n=3-4 sections per condition from 3 mice; EE: n=5 sections per condition from 3 mice). (C) ω-CTx-GVIA (1 μM) is used to isolate synaptic release from CCKBCs. Example eIPSCs from WT (black) and Npas4 KO PNs (left) in superficial CA1 (left) of enriched mice. Pairwise comparison of eIPSCs recorded in neighboring WT and Npas4 KO neurons (right, n=16 pairs).

Figure 2.5 NPAS4 regulates synaptic connectivity between individual CCKBC-PN pairs

(A-C) Electrophysiological characteristics of PV INs and CCK INs: (A) example spike trains (scale bar=50 ms, 10 mV), (B) AP full width at half max (FWHM, n = 17 PV INs, 20 CCK INs) and (C) AP frequency adaptation over time (n = 17 PV INs, 19 CCK INs). (D) Schematic of recording from synaptically connected PN and CCKCB pairs for panels E-I. Whole-cell patch clamp recordings were established from CCKBCs and synaptically connected WT or Npas4 KO PNs. (E) Examples of CCKBC APs (top) and PN uIPSCs (bottom) recorded from WT (black) and Npas4 KO (green) PNs. Scale bars=25 ms, 50 pA. (F) Average uIPSC amplitudes measured from CCKBC-WT PN and CCKBC-Npas4 KO PN pairs (WT: n=12 pairs, KO: n=10 pairs). Open circles represent individual data points. * indicates $p<0.05$. (G) Average uIPSCs recorded from CCKBC-PN pairs for WT and Npas4 KO PNs (top) and normalized by amplitude (bottom). scale bars = 10 ms, 100 pA. (H) 10-90% uIPSC rise times from CCKBC-PN pairs with WT and Npas4 KO PNs (WT: n=12 pairs, KO: n=10 pairs). (I) Decay time constant (τ) for CCKBC-PN pairs with WT and Npas4 KO PNs (WT: n=12 pairs, KO: n=10 pairs). Measurements from WT neurons are shown in black/gray; KO neurons in green. Data are shown as mean ± SEM. * indicates $p<0.05$. ***indicates $p<0.001$.

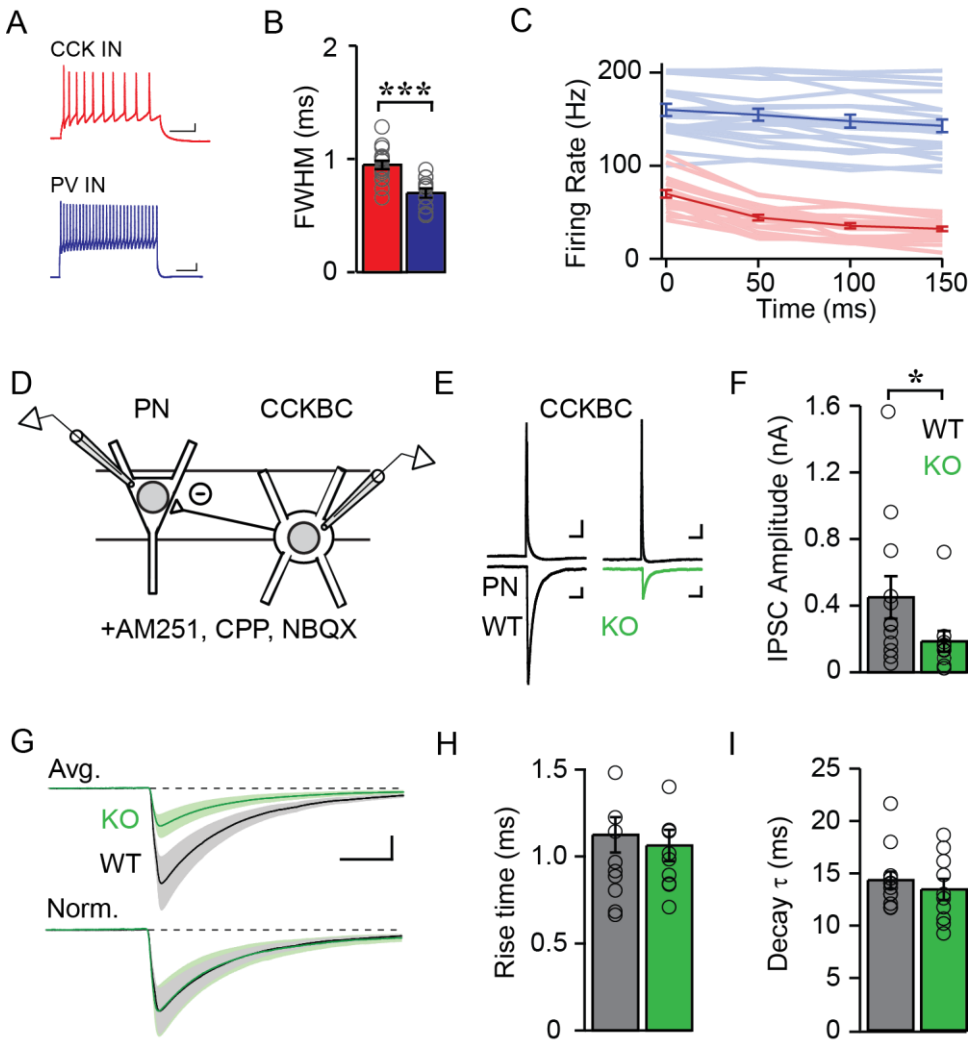
A
CCK IN
PV IN
B
FWHM (ms)
2
1
0
***
C
Firing Rate (Hz)
200
100
0
0
50
100
150
Time (ms)
D
PN
CCKBC
+AM251, CPP, NBQX
E
CCKBC
PN
WT
KO
F
IPSC Amplitude (nA)
1.6
1.2
0.8
0.4
0
*
WT
KO
G
Avg.
KO
WT
Norm.
H
Rise time (ms)
1.5
1.0
0.5
0
I
Decay τ (ms)
25
20
15
10
5
0

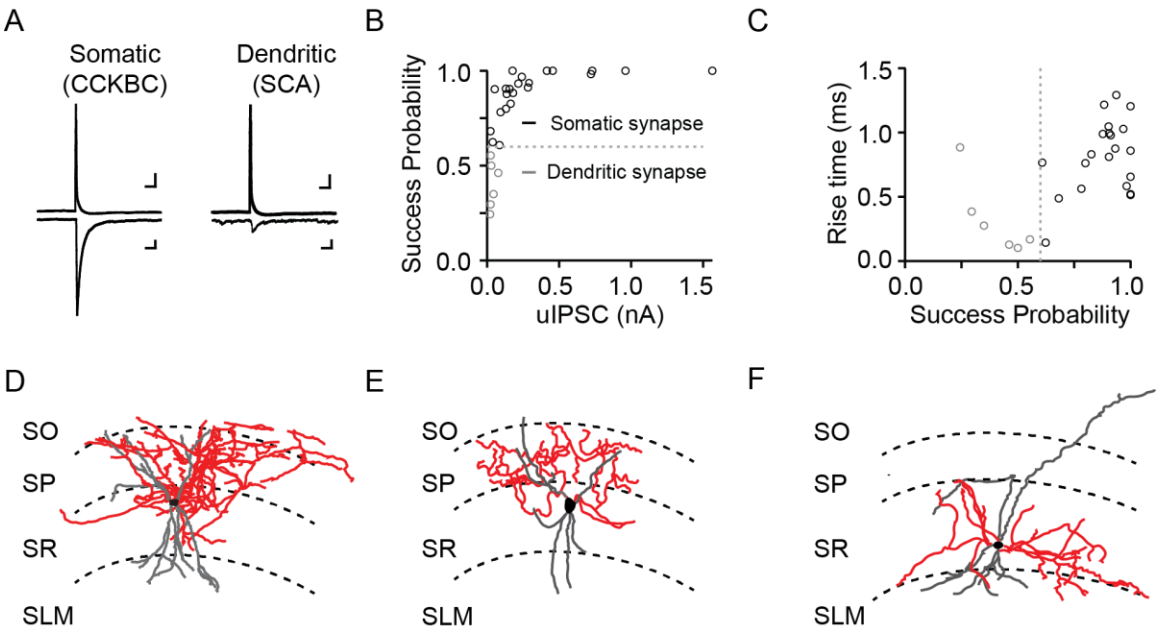

Figure 2.6 CCKBCs were differentiated from dendritic SCA interneurons by synaptic properties and morphology

(A) Examples of presynaptic APs (top) and postsynaptic uIPSCs (bottom) recorded from somatic (left) and dendritic-targeting (right) INs and PNs, respectively. Scale bar = 25 ms, 50 pA. (B) uIPSC amplitudes vs. success probability for pairs of somatic and dendritic-targeting CCK INs and PNs. Dotted line represents the cut off for somatic vs. dendritic synapses (Success probability = 0.6). (C) Success probability vs. uIPSC 10%-90% rise times (ms) for somatic and dendritic-targeting CCK INs. (D-F) Biocytin reconstructions of CCK INs, including CCKBCs (D-E) and SCA (F), showing axon (red) and dendrites (gray).

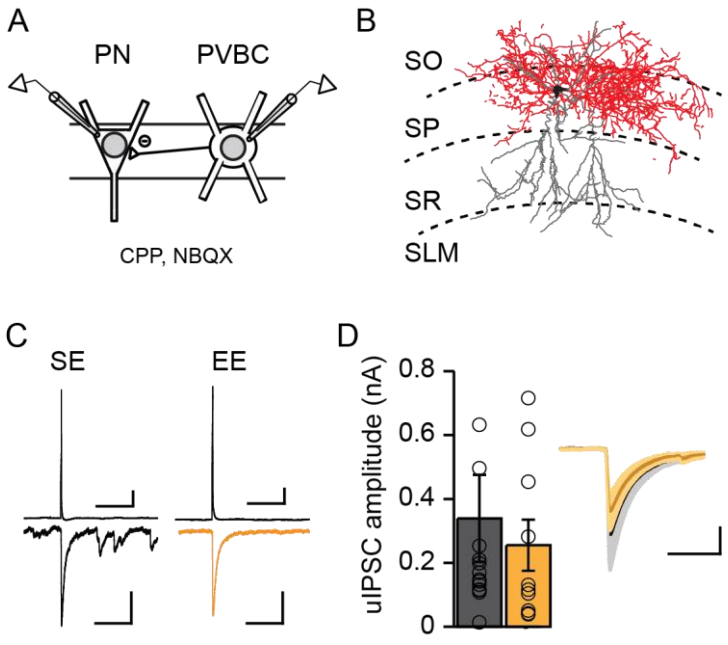

Figure 2.7 Enrichment does not affect connectivity strength between individual PVBCs and PNs in CA1

(A) Schematic of recording configuration. Whole-cell patch clamp recordings were obtained from fast-spiking putative PVBCs and postsynaptically connected WT PNs in acute hippocampal slices from mice in SE or EE. (B) Example reconstruction of a biocytin-filled PVBC, showing axon (red) and dendrites (gray). (C) Example APs and uIPSCs from PVBC-PN pairs in slices from mice in SE (black) and EE (orange). Scale bars = 50 ms and 10 mV (top) or 50 ms and 100 pA (bottom). (D) uIPSC amplitude recorded from PVBC-PN pairs is in slices from mice in SE (gray) and EE (orange) (n=14 SE and n=10 EE pairs). Scale bars = 25 ms, 100 pA.

Figure 2.8 NPAS4 regulates the number of CCKBC synapses onto PNs but does not alter synaptic properties.

(A) Success rate for CCKBC-PN pairs between WT (gray) and Npas4 KO (green) PNs (WT: n=12 pairs, KO: n=10 pairs). Open circles represent individual data points. (B) Left: Example paired-pulse uIPSCs from WT (black) and Npas4 KO (green) PNs recorded from CCKBC-PN pairs with a 20 ms inter-spike interval (ISI). Scale bar=10 ms, 50 pA. Right: Paired-pulse ratios (PPRs) for ISIs of 20 ms, 50 ms, 200 ms, and 1000 ms different between CCK-PN pairs with WT and Npas4 KO PNs (WT: n=12 pairs, KO: n=10 pairs for all ISIs). (C) uIPSC amplitude versus coefficient of variation (CV) for CCKBC-PN pairs with WT and Npas4 KO PNs (WT: n=12 pairs, KO: n=10 pairs). (D) Average CV of the uIPSC recorded in WT and Npas4 KO PNs (WT: n=12 pairs, KO: n=10 pairs). (E) uIPSC amplitude and variance of amplitude for CCKBC-PN pairs with WT (black) and Npas4 KO (green) PNs. Dotted lines indicate best linear fit for WT (R2= 0.89) and Npas4 KO (R2= 0.84) data (WT: n=12 pairs, KO: n=10 pairs). (F) Example traces of 20 APs at 40 Hz and resulting uIPSC trains for CCKBC-PN pairs with WT (black) and Npas4 KO (green) PNs. Dashed box indicates window analyzed for asynchronous release (100 ms after end of AP train). Scale bars=100 ms, 10 mV (top) and 100 ms, 100 pA (bottom). (G) Asynchronous event amplitude measured during the 100 ms following the end of CCKBC AP firing for CCKBC-PN pairs with WT and Npas4 KO PNs (WT: n=6; KO: n=8 for amplitude). Data are shown as mean ± SEM. * $p<0.05$; ** $p<0.01$.

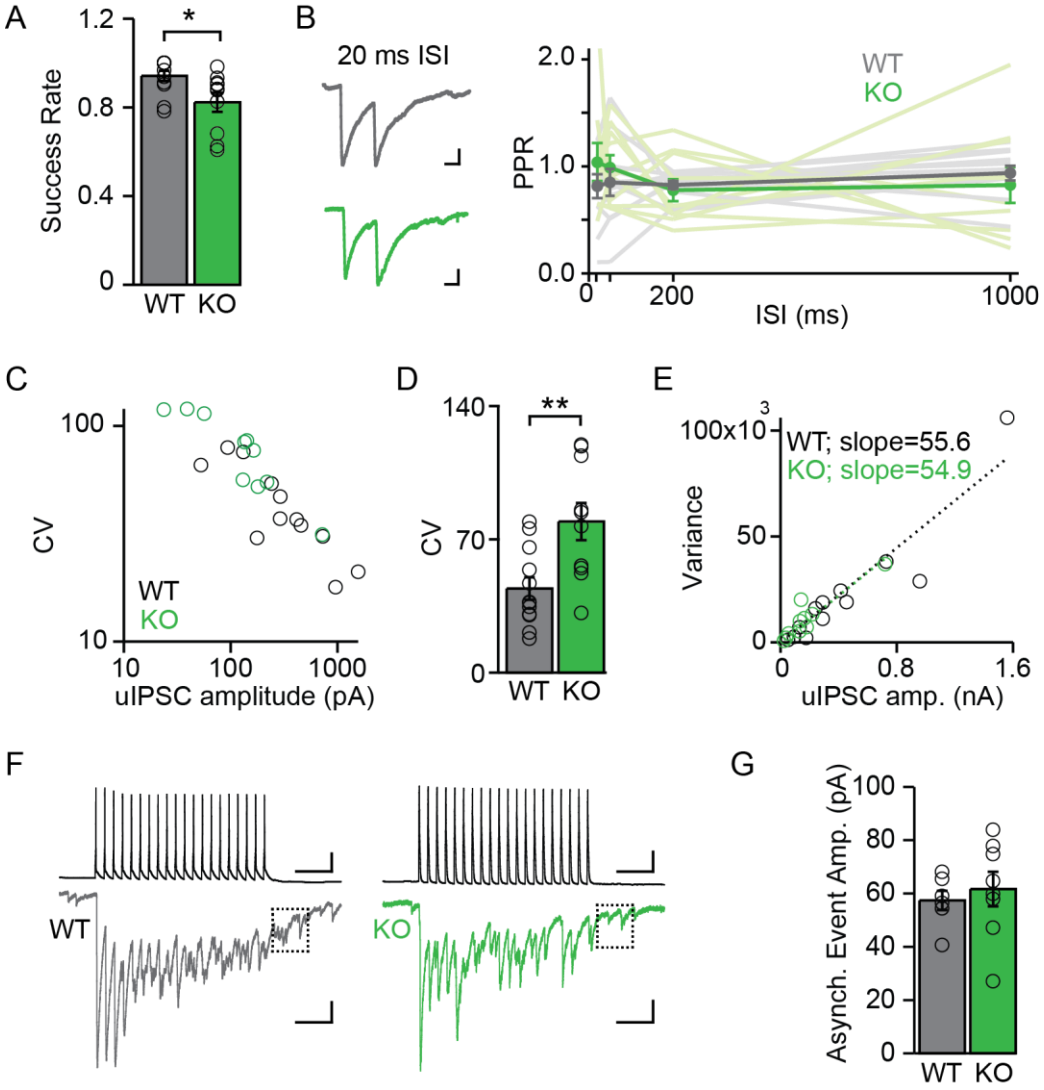
A
Success Rate
1.2
0.8
0.4
0
*
WT KO
B
20 ms ISI
PPR
2.0
1.0
0.0
WT
KO
0
200
1000
ISI (ms)
C
CV
100
10
WT
KO
10
100
1000
uIPSC amplitude (pA)
D
CV
140
70
0
**
WT KO
E
Variance
100x10^3
50
0
WT; slope=55.6
KO; slope=54.9
0
0.8
1.6
uIPSC amp. (nA)
F
WT
KO
G
Asynch. Event Amp. (pA)
100
80
60
40
20
0
WT KO

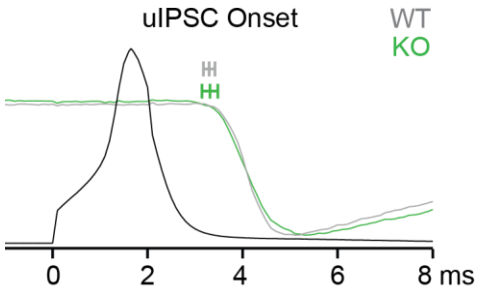

Figure 2.9 CCKBC-PN pairs with WT and KO PNs have similar uIPSC onset times

Latency to uIPSC onset between CCKBC-PN pairs with WT and *Npas4* KO PNs (WT: n=12 pairs, KO: n=10 pairs). Example AP from a CCKBC (*black*) and uIPSCs from WT (*gray*) and *Npas4* KO (*green*) PNs, respectively. Latency to uIPSC onset between CCKBC-PN pairs with WT and Npas4 KO PNs (WT: n=12 pairs, KO: n=10 pairs). Example AP from a CCKBC (black) and uIPSCs from WT (gray) and Npas4 KO (green) PNs, respectively.

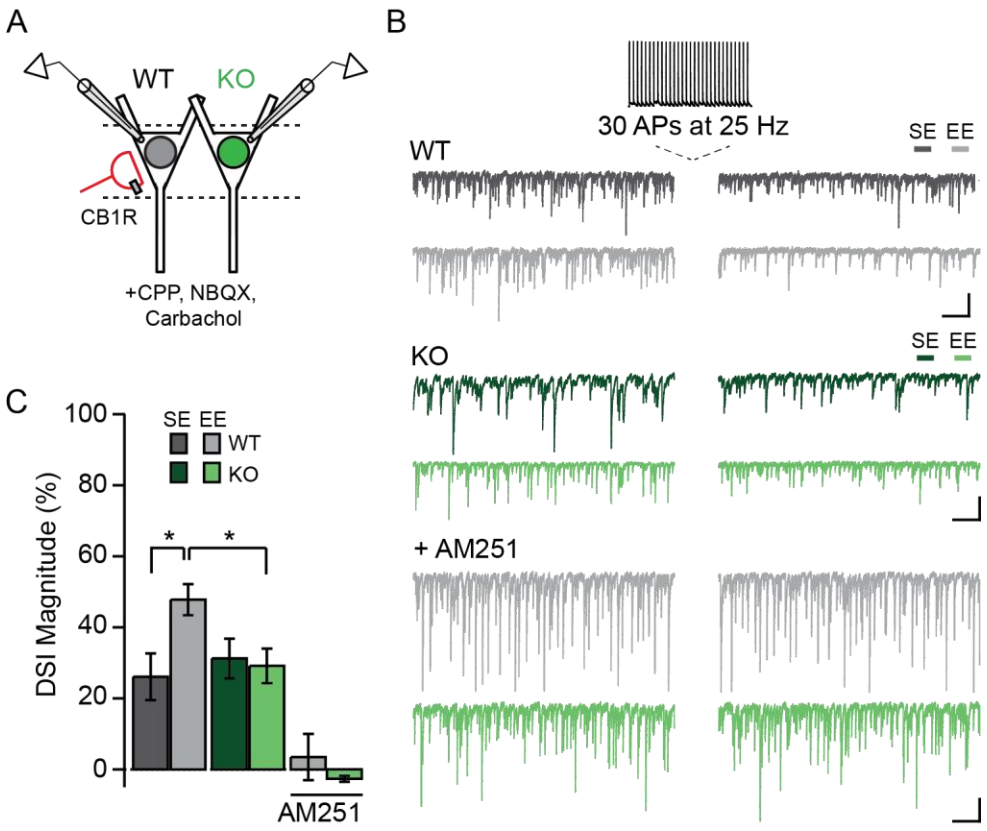

Figure 2.10 Experience-driven NPAS4 expression enhances the magnitude of DSI in PNs

(A) Schematic of recording configuration. Whole-cell patch clamp recordings were obtained from WT and Npas4 KO PNs. Spontaneous IPSCs were recorded before and after inducing DSI by firing 30 APs at 25 Hz in PN. (B) Example traces from experiment described in (A) from WT (gray) and Npas4 KO (green) PNs recorded in slices from mice in SE, EE, and EE in the presence of the CB1R antagonist AM251 (5 μM). (C) DSI magnitude (% reduction in charge after DSI induction) in WT and KO PNs from mice taken from SE, EE, and EE recorded in the presence of AM251 (SE: n=15 WT and 14 KO PNs, EE: n=14 WT and 13 KO PNs, EE with AM251: n=11 WT and 11 KO PNs). All scale bars = 500 ms, 200 pA. Data are shown as mean ± SEM. * $p<0.05$.

Chapter 2 is a reprint of the material as it appears in Hartzell AL, Martyniuk KM, Brigidi GS, Djaja NA, and Bloodgood BL (2018). The IEG *Npas4* recruits CCK basket cell synapses and enhances cannabinoid-mediated plasticity in the mouse hippocampus. In revision. The dissertation author was the primary investigator and author of this paper.

References

Alen, F., Ramirez-Lopez, M. T., Gomez de Heras, R., Rodriguez de Fonseca, F., & Orio, L. (2013). Cannabinoid receptors and cholecystokinin in feeding inhibition. Vitam Horm, 92, 165-196. doi:10.1016/B978-0-12-410473-0.00007-6

Baimbridge, K. G., Peet, M. J., McLennan, H., & Church, J. (1991). Bursting response to current-evoked depolarization in rat ca1 pyramidal neurons is correlated with lucifer yellow dye coupling but not with the presence of calbindin-d28k. Synapse, 7(4), 269-277. doi:10.1002/syn.890070404

Bartos, M., & Elgueta, C. (2012). Functional characteristics of parvalbumin- and cholecystokinin-expressing basket cells. Journal of Physiology-London, 590(4), 669-681. doi:DOI 10.1113/jphysiol.2011.226175

Berninger, B., Schinder, A. F., & Poo, M. M. (1999). Synaptic reliability correlates with reduced susceptibility to synaptic potentiation by brain-derived neurotrophic factor. Learn Mem, 6(3), 232-242.

Bloodgood, B. L., Sharma, N., Browne, H. A., Trepman, A. Z., & Greenberg, M. E. (2013). The activity-dependent transcription factor npas4 regulates domain-specific inhibition. Nature, 503(7474), 121-125. doi:10.1038/nature12743

Boudkkazi, S., Carlier, E., Ankri, N., Caillard, O., Giraud, P., Fronzaroli-Molinieres, L., & Debanne, D. (2007). Release-dependent variations in synaptic latency: A putative code for short- and long-term synaptic dynamics. Neuron, 56(6), 1048-1060. doi:10.1016/j.neuron.2007.10.037

Boudkkazi, S., Fronzaroli-Molinieres, L., & Debanne, D. (2011). Presynaptic action potential waveform determines cortical synaptic latency. J Physiol, 589(Pt 5), 1117-1131. doi:10.1113/jphysiol.2010.199653

Bullitt, E. (1990). Expression of c-fos-like protein as a marker for neuronal activity following noxious stimulation in the rat. J Comp Neurol, 296(4), 517-530. doi:10.1002/cne.902960402

Cai, D. J., Aharoni, D., Shuman, T., Shobe, J., Biane, J., Song, W., . . . Silva, A. J. (2016). A shared neural ensemble links distinct contextual memories encoded close in time. Nature, 534(7605), 115-118. doi:10.1038/nature17955

Carlson, G., Wang, Y., & Alger, B. E. (2002). Endocannabinoids facilitate the induction of ltp in the hippocampus. Nat Neurosci, 5(8), 723-724. doi:10.1038/nn879

Cembrowski, M. S., Wang, L., Sugino, K., Shields, B. C., & Spruston, N. (2016). Hipposeq: A comprehensive rna-seq database of gene expression in hippocampal principal neurons. Elife, 5, e14997. doi:10.7554/eLife.14997

Chevaleyre, V., & Castillo, P. E. (2004). Endocannabinoid-mediated metaplasticity in the hippocampus. Neuron, 43(6), 871-881. doi:10.1016/j.neuron.2004.08.036

Cobb, S.R., Buhl, E.H., Halasy, K., Paulson, O., & Somogyi, P. (1995). Synchronization of neuronal activity in the hippocampus by individual GABAertgic interneurons. Nature 378(6552): 75-78.

Cope, D. W., Maccaferri, G., Marton, L. F., Roberts, J. D., Cobden, P. M., & Somogyi, P. (2002). Cholecystokinin-immunopositive basket and schaffer collateral-associated interneurones target different domains of pyramidal cells in the ca1 area of the rat hippocampus. Neuroscience, 109(1), 63-80.

Cowansage, K. K., Shuman, T., Dillingham, B. C., Chang, A., Golshani, P., & Mayford, M. (2014). Direct reactivation of a coherent neocortical memory of context. Neuron. doi:10.1016/j.neuron.2014.09.022

Danielson, N. B., Zaremba, J. D., Kaifosh, P., Bowler, J., Ladow, M., & Losonczy, A. (2016). Sublayer-specific coding dynamics during spatial navigation and learning in hippocampal area ca1. Neuron, 91(3), 652-665. doi:10.1016/j.neuron.2016.06.020

Daw, M. I., Tricoire, L., Erdelyi, F., Szabo, G., & McBain, C. J. (2009). Asynchronous transmitter release from cholecystokinin-containing inhibitory interneurons is widespread and target-cell independent. J Neurosci, 29(36), 11112-11122. doi:10.1523/JNEUROSCI.5760-08.2009

Del Castillo, J., & Katz, B. (1954). Quantal components of the end-plate potential. J Physiol, 124(3), 560-573.

Del Pino, I., Brotons-Mas, J. R., Marques-Smith, A., Marighetto, A., Frick, A., Marin, O., & Rico, B. (2017). Abnormal wiring of cck+ basket cells disrupts spatial information coding. Nat Neurosci, 20(6), 784-792. doi:10.1038/nn.4544

Dubruc, F., Dupret, D., & Caillard, O. (2013). Self-tuning of inhibition by endocannabinoids shapes spike-time precision in ca1 pyramidal neurons. J Neurophysiol, 110(8), 1930-1944. doi:10.1152/jn.00099.2013

Dudok, B., Barna, L., Ledri, M., Szabo, S. I., Szabadits, E., Pinter, B., . . . Katona, I. (2015). Cell-specific storm super-resolution imaging reveals nanoscale organization of cannabinoid signaling. Nat Neurosci, 18(1), 75-86. doi:10.1038/nn.3892

Foster, K. A., & Regehr, W. G. (2004). Variance-mean analysis in the presence of a rapid antagonist indicates vesicle depletion underlies depression at the climbing fiber synapse. Neuron, 43(1), 119-131. doi:10.1016/j.neuron.2004.06.022

Fruh, S., Romanos, J., Panzanelli, P., Burgisser, D., Tyagarajan, S. K., Campbell, K. P., . . . Fritschy, J. M. (2016). Neuronal dystroglycan is necessary for formation and maintenance of functional cck-positive basket cell terminals on pyramidal cells. J Neurosci, 36(40), 10296-10313. doi:10.1523/JNEUROSCI.1823-16.2016

Garner, A. R., Rowland, D. C., Hwang, S. Y., Baumgaertel, K., Roth, B. L., Kentros, C., & Mayford, M. (2012). Generation of a synthetic memory trace. Science, 335(6075), 1513-1516. doi:10.1126/science.1214985

Geiller, T., Royer, S., & Choi, J. S. (2017). Segregated cell populations enable distinct parallel encoding within the radial axis of the ca1 pyramidal layer. Exp Neurobiol, 26(1), 1-10. doi:10.5607/en.2017.26.1.1

Gingrich, K. J., Roberts, W. A., & Kass, R. S. (1995). Dependence of the gabaa receptor gating kinetics on the alpha-subunit isoform: Implications for structure-function relations and synaptic transmission. J Physiol, 489 (Pt 2), 529-543.

Glickfeld, L. L., Atallah, B. V., & Scanziani, M. (2008). Complementary modulation of somatic inhibition by opioids and cannabinoids. J Neurosci, 28(8), 1824-1832. doi:10.1523/JNEUROSCI.4700-07.2008

Glickfeld, L. L., & Scanziani, M. (2006). Distinct timing in the activity of cannabinoid-sensitive and cannabinoid-insensitive basket cells. Nat Neurosci, 9(6), 807-815. doi:10.1038/nn1688

Guenthner, C. J., Miyamichi, K., Yang, H. H., Heller, H. C., & Luo, L. (2013). Permanent genetic access to transiently active neurons via trap: Targeted recombination in active populations. Neuron, 78(5), 773-784. doi:10.1016/j.neuron.2013.03.025

Hefft, S., & Jonas, P. (2005). Asynchronous gaba release generates long-lasting inhibition at a hippocampal interneuron-principal neuron synapse. Nature Neuroscience, 8(10), 1319-1328. doi:Doi 10.1038/Nn1542

Katona, I., Sperlagh, B., Sik, A., Kafalvi, A., Vizi, E. S., Mackie, K., & Freund, T. F. (1999). Presynaptically located cb1 cannabinoid receptors regulate gaba release from axon terminals of specific hippocampal interneurons. J Neurosci, 19(11), 4544-4558.

Kerchner, G. A., & Nicoll, R. A. (2008). Silent synapses and the emergence of a postsynaptic mechanism for ltp. Nat Rev Neurosci, 9(11), 813-825. doi:10.1038/nrn2501

Lavoie, A. M., & Twyman, R. E. (1996). Direct evidence for diazepam modulation of gabaa receptor microscopic affinity. Neuropharmacology, 35(9-10), 1383-1392.

Le Bé, J.-V., Silberberg, G., Wang, Y., & Markram, H. (2007). Morphological, electrophysiological, and synaptic properties of corticocallosal pyramidal cells in the neonatal rat neocortex. Cerebral Cortex, 17(9), 2204-2213. doi:10.1093/cercor/bhl127

Lee, S. H., Marchionni, I., Bezaire, M., Varga, C., Danielson, N., Lovett-Barron, M., . . . Soltesz, I. (2014). Parvalbumin-positive basket cells differentiate among hippocampal pyramidal cells. Neuron, 82(5), 1129-1144. doi:10.1016/j.neuron.2014.03.034

Lin, Y., Bloodgood, B. L., Hauser, J. L., Lapan, A. D., Koon, A. C., Kim, T. K., . . . Greenberg, M. E. (2008). Activity-dependent regulation of inhibitory synapse development by npas4. Nature, 455(7217), 1198-1204. doi:10.1038/nature07319

Maccaferri, G., Roberts, J. D., Szucs, P., Cottingham, C. A., & Somogyi, P. (2000). Cell surface domain specific postsynaptic currents evoked by identified gabaergic neurones in rat hippocampus in vitro. J Physiol, 524 Pt 1, 91-116.

Marx, M., Gunter, R. H., Hucko, W., Radnikow, G., & Feldmeyer, D. (2012). Improved biocytin labeling and neuronal 3d reconstruction. Nat Protoc, 7(2), 394-407. doi:10.1038/nprot.2011.449

Masurkar, A. V., Srinivas, K. V., Brann, D. H., Warren, R., Lowes, D. C., & Siegelbaum, S. A. (2017). Medial and lateral entorhinal cortex differentially excite deep versus superficial ca1 pyramidal neurons. Cell Rep, 18(1), 148-160. doi:10.1016/j.celrep.2016.12.012

Mayford, M., & Reijmers, L. (2015). Exploring memory representations with activity-based genetics. Cold Spring Harb Perspect Biol, 8(3), a021832. doi:10.1101/cshperspect.a021832

Minatohara, K., Akiyoshi, M., & Okuno, H. (2015). Role of immediate-early genes in synaptic plasticity and neuronal ensembles underlying the memory trace. Front Mol Neurosci, 8, 78. doi:10.3389/fnmol.2015.00078

Mody, I., & Pearce, R. A. (2004). Diversity of inhibitory neurotransmission through gaba(a) receptors. Trends Neurosci, 27(9), 569-575. doi:10.1016/j.tins.2004.07.002

Pologruto, T. A., Sabatini, B. L., & Svoboda, K. (2003). Scanimage: Flexible software for operating laser scanning microscopes. Biomed Eng Online, 2, 13. doi:10.1186/1475-925X-2-13

Poncer, J. C., McKinney, R. A., Gahwiler, B. H., & Thompson, S. M. (1997). Either n- or p-type calcium channels mediate gaba release at distinct hippocampal inhibitory synapses. Neuron, 18(3), 463-472.

Pouille, F., & Scanziani, M. (2001). Enforcement of temporal fidelity in pyramidal cells by somatic feed-forward inhibition. Science, 293(5532), 1159-1163. doi:10.1126/science.1060342

Regehr, W. G. (2012). Short-term presynaptic plasticity. Cold Spring Harb Perspect Biol, 4(7), a005702. doi:10.1101/cshperspect.a005702

Reid, C. A., & Clements, J. D. (1999). Postsynaptic expression of long-term potentiation in the rat dentate gyrus demonstrated by variance-mean analysis. J Physiol, 518(Pt 1), 121-130.

Renier, N., Adams, E. L., Kirst, C., Wu, Z., Azevedo, R., Kohl, J., . . . Tessier-Lavigne, M. (2016). Mapping of brain activity by automated volume analysis of immediate early genes. Cell, 165(7), 1789-1802. doi:10.1016/j.cell.2016.05.007

Sabatini, B. L., & Regehr, W. G. (1999). Timing of synaptic transmission. Annu Rev Physiol, 61, 521-542. doi:10.1146/annurev.physiol.61.1.521

Thomson, A. M., Bannister, A. P., Hughes, D. I., & Pawelzik, H. (2000). Differential sensitivity to zolpidem of ipsps activated by morphologically identified ca1 interneurons in slices of rat hippocampus. Eur J Neurosci, 12(2), 425-436.

Valero, M., Cid, E., Averkin, R. G., Aguilar, J., Sanchez-Aguilera, A., Viney, T. J., . . . de la Prida, L. M. (2015). Determinants of different deep and superficial ca1 pyramidal cell dynamics during sharp-wave ripples. Nat Neurosci, 18(9), 1281-1290. doi:10.1038/nn.4074

Wilson, R. I., & Nicoll, R. A. (2001). Endogenous cannabinoids mediate retrograde signalling at hippocampal synapses. Nature, 410(6828), 588-592. doi:10.1038/35069076

Wisden, W., Cope, D., Klausberger, T., Hauer, B., Sinkkonen, S. T., Tretter, V., . . . Somogyi, P. (2002). Ectopic expression of the gaba(a) receptor alpha6 subunit in hippocampal pyramidal neurons produces extrasynaptic receptors and an increased tonic inhibition. Neuropharmacology, 43(4), 530-549.

Ye, L., Allen, W. E., Thompson, K. R., Tian, Q., Hsueh, B., Ramakrishnan, C., . . . Deisseroth, K. (2016). Wiring and molecular features of prefrontal ensembles representing distinct experiences. Cell, 165(7), 1776-1788. doi:10.1016/j.cell.2016.05.010

Younts, T. J., & Castillo, P. E. (2014). Endogenous cannabinoid signaling at inhibitory interneurons. Curr Opin Neurobiol, 26, 42-50. doi:10.1016/j.conb.2013.12.006

Zhu, P. J., & Lovinger, D. M. (2007). Persistent synaptic activity produces long-lasting enhancement of endocannabinoid modulation and alters long-term synaptic plasticity. J Neurophysiol, 97(6), 4386-4389. doi:10.1152/jn.01228.2006

Chapter 3. What's next?

Hypotheses regarding the molecular mechanism underlying *Npas4*-mediated CCK basket cell synapse recruitment

Our findings in Chapter 2 establish a role for the inducible transcription factor (ITF) NPAS4 in mediating the recruitment of cholecystokinin-expressing basket cell (CCKBC) synapses onto the somata of hippocampal pyramidal neurons (PNs). 270 putative *Npas4* target genes have been identified (Bloodgood et al., 2013; Lin et al., 2008), including 16 that affect inhibitory input onto PNs in organotypic hippocampal slice cultures (Bloodgood et al., 2013). However, the molecular mechanism responsible for CCKBC-specific synapse recruitment downstream of activity-dependent *Npas4* expression, without affecting parvalbumin-expressing basket cell (PVBC) synapses, is unknown.

CCKBC and PVBC synapses, while both form on PN somata in CA1, exhibit vast biological differences, including in their protein, channel, and receptor composition, raising the possibility that these subtypes employ different mechanisms for synapse formation. While many of the differences in protein expression have been described, little is known about subtype-specific synapse formation or adaptations of the GABAergic postsynaptic density. Recently, however, the neuronal dystrophin-glycoprotein complex (DGC) was identified as a necessary component for the formation of CCKBC terminals on pyramidal cells, but not for PVBC terminals (Früh et al., 2016). This provides a compelling starting point for investigating the molecular mechanism by which *Npas4* mediates the cell type-specific recruitment of CCKBC synapses onto active PNs.

The DGC is a transmembrane complex most well-known for its role in muscle tissue, as mutations of its components can lead to muscular dystrophies (McNally and Pytel, 2007). However, defects in the DGC are also associated with several brain pathologies, ranging from mild cognitive impairment to gross neuronal migration disorders (Waite et al., 2012). Indeed, the DGC is expressed in neurons in the central nervous system, where it interacts with the extracellular matrix and is involved in the organization of γ-aminobutyric acid $(GABA)_A$ receptors in the postsynaptic density at a subset of inhibitory synapses (**Figure 3.1**; Brunig et al., 2002; Kneusel et al., 1999; Levi et al., 2002; Waite et al., 2012).

In contrast to the muscular DGC, the neuronal DGC has not been purified as an intact complex, and its constituent proteins have therefore only been probed via immunochemical experiments (Waite et al., 2012). However, several of the components and their associations with one another are fairly well-understood (**Figure 3.1**). The central component of the complex is dystroglycan, for which a single gene encodes an extracellular α isoform, which can interact with the extracellular matrix, and a transmembrane β isoform. The β isoform binds the cytoplasmic protein dystrophin, which interacts with actin filaments. The neurexin-neuroligin trans-synaptic adhesion complexes allow the recruitment of the scaffolding protein gephyrin to the inhibitory postsynaptic density, where it mediates $GABA_A$ receptor clustering. This occurs following neuroligin2-mediated activation of the guanine nucleotide exchange factor (GEF) collybistin. The DGC is potentially recruited to the postsynaptic density through a neurexin-dystroglycan interaction and an indirect interaction with neuroligin2 mediated by the scaffolding protein S-SCAM. SynArfGEF (IQSeq3) associates with the complex,

where it might act to induce actin remodeling via activation of Arf6, resulting in the stabilization of $GABA_A$ receptors (Waite et al., 2012).

Recently, it was shown that ablation of dystroglycan in neurons leads to the selective loss of presynaptic terminals expressing CCK8, vesicular GABA transporter 3 (Vglut3), and cannabinoid receptor 1 (CB1R), all of which are specifically expressed at CCKBC synapses, in the pyramidal cell layer of CA1 (**Figure 3.2**; Früh et al., 2016). In contrast, presynaptic terminals expressing synaptotagmin2 and PV are not affected by neuronal ablation of dystroglycan (Früh et al., 2016). This phenotype is found both in adults and at a time point right after initial synaptogenesis during development, consistent with a role for dystroglycan in synapse formation (Früh et al., 2016).

In order to address the hypothesis that NPAS4 might mediate selective CCKBC synapse recruitment through this mechanism, we queried the list of putative NPAS4 targets (Bloodgood et al., 2013; Lin et al., 2008) for genes that encode components of the DGC. The most promising candidate that emerged is the gene IQ Motif and Sec7 Domain 3 (*IQsec3/SynArfGEF/BRAG3*), which encodes for a guanine nucleotide exchange factor that is associated with the DGC (Fukaya et al., 2011). NPAS4 is bound at the putative *IQsec3* promotor and expression is induced by neural activity, but not in NPAS4 knockout tissue (Bloodgood et al., 2013). Furthermore, *IQsec3* knockdown via RNA interference (RNAi) reveals a miniature inhibitory postsynaptic current (mIPSC) phenotype in organotypic hippocampal slices cultures (Bloodgood et al., 2013). It is therefore possible that *Npas4* drives the activity-dependent selective recruitment of CCKBC synapses by upregulating expression of *IQsec3*.

Another component of the DGC that shows a less promising connection to NPAS4 expression, but is worth mentioning, is *β-dystrobrevin*. *β-dystrobrevin* is bound at its promoter by NPAS4, but its expression does not appear inducible by neural activity (Bloodgood et al., 2013). Similarly, a candidate that appears to be an NPAS4 target but is less tightly associated with the DGC is nitric oxide synthase 1 adaptor protein (*NOS1AP*), which is bound by NPAS4, inducible by neural activity and results in an mIPSC phenotype when knocked down in organotypic hippocampal cultures by RNAi (Bloodgood et al., 2013). *NOS1AP* is an adaptor protein that binds to neuronal nitric oxide synthase (nNOS) via a C-terminal PDZ-binding domain and an N-terminal phosphotyrosine binding domain that can mediate interactions between nNOS and other proteins. *NOS1AP* has been shown to associate with the DGC component syntrophin (Brenman et al., 1996).

Working out the biological mechanism of *Npas4*-mediated selective recruitment of CCKBC synapses is one of the major next challenges toward fully understanding how an ITF can impact cellular and circuit computations. The challenge arises in part because little is known about subtype-specific differences in synapse formation or adaptations of the inhibitory postsynaptic density. Luckily, recent insight into the DGC as a CCKBC-specific mechanism for synapse formation (Früh et al., 2016) has provided a convenient starting point for investigating this question, made promising by the DGC components, most notably *IQSec3*, that are putative NPAS4 targets involved in the regulation of inhibitory synapses (Bloodgood et al., 2013). Testing this hypothesis would require asking whether conditional loss of *IQSec3* in an *Npas4* wildtype (WT) background is necessary and sufficient to replicate the *Npas4* knockout *(*KO) phenotype *in vivo*.

Seeking the interneuron subtypes mediating the proximal dendritic *Npas4* phenotype

Npas4 is a known regulator of inhibitory synapses in two domains along the somato-dendritic axis of CA1 PNs. While Chapter 2 describes significant progress made toward understanding the specifics of the *Npas4*-mediated recruitment of somatic inhibitory synapses, the *Npas4*-dependent loss of inhibitory synapses in the proximal apical dendrites (Bloodgood et al., 2013) has not been similarly investigated. Parallel to the case of somatic inhibition, inhibitory synapses formed on the proximal apical dendrites of CA1 pyramidal cells originate primarily from two interneuron (IN) subtypes, the CCK-expressing Schaffer collateral-associated INs (SCAs; **Figure 3.3**) and the PV-expressing bistratified INs (**Figure 3.4**). However, relative to the case of somatic inhibition, less is known about the channels and receptors governing neurotransmission from these IN subtypes, making the molecular and pharmacological toolkit available to probe their synapses less complete.

Both SCA and bistratified INs have axons that ramify almost exclusively in stratum radiatum (SR) and stratum oriens (SO), overlapping with the Schaffer collateral pathway originating from the CA3 subregion (Buhl et al., 1994; Cope et al., 2002; Pawelzik et al., 1997; Vida et al., 1998). The somata of SCAs are located predominantly in SR (Cope et al., 2002; Vida et al., 1998), with dendrites spanning all hippocampal layers (Klausberger, 2009). The somata of bistratified INs, in contrast, reside mainly in the pyramidal cell layer, with a small subset located in SO. The dendrites of bistratified cells extend into SO and SR, where, like PVBCs, they form gap junctions extensively with other interneurons (Klausberger, 2009).

SCAs are molecularly and physiologically similar to CCKBCs, differing mainly in their morphology. Both cell types express cholecystokinin and cannabinoid receptor 1 (CB1R) and share very similar passive and active membrane properties (Cope et al., 2002). Likewise, bistratified INs are molecularly and physiologically analogous to PVBCs, with the major difference being their morphology. In addition to parvalbumin, they express somatostatin, neuropeptide Y, and high levels of extrasynaptic $GABA_A$ receptors containing the α1 subunit (Baude et al., 2007; Klausberger et al., 2004; Pawelzik et al., 2002). Like PVBCs, they are fast-spiking, however they exhibit longer membrane time constants and higher input resistances relative to their basket cell counterparts (Buhl et al., 1996).

Because of the similar protein expression and physiological profiles between the two basket cell subtypes and their dendritic IN counterparts, the fact that CCKBC synapses are recruited downstream of *Npas4* expression might lead one to hypothesize that SCA INs mediate the dendritic *Npas4* phenotype. However, while *Npas4* expression results in the enhancement of somatic inhibition, it mediates the loss of dendritic inhibition (**Figure 1.11**; Bloodgood et al., 2013), suggesting that the dendritic and somatic inhibitory synapse phenotypes might result from entirely different signaling pathways. This necessitates an agnostic approach to the question of which proximal dendrite-targeting INs make the affected synapses.

As opposed to somatic inhibition, which functions to gate the spiking behavior of pyramidal cells, dendritic inhibition serves a role in governing the integration of excitatory signals arriving to the dendrites (Miles et al., 1996). Further functional distinctions can be drawn between subgroups of inhibitory synapses based on where on

the PN dendritic arbor they form. In order for excitatory input to propagate to the PN soma and cause the cell to spike, it must converge with other sources of depolarization or back-propagating action potentials (bAPs) to cause regenerative dendritic spikes (Spruston et al., 2008). The influence of inhibitory synapses formed onto dendritic spines is compartmentalized within the spine, where activation can attenuate calcium transients and grade the strength of the excitatory input in a compartmentalized manner (Chiu et al., 2013). In contrast, inhibitory synapses formed onto a dendritic shaft can affect all excitatory inputs made onto that branch segment (Liu, 2004), and in this way can shape excitatory signal propagation by both attenuating bAPs and directly curbing dendritic spikes (Golding and Spruston, 1998; Higley, 2014; Major et al., 2013; Stokes et al., 2014).

The ability of inhibitory synapses to attenuate the summation of coactive excitatory inputs suggests that they can affect synapse plasticity in addition to directly shaping the spread of depolarizing current. Indeed, modeling of inhibitory and excitatory synapses on PN dendrites suggests that the activation of inhibitory synapses can alter the likelihood of long-term potentiation or depression expressed at the excitatory synapses, depending on the relative locations of the inhibitory and excitatory inputs (Bar-Ilan et al., 2012). Furthermore, uncaging GABA at locations where bAPs and glutamate uncaging converge can result in the shrinkage and elimination of spines within 15 μm of the uncaging site (Hayama et al., 2013).

While *Npas4* has been shown to reduce inhibition in the proximal apical dendrites of CA1 PNs (Bloodgood et al., 2013), it is not known whether *Npas4* expression affects all inhibitory synapses equally, or preferentially destabilizes those made onto dendritic

spines versus shafts. Furthermore, it is not known whether specific subtypes of dendrite-projecting interneurons bias their synapses to dendritic spines versus shafts of CA1 PNs. However, the distribution of inhibitory synapses onto different compartments of CA1 PNs along the somato-dendritic axis offers some insight. Oblique dendrites of CA1 PNs, particularly those in distal SO and SR, are densely spiny, whereas proximal apical and basal dendrites are sparsely spiny or spine-free (Megias et al., 2001). Furthermore, inhibitory synapses forming on dendritic spines have only been observed in stratum lacunosum-moleculare (SLM) (Megias et al., 2001). Since no *Npas4* inhibitory synapse phenotype has been observed in SLM (Bloodgood et al., 2013), it is likely that activity-dependent *Npas4* expression results in the loss of dendritic shaft inhibitory synapses in proximal SR. If this is indeed true, *Npas4*-mediated loss of dendritic inhibitory synapses could permit enhanced convergence of excitatory signals and heightened potential for the expression of plasticity at excitatory synapses. On the circuit level, activation of a common input that synapses onto multiple PNs would result in coordinated plasticity at the coincidentally active synapses, resulting in the potential for the cohort of PNs to fire as an ensemble during subsequent activation of the common input. Due to the differences in membrane properties, excitatory drives, and neuromodulatory responses between subtypes of INs, the identity of the IN subtype(s) that make the dendritic synapses destabilized by *Npas4* expression could shift the circuit conditions under which heightened excitability and plasticity of dendritic excitatory inputs could occur. These hypotheses motivate the importance of investigating the dendritic *Npas4* phenotype and the resulting changes for circuit activity and plasticity in more detail.

Implications of Npas4-mediated CCKBC synapse recruitment on place cell emergence and function

Investigating the consequences of *Npas4* expression at the microcircuit level will provide important insight into how neural activity, through changing gene expression, is capable of altering connections between neurons and thereby shaping information flow through the hippocampal circuit. The experiments in Chapter 2 demonstrate that activity-dependent *Npas4* expression results in the recruitment of CCKBC synapses to the somata of CA1 PNs. In the behaving animal, many CA1 PNs that express *Npas4* in response to exploration of a novel environment are likely place cells, activated when an animal traverses the cells' spatial receptive fields, or "place fields" (O'Keefe and Dostrovsky, 1971; O'Keefe and Nadel, 1978; Wilson and McNaughton, 1993). An obvious next question is how the *Npas4*-mediated recruitment of CCKBC synapses affects the hippocampal circuit on a functional level, particularly with respect to place cells and spatial navigation. Unfortunately, due in part to the difficulties in genetically targeting CCKBCs, limited data exists on the firing characteristics or role of this IN subtype during awake behavior. Still, the available data combined with known properties of CCKBCs suggests some compelling and experimentally tractable hypotheses.

In mice in which CCKBCs lack the tyrosine kinase receptor ErbB4 globally throughout development, the number of CCKBC synapses made onto both PNs and PVBCs is dramatically reduced in both juvenile and adult mice (Del Pino et al., 2017), allowing for the best available glimpse into the role of CCKBCs in hippocampal function, despite obvious caveats in interpretation. In this model, the power of theta oscillations during exploration was decreased and spatial learning and memory deficits were observed (Del Pino et al., 2017). Spatial code by putative place cells was also defective, with fewer PNs demonstrating spatial selectivity and recorded single units showing

reduced spatial coherence and spatial information per spike (**Figure 3.5**; Del Pino et al., 2017). Additionally, place cells in ErbB4 conditional knock out mice were less stable across the recording epoch. While these results support a role for CCKBC inhibition in hippocampal function, particularly with regard to spatial coding, it is unknown whether these defects arise from developmental loss of CCKBC input or whether they would persist in the case of acute loss of CCKBC synapses after development, which is more analogous to the *Npas4* KO model. Furthermore, since this mouse model drives loss of ErbB4 in CCKBCs in multiple brain regions, including regions upstream of CA1 such as CA3 and the entorhinal cortex (EC), it is impossible to know whether the observed deficits arise from local CA1 circuit defects, or whether they arise from upstream changes. Still, it motivates an investigation into whether a CA1-specific loss of *Npas4* post-developmentally would result in a consistent spatial coding phenotype.

Other hypotheses regarding a role for CCKBC inhibition in cognitively-relevant hippocampal circuit dynamics involve the expression of depolarization-induced suppression of inhibition (DSI) at CCKBC-PN synapses. When an animal traverses into the center of a PN's place field, the PN will discharge action potentials at around 20 Hz (Leutgeb et al., 2007). This stimulus is sufficient to trigger endocannabinoid release from the PN and induce DSI at CCKBC-PN synapses (Neu et al., 2007), relieving the PN of a portion of its GABAergic input while other cells are still inhibited by CCKBC activity. The consequence of this would be a situation in which the "signal" of the place cell would be enhanced relative to the "noise" of the circuit, effectively enhancing the signal-to-noise ratio of the network (Bartos and Elgueta, 2012; Klausberger & Somogyi, 2008). A compelling question to ask, therefore, is whether activity-driven *Npas4* expression

would enhance the dynamic range of putative place cell activity relative to network activity, allowing PNs with an activity history consistent with *Npas4*-mediated recruitment of CCKBC synapses to achieve a higher signal-to-noise ratio when an animal traverses into a place field.

A second hypothesis for how *Npas4*-mediated recruitment of CCKBC input might shape hippocampal circuit dynamics through DSI expression involves the phenomenon of phase precession (O'Keefe and Recce, 1993). As an animal traverses an environment, an oscillation of the local field potential in the range of 4-7 Hz, termed the theta rhythm, can be observed (Bragin et al., 1995; Buzsaki and Draguhn, 2004). As an animal nears the place field for a particular PN, the PN begins to fire slightly in advance of the peak of the theta wave, with each successive spike occurring earlier and earlier with respect to the local field potential as the animal nears the center of the PN's place field. This phenomenon is termed "phase precession" (**Figure 3.6**; O'Keefe and Recce, 1993). A role for DSI in regulating phase precession was proposed by Fruend et al., 2003. Fruend and colleagues hypothesized that the burst firing of PNs observed when an animal enters their place fields, combined with the activation of cholinergic fibers that occurs with theta activity, are ideal for inducing DSI at CCKBC-PN synapses. The temporary reduction in CCKBC-mediated inhibition in combination with increased excitation of the PN might be the mechanism by which it can dissociate itself from theta entrainment and fire at earlier and earlier phases of the theta cycle as the animal enters its place field. It is interesting to consider, therefore, the possibility that *Npas4*-mediated CCKBC synapse recruitment might enhance phase precession in CA1 PNs.

Our findings in Chapter 2 establish a role for the inducible transcription factor NPAS4 in mediating the recruitment of CCKBC synapses onto the somata of hippocampal PNs, thereby increasing the proportion of their inhibitory somatic input that is susceptible to temporary suppression via DSI expression. These findings open the door to numerous exciting hypotheses regarding how *Npas4* expression might restructure dendritic inhibition in an interneuron subtype-specific manner, shape ensemble firing in the hippocampus, improve the signal-to-noise ratio of place cells, enhance place coding, and augment phase precession in the hippocampus. Perhaps most exciting, however, is that this result provides the first known example of a specific functional output of inducible transcription factor expression and provides novel insight into how neural activity can restructure hippocampal circuits. It also constitutes the only activity-dependent mechanism for CCKBC synapse structural plasticity has thus far been demonstrated.

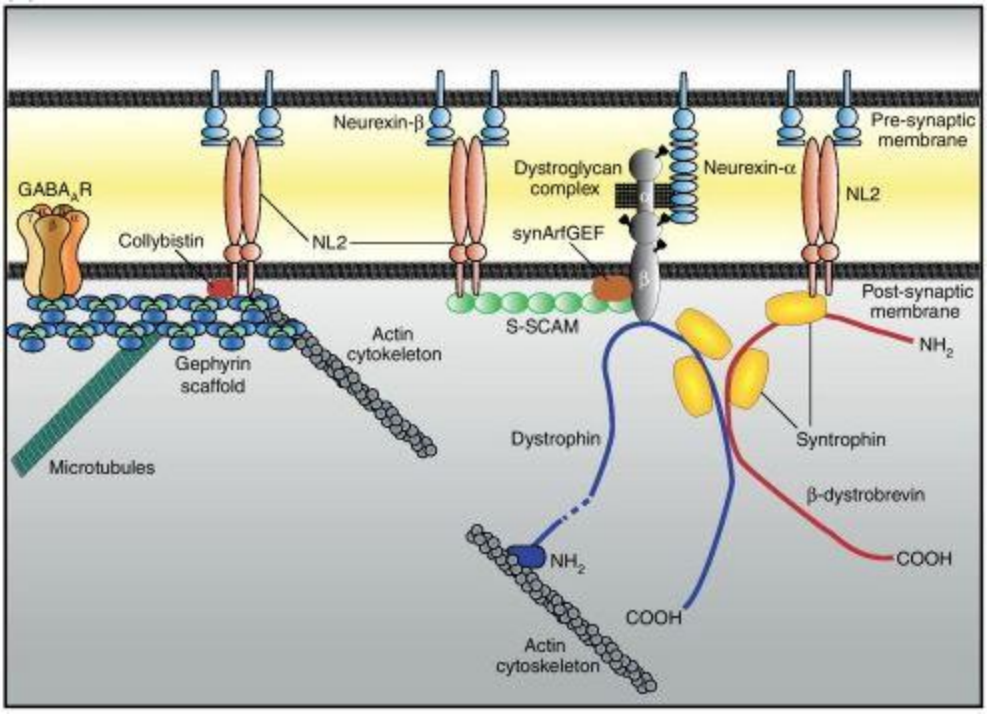

Figure 3.1 Theoretical model of the dystrophin-glycoprotein complex at a neuronal inhibitory synapse

The dystroglycan-glycoprotein complex is associated with a subset of GABAergic synapses in the hippocampus, where it participates in anchoring $GABA_A$ receptors. Neurexin-neuroligin trans-synaptic adhesion complexes allow the recruitment of the scaffolding protein gephyrin to the inhibitory postsynaptic density, where it mediates $GABA_A$ receptor clustering. This occurs following neuroligin2-mediated activation of the GEF collybistin. The DGC is potentially recruited to the postsynaptic density through a neurexin-dystroglycan interaction and an indirect interaction with neuroligin2 mediated by the scaffolding protein S-SCAM. synArfGEF (IQSeq3) associates with the complex, where it might act to induce actin remodeling via activation of Arf6, resulting in stabilization of $GABA_A$ receptors. Reprinted with permission from Waite, A., Brown, S. C., & Blake, D. J. (2012). The dystrophin-glycoprotein complex in brain development and disease. Trends Neurosci, 35(8), 487-496. doi:10.1016/j.tins.2012.04.004.

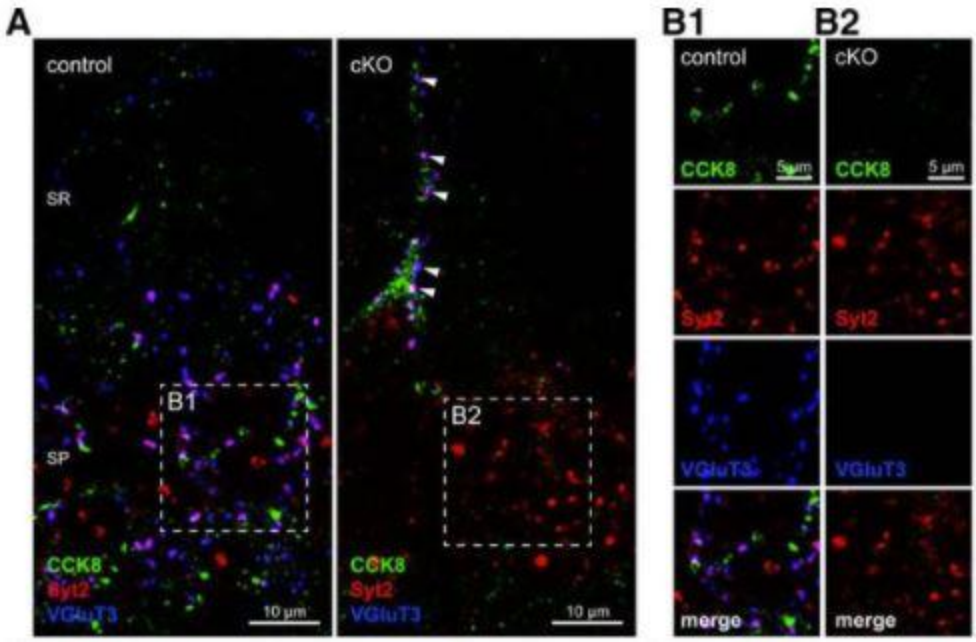

Figure 3.2 Neuronal ablation of dystroglycan results in the specific loss of CCKBC presynaptic terminals from CA1 pyramidal neurons

Ablation of dystroglycan in neurons leads to the selective loss of presynaptic terminals expressing CCK8 and vesicular GABA transporter 3 (Vglut3) in the pyramidal cell layer of CA1, both of which are markers of CCKBC synapses. (A) Immunofluorescent labeling of CCKBC synapse markers CCK8 and Vglut3 are missing around the somata of pyramidal neurons. (B1-B2) Separate channels of (A). Reprinted with permission from Fruh, S., Romanos, J., Panzanelli, P., Burgisser, D., Tyagarajan, S. K., Campbell, K. P., . . . Fritschy, J. M. (2016). Neuronal Dystroglycan Is Necessary for Formation and Maintenance of Functional CCK-Positive Basket Cell Terminals on Pyramidal Cells. J Neurosci, 36(40), 10296-10313. doi:10.1523/jneurosci.1823-16.2016.

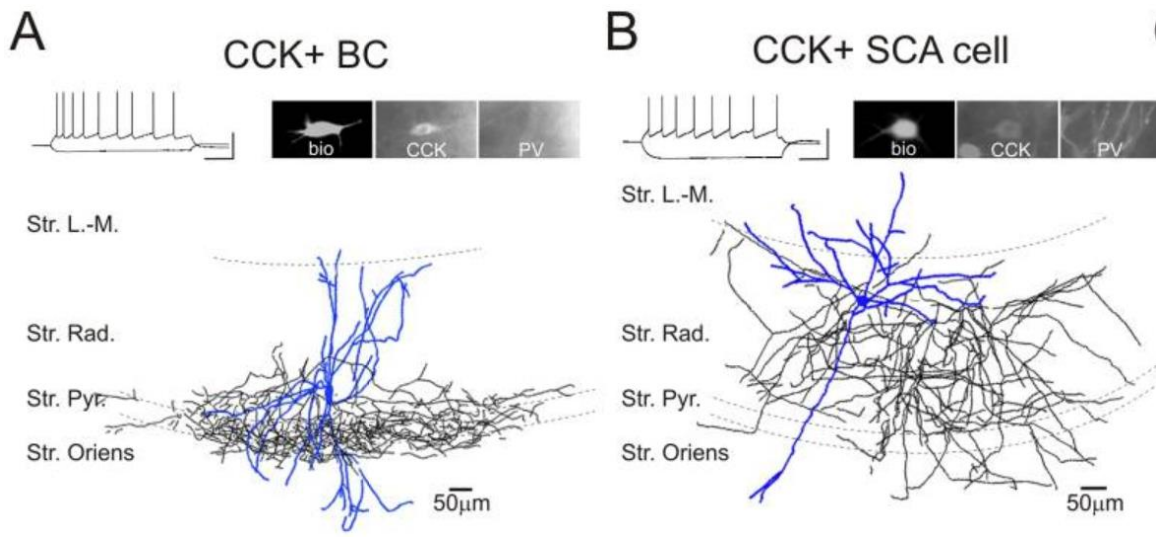

Figure 3.3 Schaffer collateral associated interneurons target the proximal apical and basal dendrites of CA1 pyramidal neurons and share characteristics with CCK basket cells

Schaffer collateral associated interneurons target the proximal apical and basal dendrites of CA1 pyramidal neurons. They share similar electrophysiological and protein expression characteristics with CCK basket cells, such as spike frequency adaptation in response to a depolarizing current pulse and immunoreactivity for cholecystokinin. Image shows example current clamp recordings, immunostaining, and biocytin reconstruction of a CCK-expressing basket cell (A) and Schaffer collateral associated interneuron (B). Reprinted with permission from Lee, S. H., Foldy, C., & Soltesz, I. (2010). Distinct endocannabinoid control of GABA release at perisomatic and dendritic synapses in the hippocampus. J Neurosci, 30(23), 7993-8000. doi:10.1523/jneurosci.6238-09.2010.

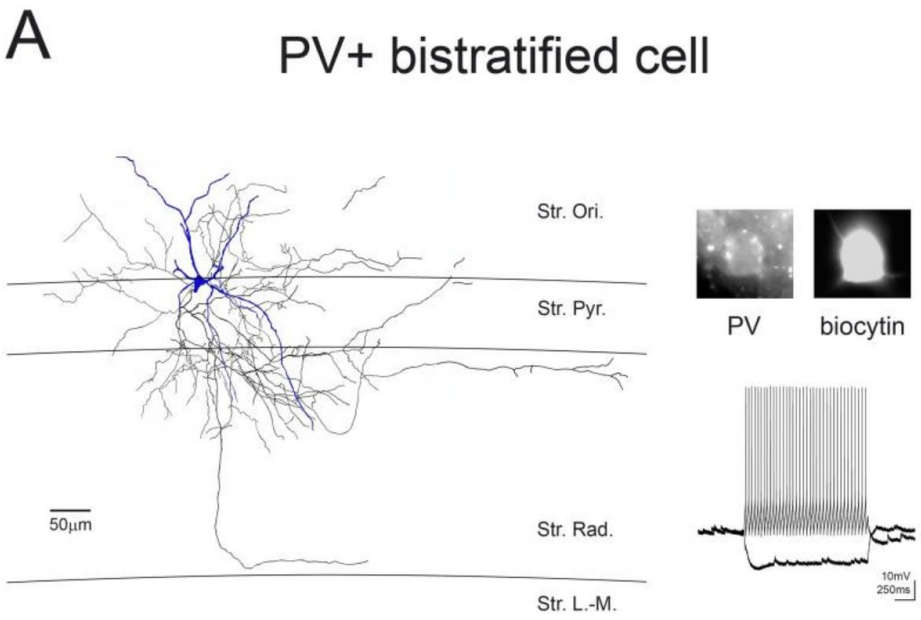

Figure 3.4 Bistratified interneurons target the proximal apical and basal dendrites of CA1 pyramidal neurons and share characteristics with PV basket cells

Bistratified interneurons target the proximal apical and basal dendrites of CA1 pyramidal neurons and share electrophysiological and protein expression characteristics with PV basket cells, including fast, high-frequency action potentials in response to depolarizing current injection and expression of parvalbumin. Image shows example current clamp recordings, immunostaining, and biocytin reconstruction of a PV-expressing bistratified interneuron. Reprinted with permission from Lee, S. Y., Foldy, C., Szabadics, J., & Soltesz, I. (2011). Cell-type-specific CCK2 receptor signaling underlies the cholecystokinin-mediated selective excitation of hippocampal parvalbumin-positive fast-spiking basket cells. J Neurosci, 31(30), 10993-11002. doi:10.1523/jneurosci.1970-11.2011.

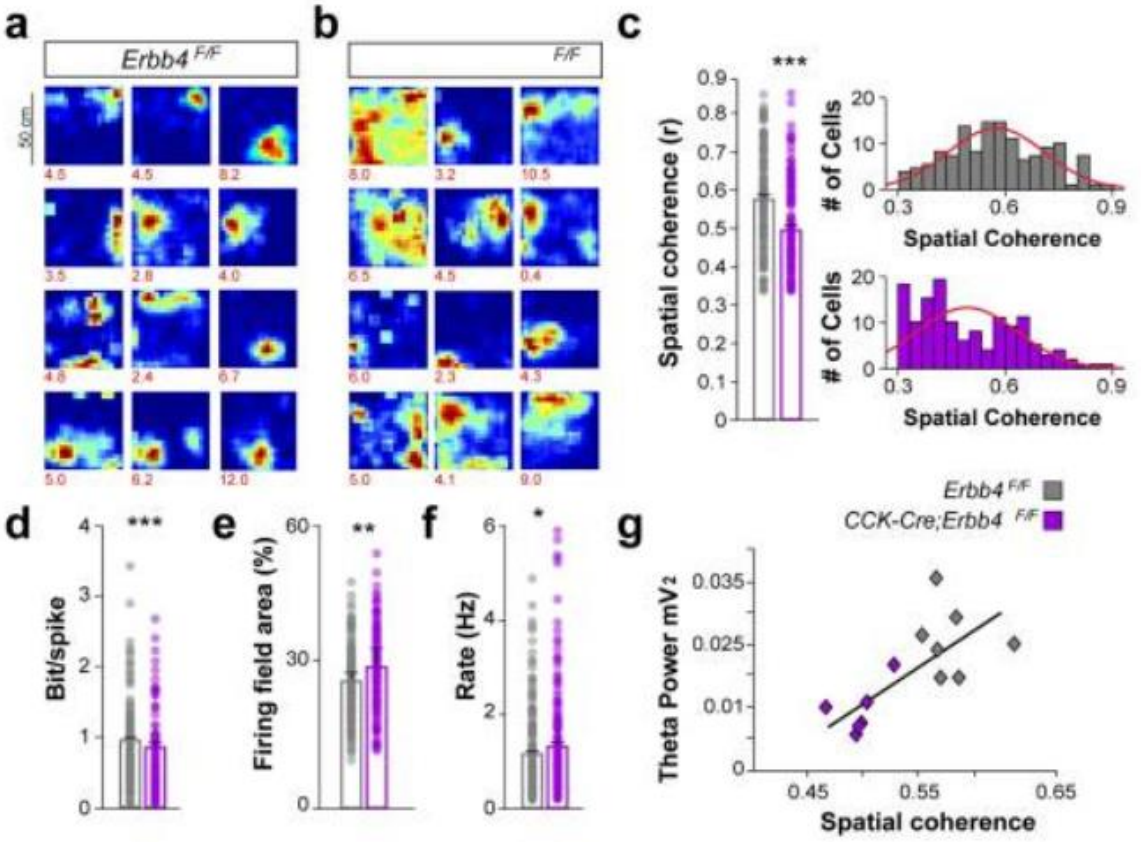

Figure 3.5 CA1 pyramidal cells in ErbB4 conditional knockout mice show defective place coding

ErbB4 conditional knock out mice, in which CCK basket cells do not express ErbB4 and provide significantly less input to hippocampal PNs, show impaired place coding, including lower spatial coherence of place fields and less spatial information per spike. (A-B) Firing rate maps showing place fields in control (A) and ErbB4 conditional knock out (B) mice. (C) Spatial coherence in control and ErbB4 conditional knock out mice. (D-F) Spatial information, firing field areas, and firing rates from control and ErbB4 conditional knock out mice. (G) Correlation between theta power and spatial coherence for control and ErbB4 mutant mice. Reprinted with permission from Del Pino, I., Brotons-Mas, J. R., Marques-Smith, A., Marighetto, A., Frick, A., Marin, O., & Rico, B. (2017). Abnormal wiring of cck+ basket cells disrupts spatial information coding. Nat Neurosci, 20(6), 784-792. doi:10.1038/nn.4544

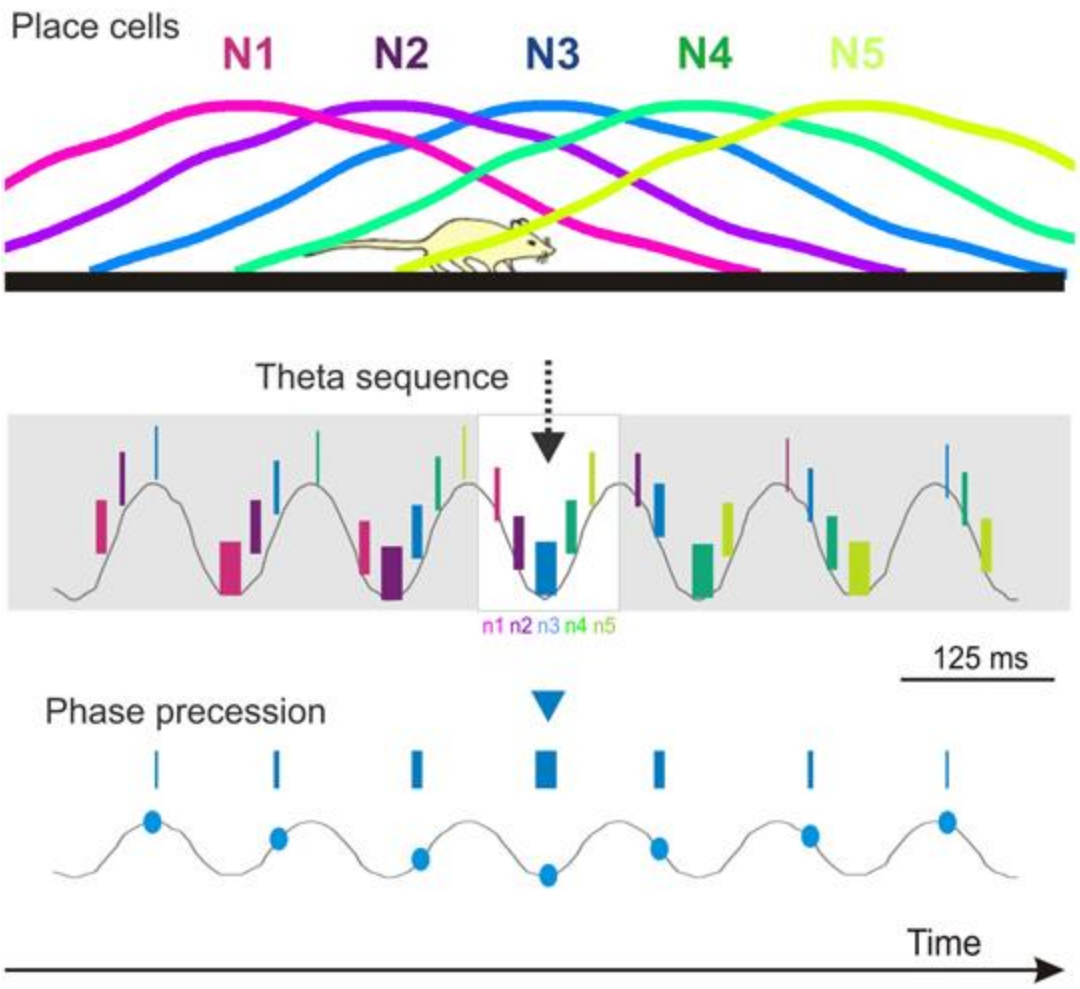

Figure 3.6 Phase precession in the hippocampus

As an animal traverses an environment, an oscillation of the local field potential in the range of 4-7 Hz, termed the theta rhythm, can be observed (Bragin et al., 1995; Buzsaki and Draguhn, 2004). As an animal nears the place field for a particular PN, the PN begins to fire slightly in advance of the peak of the theta wave, with each successive spike occurring earlier and earlier with respect to the local field potential as the animal nears the center of the PN's place field. Top: Place cell sequences of five neurons (n1-n5) firing as a rodent traverses a linear track. Middle: Temporal sequences of the firing of n1-n5 during theta oscillations. Bottom: Phase precession of place cell n3. From Dragoi, G. (2013). Internal operations in the hippocampus: single cell and ensemble temporal coding. Front Syst Neurosci, 7, 46. doi:10.3389/fnsys.2013.00046.

References

Bar-Ilan, L., Gidon, A., & Segev, I. (2012). The role of dendritic inhibition in shaping the plasticity of excitatory synapses. Frontiers in Neural Circuits, 6, 118. http://doi.org/10.3389/fncir.2012.00118

Bartos, M., & Elgueta, C. (2012). Functional characteristics of parvalbumin- and cholecystokinin-expressing basket cells. Journal of Physiology-London, 590(4), 669-681. doi:DOI 10.1113/jphysiol.2011.226175

Baude, A., Bleasdale, C., Dalezios, Y., Somogyi, P., & Klausberger, T. (2007). Immunoreactivity for the GABAA receptor alpha1 subunit, somatostatin and Connexin36 distinguishes axoaxonic, basket, and bistratified interneurons of the rat hippocampus. Cereb Cortex, 17(9), 2094-2107. doi:10.1093/cercor/bhl117

Bloodgood, B. L., Sharma, N., Browne, H. A., Trepman, A. Z., & Greenberg, M. E. (2013). The activity-dependent transcription factor npas4 regulates domain-specific inhibition. Nature, 503(7474), 121-125. doi:10.1038/nature12743

Bragin, A., Jandó, G., Nádasdy, Z., Hetke, J., Wise, K, & Buzsáki, G. (1995). Gamma (40-100 Hz) oscillation in the hippocampus of the behaving rat. J. Neurosci. 15(1 Pt 1): 47-60.

Brenman, J. E., Chao, D. S., Gee, S. H., McGee, A. W., Craven, S. E., Santillano, D. R., . . . Bredt, D. S. (1996). Interaction of nitric oxide synthase with the postsynaptic density protein PSD-95 and alpha1-syntrophin mediated by PDZ domains. Cell, 84(5), 757-767.

Brunig, I., Suter, A., Knuesel, I., Luscher, B., & Fritschy, J. M. (2002). GABAergic terminals are required for postsynaptic clustering of dystrophin but not of GABA(A) receptors and gephyrin. J Neurosci, 22(12), 4805-4813.

Buhl, E.H., Halasy, K., Somogyi, P. (1994). Diverse sources of hippocampal unitary inhibitory postsynaptic potentials and the number of synaptic release sites. Nature 368(6474): 823-828.

Buhl, E. H., Szilagyi, T., Halasy, K., & Somogyi, P. (1996). Physiological properties of anatomically identified basket and bistratified cells in the CA1 area of the rat hippocampus in vitro. Hippocampus, 6(3), 294-305. doi:10.1002/(SICI)1098-1063(1996)6:3<294::AID-HIPO7>3.0.CO;2-N

Buzsáki, G. and Draguhn, A. (2004). Neuronal oscillations in cortical networks. Science 304(5679): 1926-1929.

Chiu, C. Q., Lur, G., Morse, T. M., Carnevale, N. T., Ellis-Davies, G. C., & Higley, M. J. (2013). Compartmentalization of GABAergic inhibition by dendritic spines. Science, 340(6133), 759-762. doi:10.1126/science.1234274

Cope, D. W., Maccaferri, G., Marton, L. F., Roberts, J. D., Cobden, P. M., & Somogyi, P. (2002). Cholecystokinin-immunopositive basket and Schaffer collateral-associated

interneurones target different domains of pyramidal cells in the CA1 area of the rat hippocampus. Neuroscience, 109(1), 63-80.

Del Pino, I., Brotons-Mas, J. R., Marques-Smith, A., Marighetto, A., Frick, A., Marin, O., & Rico, B. (2017). Abnormal wiring of cck+ basket cells disrupts spatial information coding. Nat Neurosci, 20(6), 784-792. doi:10.1038/nn.4544

Dragoi, G. (2013). Internal operations in the hippocampus: single cell and ensemble temporal coding. Front Syst Neurosci, 7, 46. doi:10.3389/fnsys.2013.00046

Freund, T. F. (2003). Interneuron Diversity series: Rhythm and mood in perisomatic inhibition. Trends Neurosci, 26(9), 489-495. doi:10.1016/s0166-2236(03)00227-3

Fruh, S., Romanos, J., Panzanelli, P., Burgisser, D., Tyagarajan, S. K., Campbell, K. P., . . . Fritschy, J. M. (2016). Neuronal Dystroglycan Is Necessary for Formation and Maintenance of Functional CCK-Positive Basket Cell Terminals on Pyramidal Cells. J Neurosci, 36(40), 10296-10313. doi:10.1523/jneurosci.1823-16.2016

Fukaya, M., Kamata, A., Hara, Y., Tamaki, H., Katsumata, O., Ito, N., . . . Sakagami, H. (2011). SynArfGEF is a guanine nucleotide exchange factor for Arf6 and localizes preferentially at post-synaptic specializations of inhibitory synapses. J Neurochem, 116(6), 1122-1137. doi:10.1111/j.1471-4159.2010.07167.x

Golding, N. L., & Spruston, N. (1998). Dendritic sodium spikes are variable triggers of axonal action potentials in hippocampal CA1 pyramidal neurons. Neuron, 21(5), 1189-1200.

Hayama, T., Noguchi, J., Watanabe, S., Takahashi, N., Hayashi-Takagi, A., Ellis-Davies, G. C. R., … Kasai, H. (2013). GABA promotes the competitive selection of dendritic spines by controlling local Ca2+ signaling. Nature Neuroscience, 16(10), 1409–1416. http://doi.org/10.1038/nn.3496

Higley, M. J. (2014). Localized GABAergic inhibition of dendritic Ca(2+) signalling. Nat Rev Neurosci, 15(9), 567-572. doi:10.1038/nrn3803

Klausberger, T., Marton, L. F., Baude, A., Roberts, J. D., Magill, P. J., & Somogyi, P. (2004). Spike timing of dendrite-targeting bistratified cells during hippocampal network oscillations in vivo. Nat Neurosci, 7(1), 41-47. doi:10.1038/nn1159

Klausberger, T. and Somogyi, P. (2008). Neuronal diversity and temporal dynamics: the unity of hippocampal circuit operations. Science 321(5885):53-7

Klausberger, T. (2009). GABAergic interneurons targeting dendrites of pyramidal cells in the CA1 area of the hippocampus. Eur J Neurosci, 30(6), 947-957. doi:10.1111/j.1460-9568.2009.06913.x

Knuesel, I., Mastrocola, M., Zuellig, R. A., Bornhauser, B., Schaub, M. C., & Fritschy, J. M. (1999). Short communication: altered synaptic clustering of GABAA receptors in mice lacking dystrophin (mdx mice). Eur J Neurosci, 11(12), 4457-4462.

Lee, S. H., Foldy, C., & Soltesz, I. (2010). Distinct endocannabinoid control of GABA release at perisomatic and dendritic synapses in the hippocampus. J Neurosci, 30(23), 7993-8000. doi:10.1523/jneurosci.6238-09.2010

Lee, S. Y., Foldy, C., Szabadics, J., & Soltesz, I. (2011). Cell-type-specific CCK2 receptor signaling underlies the cholecystokinin-mediated selective excitation of hippocampal parvalbumin-positive fast-spiking basket cells. J Neurosci, 31(30), 10993-11002. doi:10.1523/jneurosci.1970-11.2011

Leutgeb, J. K., Leutgeb, S., Moser, M. B., & Moser, E. I. (2007). Pattern separation in the dentate gyrus and CA3 of the hippocampus. Science, 315(5814), 961-966. doi:10.1126/science.1135801

Levi, S., Grady, R. M., Henry, M. D., Campbell, K. P., Sanes, J. R., & Craig, A. M. (2002). Dystroglycan is selectively associated with inhibitory GABAergic synapses but is dispensable for their differentiation. J Neurosci, 22(11), 4274-4285. doi:20026440

Lin, Y., Bloodgood, B. L., Hauser, J. L., Lapan, A. D., Koon, A. C., Kim, T. K., . . . Greenberg, M. E. (2008). Activity-dependent regulation of inhibitory synapse development by npas4. Nature, 455(7217), 1198-1204. doi:10.1038/nature07319

Major, G., Larkum, M. E., & Schiller, J. (2013). Active properties of neocortical pyramidal neuron dendrites. Annu Rev Neurosci, 36, 1-24. doi:10.1146/annurev-neuro-062111-150343

McNally, E. M., & Pytel, P. (2007). Muscle diseases: the muscular dystrophies. Annu Rev Pathol, 2, 87-109. doi:10.1146/annurev.pathol.2.010506.091936

Megias, M., Emri, Z., Freund, T. F., & Gulyas, A. I. (2001). Total number and distribution of inhibitory and excitatory synapses on hippocampal CA1 pyramidal cells. Neuroscience, 102(3), 527-540.

Miles, R., Tóth, K., Gulyás, A.I., Hájos, N., & Freund, T.F. (1996). Differences between somatic and dendritic inhibition in the hippocampus. Neuron 16(4): 815-823.

Neu, A., Földy, C., & Soltesz, I. (2007). Postsynaptic origin of CB1-dependent tonic inhibition of GABA release at cholecystokinin-positive basket cell to pyramidal cell synapses in the CA1 region of the rat hippocampus. The Journal of Physiology, 578(Pt 1), 233–247. http://doi.org/10.1113/jphysiol.2006.115691

O'Keefe, J., & Dostrovsky, J. (1971). The hippocampus as a spatial map. Preliminary evidence from unit activity in the freely-moving rat. Brain Res, 34(1), 171-175.

O'Keefe, J. and Nadel, L. (1978). The hippocampus as a cognitive map. Oxford University Press, Oxford.

O'Keefe, J., & Recce, M. L. (1993). Phase relationship between hippocampal place units and the EEG theta rhythm. Hippocampus, 3(3), 317-330. doi:10.1002/hipo.450030307

Pawelzik, H., Bannister, A. P., Deuchars, J., Ilia, M., & Thomson, A. M. (1999). Modulation of bistratified cell IPSPs and basket cell IPSPs by pentobarbitone sodium, diazepam and Zn2+: dual recordings in slices of adult rat hippocampus. Eur J Neurosci, 11(10), 3552-3564

Pawelzik, H., Hughes, D. I., & Thomson, A. M. (2002). Physiological and morphological diversity of immunocytochemically defined parvalbumin- and cholecystokinin-positive interneurones in CA1 of the adult rat hippocampus. J Comp Neurol, 443(4), 346-367.

Spruston, N. (2008). Pyramidal neurons: dendritic structure and synaptic integration. Nat Rev Neurosci, 9(3), 206-221. doi:10.1038/nrn2286

Stokes, C. C., Teeter, C. M., & Isaacson, J. S. (2014). Single dendrite-targeting interneurons generate branch-specific inhibition. Front Neural Circuits, 8, 139. doi:10.3389/fncir.2014.00139

Vida, I., Halasy, K., Szinyei, C., Somogyi, P., & Buhl, E. H. (1998). Unitary IPSPs evoked by interneurons at the stratum radiatum-stratum lacunosum-moleculare border in the CA1 area of the rat hippocampus in vitro. J Physiol, 506 (Pt 3), 755-773.

Waite, A., Brown, S. C., & Blake, D. J. (2012). The dystrophin-glycoprotein complex in brain development and disease. Trends Neurosci, 35(8), 487-496. doi:10.1016/j.tins.2012.04.004

Wilson, M. and McNaughton, B. (1993). Dynamics of the hippocampal ensemble code for space. Science 261(5124): 1055-1058.